IMAGE: A MAP OF THE STARS OF THE ORION CONSTELLATION

Print ISSN: 2631-8490 Online ISSN: 2631-8504

JournalPreview

London Journal of Research in Science: Natural & Formal

Volume 26 | Issue 2 | Compilation 1.0

Great Britain Journals Press

WWW.JOURNALSPRESS.COM

Journal Content
In this Issue

Great Britain Journals Press

Soil Quality at Twiga 1, Waste Site in Turkana County, Kenya

John Kioko Munyao & Dr. Esther Lesan Kitur

ABSTRACT

The exploration and production of petroleum resources create both opportunities and environmental challenges for sustainable development. In Kenya, the Government, along with private investors, has pursued oil and gas activities in the Anza, Mandera, Lamu and Tertiary Rift Basins. Initially, sixty-three petroleum exploration blocks were established under Gazette Notice No. 3344 on May 13, 2016, but this number was later streamlined to fifty through Gazette Notice No. 4832 on April 16, 2025. This study investigates how petroleum exploration activities influence soil quality at the Twiga 1 waste consolidation site, providing insights into the environmental consequences of hydrocarbon operations in Turkana County (Block T7, previously 13T, Tertiary Rift Basin). It focused on concentrations of lead (Pb) and cadmium (Cd). A descriptive cross-sectional and experimental design was used. Soil samples were collected using the grid sampling method. Soil samples were collected using a soil auger, enabling systematic retrieval of subsurface material for subsequent analysis and samples were transported to the laboratory in well-labeled aluminum containers. Heavy metal concentrations in the samples were determined using an Atomic Absorption Spectrometer (AAS-7000, Shimadzu). The study objectives were to i) assess the levels of lead and cadmium in the soil at the Twiga 1 waste consolidation site, ii) determine the levels during the wet and dry seasons and iii) compare the levels with established environmental Standards.

Keywords: heavy metals, soil contamination, petroleum industry, climate variability, environmental safety standards introduction.

Classification: LCC Code: TD878, S592.17, QE379

Language: English

Great Britain Journals Press

LJP Copyright ID: 925611
Print ISSN: 2631-8490
Online ISSN: 2631-8504

London Journal of Research in Science: Natural & Formal

Volume 26 | Issue 2 | Compilation 1.0

Soil Quality at Twiga 1, Waste Site in Turkana County, Kenya

John Kioko Munyao[α] & Dr. Esther Lesan Kitur[σ]

ABSTRACT

The exploration and production of petroleum resources create both opportunities and environmental challenges for sustainable development. In Kenya, the Government, along with private investors, has pursued oil and gas activities in the Anza, Mandera, Lamu and Tertiary Rift Basins. Initially, sixty-three petroleum exploration blocks were established under Gazette Notice No. 3344 on May 13, 2016, but this number was later streamlined to fifty through Gazette Notice No. 4832 on April 16, 2025. This study investigates how petroleum exploration activities influence soil quality at the Twiga 1 waste consolidation site, providing insights into the environmental consequences of hydrocarbon operations in Turkana County (Block T7, previously 13T, Tertiary Rift Basin). It focused on concentrations of lead (Pb) and cadmium (Cd). A descriptive cross-sectional and experimental design was used. Soil samples were collected using the grid sampling method. Soil samples were collected using a soil auger, enabling systematic retrieval of subsurface material for subsequent analysis and samples were transported to the laboratory in well-labeled aluminum containers. Heavy metal concentrations in the samples were determined using an Atomic Absorption Spectrometer (AAS-7000, Shimadzu). The study objectives were to i) assess the levels of lead and cadmium in the soil at the Twiga 1 waste consolidation site, ii) determine the levels during the wet and dry seasons and iii) compare the levels with established environmental standards. Heavy metal concentrations were very low at all sites and in both seasons, remaining well below WHO and US EPA limits. During the wet season, mean concentrations (mg/kg) were as follows: Pb, 0.003–0.035, and Cd, 0.000–0.003. During the dry season, slightly higher values were recorded than in the wet season: Pb (0.000–0.044) and Cd (0.000–0.004). Although the differences were minor, they showed seasonal variation, with higher dry-season concentrations linked to limited leaching, moisture loss from evaporation, and dust deposition from the atmosphere. All measured concentrations were well below the guidelines limits established by the World Health Organization (WHO) for lead (Pb: 100 mg/kg) and cadmium (Cd: 1–3 mg/kg) as well as those set by the U.S. Environmental Protection Agency (EPA) (Pb: 400 mg/kg; Cd: 70 mg/kg). The soils are therefore uncontaminated and safe for farming, living and ecological purposes. At a significance level of α = 0.05, comparison of p-values for heavy metal concentrations between the wet and dry seasons supports the hypothesis that heavy metal levels are significantly higher during the dry season at the Twiga 1 waste consolidation site. Lead (0.001–0.055) shows significant differences, while cadmium (0.000–0.046) provides strong evidence for higher levels in the dry season. Heavy metal concentrations were significantly higher in the dry season than in the wet season, yet they remained below the limits established by the World Health Organization (WHO) and the U.S. Environmental Protection Agency (EPA). The dry season-associated rise in metal concentrations demonstrates the impact of climatic changes on soil chemical properties. Although the soils at the Twiga 1 waste consolidation site are safe, ongoing monitoring is recommended to protect long-term soil health and environmental integrity around petroleum operations.

Keywords: heavy metals, soil contamination, petroleum industry, climate variability, environmental safety standards.

Author α σ: Department of Environmental Sciences and Education.

London Journal of Research in Science: Natural & Formal

I. INTRODUCTION

1.1: Background Information

Heavy metals are introduced into the environment during upstream petroleum production through various interconnected pathways related to drilling activities, extraction, and waste management activities. During drilling and production, additives and chemicals in drilling fluids such as barite may contain trace heavy metals, including cadmium and lead, which can be released into surrounding soils and water (Smith et al., 2018). Furthermore, produced water generated during oil and gas extraction can contain naturally occurring heavy metals that are mobilized from reservoir rocks, notably lead and cadmium (*Brown et al., 2017)*. The corrosion of drilling and production equipment further contributes to environmental contamination by releasing metals such as cadmium and lead (*Jones et al., 2019*). Areas with naturally high background concentrations of these metals, particularly in the Middle East and parts of Africa, are especially susceptible to contamination, as improper disposal of produced water, drilling cuttings, and other oilfield wastes can markedly exacerbate environmental heavy metal levels (*Johnson et al., 2020*). Oil spills and leakages occurring during exploration and production can release persistent heavy metals into the environment, leading to their accumulation in soils and sediments and causing long-term ecological impacts (*Pandiyan et al., 2021*). The buildup of lead and cadmium in soils and aquatic systems contributes to extensive environmental degradation, posing severe risks to communities reliant on agriculture and fisheries. These metals bioaccumulate in plants and animals, disrupting food webs, decreasing biodiversity, and inflicting potentially irreversible ecological damage (*Phaenark et al., 2024*). Heavy metal contamination can impair plant growth and photosynthetic activity, leading to reduced vegetation cover and a decline in the carbon sequestration capacity of ecosystems (*Pandiyan et al., 2021*). The consequent loss of natural carbon sinks may further exacerbate climate change by limiting atmospheric CO_2 removal. Additionally, degraded ecosystems may release_stored carbon through the decomposition of vegetation and soil organisms, creating a feedback loop that further increases atmospheric CO_2 concentrations. Exposure to cadmium and lead also poses significant human health risks. Lead exposure is linked to neurological damage, particularly in children, while cadmium is a recognized carcinogen associated with renal dysfunction and skeletal disorders (*Rozirwan et al., 2024*). Beyond these direct health effects, such impacts can indirectly contribute to climate change by increasing healthcare demands and energy consumption, thereby elevating carbon emissions. In Kenya, the government, in partnership with oil and gas investors, has conducted extensive petroleum exploration across multiple sedimentary basins, including Anza, Mandera, Lamu, and the Tertiary Rift Basin, with fifty exploration blocks officially gazetted.The study focuses on Twiga 1, a waste consolidation site within Block T7 (formerly Block 13T) in the Tertiary Rift Basin. Since the onset of petroleum operations, communities in Turkana County have reported heightened livestock mortality, particularly among goats. Oilfield wastes are known to contain toxic heavy metals such as lead, chromium, cadmium and nickel, which are harmful to grazing animals and can accumulate in contaminated soils *(Stimmel et al., 1989;* Wyszkowski &Kordala, 2024). Consequently, a detailed soil Analysis of the Twiga 1 waste consolidation site is necessary to determine whether heavy metals have accumulated to levels that pose a risk to livestock, human health and the surrounding environment in Block T7 of the Tertiary Rift Basin.

II. METHODOLOGY

2.1: The study was conducted at the Twiga 1 waste consolidation site in Turkana County, Kenya, as shown in Figure 2.2. Twiga 1 is a well pad located in Block T7 (formerly Block 13T) within the Tertiary Basin, licensed by the National Environment Management Authority (NEMA), No. PR/10351. The well was drilled in 2012 and it was one of the few sites in the basin where commercially viable crude oil deposits were discovered. Since 2014, Tullow Kenya B.V. has been using the Twiga 1 site, Longitude:

35° 42′ 57.43″ E, Latitude: 2° 24′ 10.88″ N) as a temporary storage area for drill cuttings from other wells in the basin, even though the site was not licensed as a waste holding facility. Located in a semi-arid zone, the region experiences rainfall concentrated in two distinct periods: the long rains between April and June and the short rains from October to December. With an annual average rainfall often falling below 500 mm, the area faces challenges in maintaining adequate soil moisture, which, coupled with sparse vegetation cover, increases susceptibility to soil erosion. These climatic conditions have significant implications for agricultural productivity and natural resource management, highlighting the need for sustainable land-use strategies tailored to such rainfall variability. Humidity levels in Turkana are generally low, averaging between 30% and 50% which can exacerbate the impacts of drought and influence soil properties. The area experiences moderate to strong winds, particularly during dry seasons and wind patterns which contribute to soil erosion and affect the dispersal of pollutant.

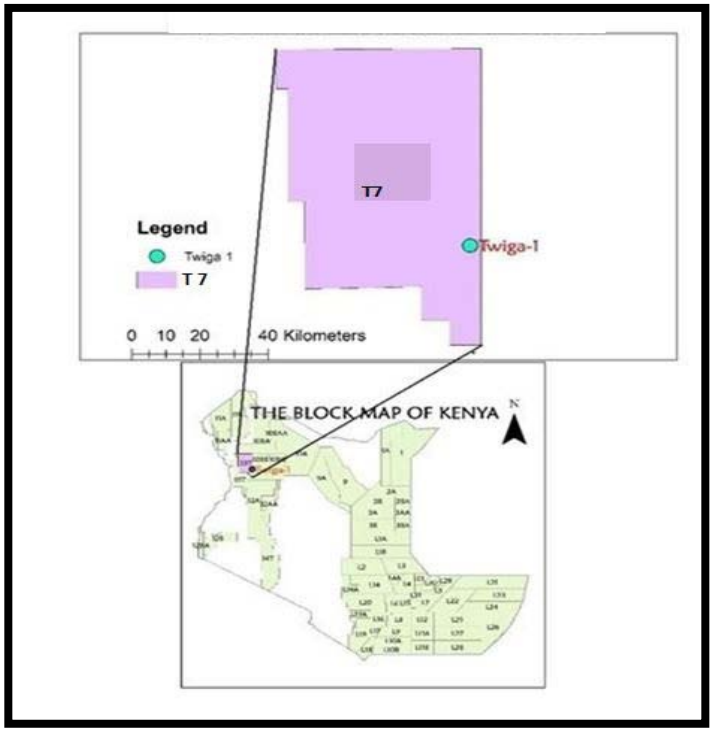

Fig. 2.1: A map of Kenya showing Twiga 1, a waste consolidated site.

2.2 Sampling of soil samples

Sampling was conducted once a month for four months, between April and August 2025, across four grids (Fig. 2.2). The sampling points were referenced using GPS coordinates. (Table 2.1). Soil samples (300 g from each sampling point) were collected from 24 sampling sites using a soil auger at a depth of 0–6 cm and transferred into clean, labeled aluminum containers. The containers were labeled to indicate the sampling date and sampling points. The samples were then transported to the laboratory for Analysis. In the laboratory, the samples were dried in an oven at a temperature of 800 degree centigrade. The dried soil samples were pulverized to a particle size of 150 microns using a pulverizer to increase their surface area.

for Analysis. In the laboratory, the samples were dried in an oven at a temperature of 800 degree centigrade. The dried soil samples were pulverized to a particle size of 150 microns using a pulverizer to increase their surface area

Table 1: Geographical coordinates and elevation

Identity	Coordinates		
	Latitude N	Longitude E	Elevation
A1	35° 42′ 54.73″	2°24′13.23″	705m
A2	35° 42′ 56.69″	2° 24′ 13.26″	705mm
A3	35.716265,	2° 24′ 13.26″	703m
A4	35° 43′ 0.49″	2° 24′ 13.24″	703m
A5	35° 43′ 2.47″	2° 24′ 13.24″	696m
A6	35° 43′ 4.45″	2° 24′ 13.22″	697m
B1	35° 42′ 54.75″	2° 24′ 11.24″	704m
B2	35° 42′ 56.57″	2° 24′ 11.28″	705m
B3	35° 42′ 58.50″	2° 24′ 11.28″	705m
B4	35° 43′ 0.46″	2° 24′ 11.25″	700m
B5	35° 43′ 2.54″	2° 24′ 11.32″	702m
B6	35° 43′ 4.32″	2° 24′ 11.52″	697m
C1	35° 42′ 54.64″	2° 24′ 9.36″	701m
C2	35° 42′ 56.56″	2° 24′ 9.31″	710m
C3	35° 42′ 58.58″	2° 24′ 9.35″	706m
C4	35° 43′ 0.53″	2° 24′ 9.29″	700m
C5	35° 43′ 2.43″	2° 24′ 9.36″	699m
C6	35° 43′ 4.40″	2° 24′ 9.35″	696m
D1	35° 42′ 54.69″	2° 24′ 7.61″	700m
D2	35° 42′ 56.62″	2° 24′ 7.54″	699m
D3	35° 42′ 58.56″	2° 24′ 7.49″	703m
D4	35° 43′ 0.50″	2° 24′ 7.50″	699m
D5	35° 43′ 2.45″	2° 24′ 7.43″	699m
D6	35° 43′ 4.42″	2° 24′ 7.40″	695m

Fig 2.2: Map of Twiga 1, waste consolidation site showing twenty-four sampling points

2.3: Preparation and digestion for metal analysis using AAS

Each sample was dried in an oven at 80 °C, followed by pulverization to 150 microns. A 2.5000 g portion of the pulverized soil sample was weighed using a four-decimal analytical balance and transferred into a 150 ml glass beaker. Twenty milliliters of distilled water were added to form a slurry, followed by 5 ml of nitric acid. The mixture was then placed on a sand bath. The samples were left to digest until no more brown fumes were produced and the contents became clear. The contents were left to cool and then filtered through Whatman No. 42 filter paper into a 100 ml volumetric flask, followed by several washings. Finally, the volume was made up to the mark with deionized water and labeled accordingly. A blank sample was prepared in the same manner as the soil sample.

2.4: Preparation of working standards from a 100ppm stock solution

Working standard solutions in the range of 0 ppm to 30 ppm were prepared from a 100-ppm analytical grade stock solution of lead and cadmium using the Dilution formula

$$C_1V_1 = C_2V_2$$

C_1 = Original stock solution concentration

V_1 = Volume of stock solution to be taken

C2 = Expected new concentration of working standards

V2 = Expected volume of working standards

2.5: Sample Analysis using AAS

The working standards were analysed using an Atomic Absorption Spectrometer (AAS-7000, Shimadzu) and calibration curves were plotted based on the absorbance and concentration readings in

ppm. The samples containing the analytes of interest were then analysed and their concentrations were determined using the calibration curves of the standards.

2.6: Statistical methods used to analyze the data

2.6.1 Calibration curves

Calibration curves were used to establish the relationship between concentration and absorbance. Linear regression analysis was employed to examine trends in the data. A t-test was used to compare standard reference values with sample results, and summary tables were generated to present heavy metal concentrations across the various sampling sites. The measured values were then compared with permissible limits for lead and cadmium, to evaluate soil safety. This was to determine whether the concentrations exceed acceptable limits, thereby posing potential risks to human health. In such cases, awareness was raised among the nearby community, relevant government agencies and policymakers to facilitate appropriate environmental interventions and ensure public safety. In this study, the recommended instrument parameters for lead were used as outlined below. An electrodeless discharge lamp (EDL) served as the light source, with acetylene as the fuel and air as the support gas under oxidising flame conditions. For precise and sensitive lead determination, the wavelength was set at 217 nm with a spectral bandpass of 1.0 nm. Cadmium analysis was carried out using an electrodeless discharge lamp (EDL) operated at 3.5 mA, with acetylene as the fuel and air as the support gas under oxidizing flame conditions. The wavelength was set at 228 nm with a 0.5 nm spectral bandpass to achieve optimal detection accuracy.

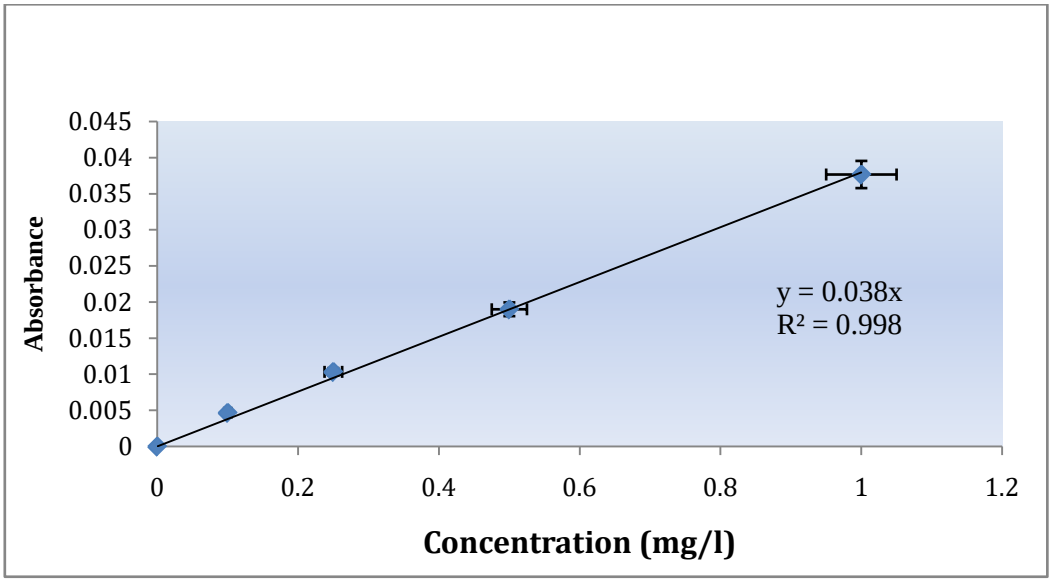

Figure 2.3 : Calibration curve for Pb for 5 standards

In this study, the recommended instrument parameters for lead were used as outlined below. An electrodeless discharge lamp (EDL) was employed as the light source. Acetylene was used as the fuel, with air serving as the support gas under oxidizing flame conditions. The wavelength was set at 217 nm with a spectral band pass of 1.0 nm to achieve optimal precision and sensitivity in lead determination

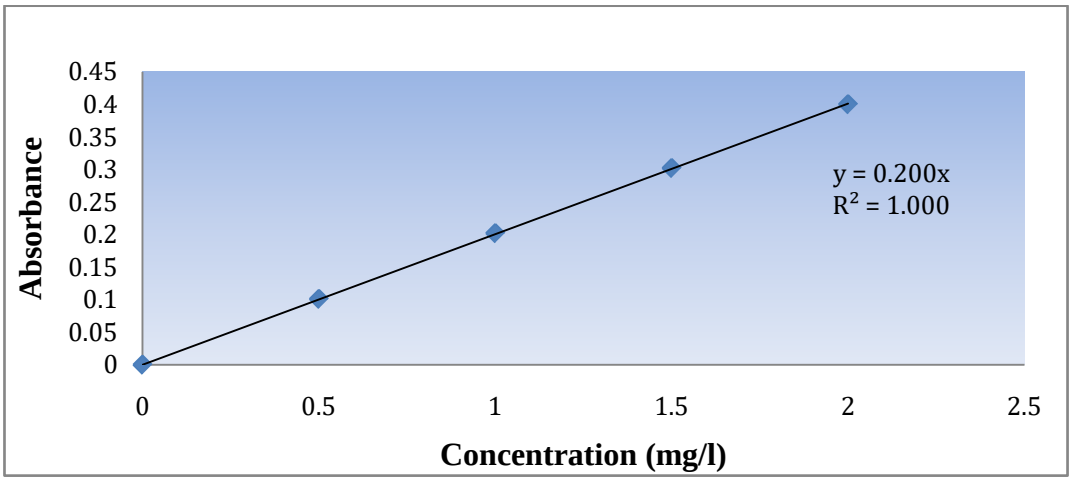

Figure 2.4: Calibration curve for Cd for 5 standards

In this study, cadmium analysis was conducted using an electrodeless discharge lamp at 3.5 mA, with acetylene as the fuel and air as the support gas under oxidizing flame conditions. The wavelength was set at 228 nm with a 0.5 nm spectral band pass for optimal detection accuracy.

III. RESULTS, DISCUSSION

3.1: Lead (Pb)

Table 1: Summary of the statistical analysis of lead concentration in the soil samples during wet and dry season

Lead concentration in the soil samples during wet season												
Method	**A1**	**A2**	**A3**	**A4**	A5	A6	B1	B2	B3	B4	B5	B6
	0.041	0.030	0.012	0.040	0.022	0.031	0.031	0.043	0.032	0.012	0.04	0.00
	0.022	0.042	0.023	0.031	0.021	0.032	0.023	0.032	0.023	0.023	0.032	0.010
	0.034	0.031	0.021	0.032	0.040	0.023	0.023	0.031	0.034	0.021	0.024	0.000
Mean	0.032	0.034	0.019	0.034	0.028	0.029	0.026	0.035	0.030	0.019	0.032	0.003
SD	0.008	0.005	0.005	0.004	0.008	0.004	0.004	0.0054	0.006	0.0058	0.0065	0.047
P-value	0.01	0.010	0.01	0.0	0.01	0.01	0.01	0.0	0.01	0.031	0.01	0.01
	C1	**C2**	**C3**	**C4**	C5	C6	D1	D2	D3	D4	D5	D6
	0	0	0	0.032	0.013	0.042	0	0.032	0.00	0.047.	0.032	0.024
	0	0	0	0.023	0.023	0.023	0	0.024	0.000	0.032	0.024	0.033
	0	0	0	0.031	0.021	0.032	0	0.013	0.000	0. 032	0.035	0.035
Mean	0	0	0	0.029	0.019	0.032	0	0.023	0.000	0.037	0.030	0.030
SD	0	0	0	0.005	0.005	0.010	0	0.009	0.0	0.009	0.006	0.006
P-Value	0	0	0	0.010	0.025	0.010	0	0.053	0.000	0.018	0.00	0.01
	Lead concentration in the samples during dry season											
	A1	A2	A3	A4	A5	A6	B1	B2	B3	B4	B5	B6

	0.034	0.042	0.024	0.032	0.034	0.035	0.023	0.036	0.032	0.031	0.032	0.025
	0.043	0.044	0.033	0.045	0.024	0.024	0.024	0.040	0.024	0.044	0.021	0.013
	0.035	0.032	0.035	0.035	0.035	0.033	0.035	0.024	0.035	0.035	0.043	0.014
Mean	0.037	0.039	0.031	0.037	0.031	0.031	0.027	0.033	0.030	0.037	0.032	0.017
SD	0.045	0.045	0.045	0.045	0.045	0.045	0.045	0.045	0.045	0.045	0.045	0.045
P-Value	0.001	0.01	0.00	0.55	0.009	0.01	0.018	0.00	0.006	0.005	0.035	0.045
	C1	**C2**	**C3**	**C4**	C5	C6	D1	D2	D3	D4	D5	D6
	0	0	0	0.043	0.023	0.045	0	0.040	0	0.041	0.044	0.035
	0	0	0	0.031	0.035	0.031	0	0.031	0	0.042	0.031	0.042
	0	0	0	0.042	0.036	0.040	0	0.035	0	0.045	0.040	0.054
Mean	0	0	0	0.039	0.031	0.039	0	0.035	0	0.043	0.038	0.044
SD	0	0	0	0.006	0.007	0.0071	0	0.005	0	0.0021	0.00665	0.0096
P- value	0	0	0	0.004	0.01	0.01	0	0.005	0	0.000	0.01	
WHO	100 mg/kg											
US EPA	400 mg/kg											

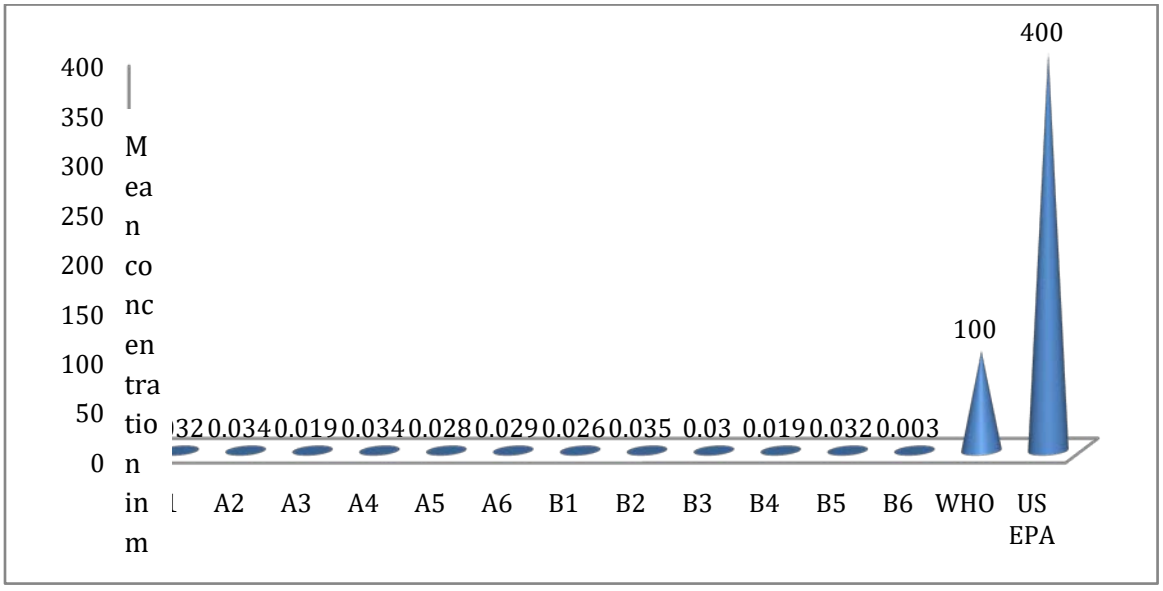

Figure 2.5: Summary of the statistical analysis of lead concentration in the soil samples during wet season

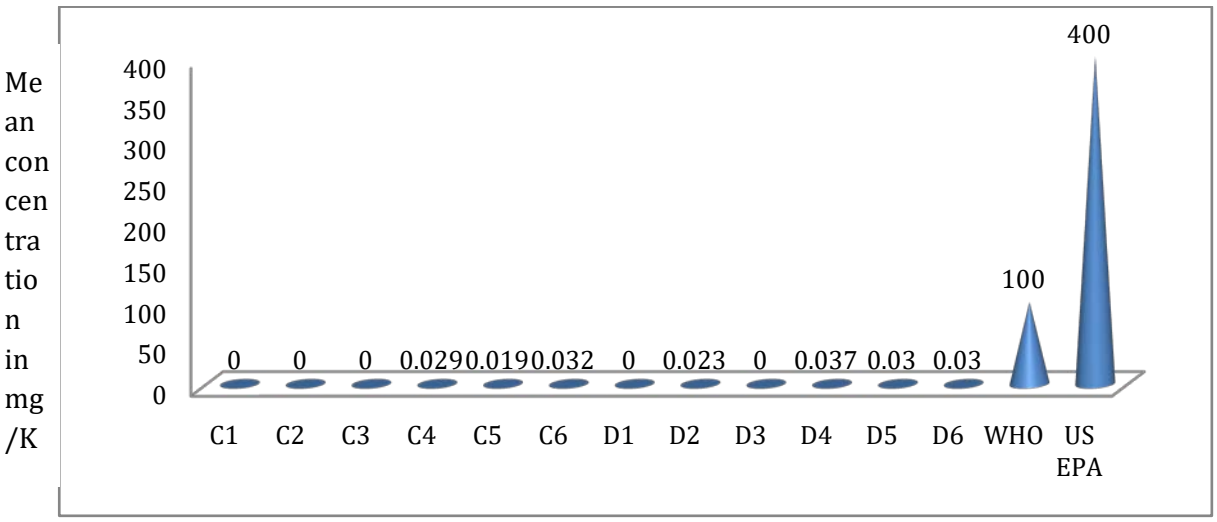

Figure 2.6: Summary of the statistical analysis of lead concentration in the soil samples during wet season

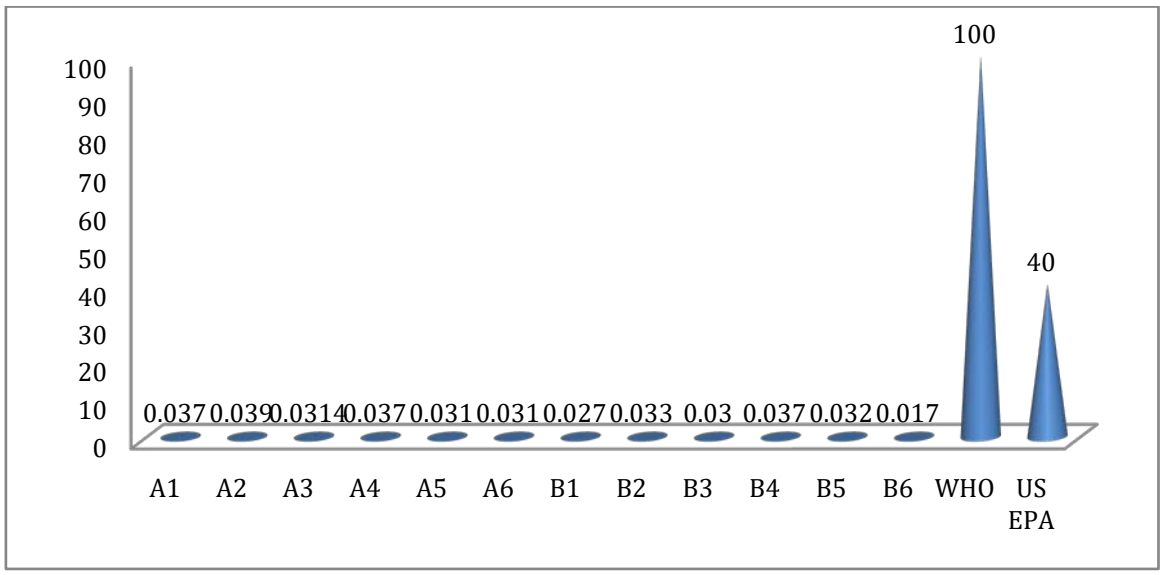

Figure 2.7: Summary of the statistical analysis of lead concentration in the soil samples during dry season

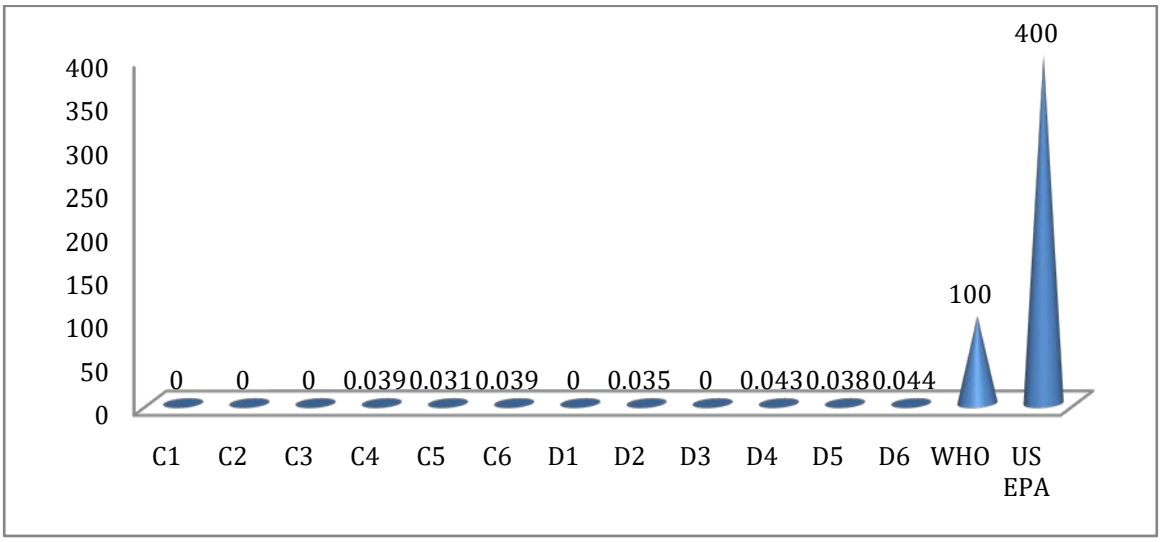

Figure 2.8: Summary of the statistical analysis of lead concentration in the soil samples during the dry season.

The results of the research showed 0.003–0.043 mg·kg^{-1} lead with several undetected, the results are remarkably low compared to petroleum operation facilities globally, which contain soils and drilling cuttings with excessive levels of heavy metals. *Mugendi et al. (2019)* reported lead (Pb) concentrations ranging from tens to hundreds of mg·kg^{-1} in soils and mud cuttings from the Twiga-1 well in Kenya's South Lokichar Basin, while *Brown et al. (2020)* documented concentrations of 25–180 mg·kg^{-1} in reserve pits surrounding drilling sites in Nigeria. *Abuzaid et al. (2022)* reported Pb concentrations of 40–220 mg·kg^{-1} in soils from petroleum plants in Saudi Arabia, while *Smith et al. (2020)* recorded levels of 15–95 mg·kg^{-1} in soils contaminated with drilling wastes in Texas, USA.,. In the Daqing oilfield in China, lead levels of 20–160 mg·kg^{-1} were observed around oil production terminals (*Liang et al., 2020*).

Comparatively, the results are orders of magnitude lower, providing significant evidence for background unadulterated soils at a petroleum-influenced site. This offers new baseline measurements that assist in separating natural conditions from petroleum-induced contamination. It established a seasonal baseline of petroleum-associated land soils with minimal contamination. It demonstrated that not all sites where petroleum activities are performed are contaminated, refuting flawed assumptions in literature. International comparative findings highlighted that, the site substantially differs from very contaminated petroleum sites in Africa, Asia and North America. In general, the findings corroborate the need for site-specific monitoring, emphasizing that contamination is not uniform in petroleum terminals.

3.2: Cadmium (Cd)

Cadmium concentrations in the research during both wet and dry seasons were extremely low, ranging from 0.001 to 0.005 mg·kg^{-1}, with many undetected values as shown in Table 2 and figure 2.5, 2.6, 2.7 and 2.8. They are several orders of magnitude lower than concentrations measured at petroleum operation sites worldwide, where drilling fluids, cuttings, and produced water contribute to elevated cadmium levels. For instance, *Brown et al., (2020)* recorded concentrations of 1.5 to 6.8 mg·kg^{-1} of cadmium in soils near oil drilling pits in the Niger Delta,

Nigeria, they recorded 2–12 mg·kg^{-1} in the neighbourhood of petroleum facilities in Saudi Arabia by *Abuzaid et al. (2022*). In the Daqing oilfield of China, *Liang et al. (2020)* reported 3–15 mg·kg^{-1} cadmium in the soils of the oil production terminals and *Smith et al., 2020*) reported 1–4 mg·kg^{-1} in petroleum-impacted soils of Texas, USA. Similar ranges have also been reported in the petroleum fields of Egypt's Gulf of Suez, where cadmium was found to be up to 5–10 mg·kg^{-1} (El-Sorogy et., 2018). Compared with these values, the present findings indicate that cadmium concentrations in the study area are well below international guidelines limits (EU: 1–3 mg·kg^{-1}; US EPA: 70 mg·kg^{-1}) and therefore the soils remain uncontaminated and are suitable for agricultural and ecological use. The results represent a significant contribution by providing a baseline reference for uncontaminated petroleum-adjacent soils, showing that not all oilfield-related sites are affected by cadmium pollution. The research established a seasonal baseline characterised by largely non-detectable to trace cadmium concentrations, which contrasted sharply with petroleum contamination hotspots reported worldwide. It illustrated the absence of petroleum-based cadmium pollution despite the location's proximity to petroleum activities. Evidence from global comparisons indicates that, whereas oilfields in other regions exhibit cadmium concentrations ranging from 1–15 mg·kg^{-1}, the site in question displays quasi-zero levels. These findings emphasise that cadmium hazards are more site-specific rather than widespread across petroleum regions. While cadmium in petroleum sites around the world is typically in the 1–15 mg·kg^{-1} range, my results (0.001–0.005 mg·kg^{-1}) are more or less negligible. During the dry season, dilution and leaching of lead and cadmium in the soil are minimised due to low rainfall amounts. Additionally, high temperatures and evaporation rates reduce soil moisture content, resulting in higher trace metal concentrations on a dry-weight basis. On the other hand, the dry season is also characterised by the deposition of wind-borne dust, which adds trace metals to the surface soil. On the contrary, the wet season is marked by high rainfall, which enhances the dilution and leaching of trace metals in the soil. As a result, the soil trace metal concentration is relatively low. However, in the context of climate change, rising temperatures and increased likelihood of drought enhance the buildup of trace metals in the soil. In the long run, high temperatures, low soil moisture, sparse biota, and the soil's chemical composition affect the mobility of trace metals in the soil.

Table 2: Cadmium concentration in the soil samples during wet and dry season in (mg/kg

	Cadmium concentration in the soil samples during wet season in (mg/kg											
Method	A1	A2	A3	A4	A5	A6	B1	B2	B3	B4	B5	B6
AAS	0	0	0	0	0.002	0.003	0.001	0	0	0.001	0.001	0
	0	0	0	0	0.001	0.002	0.002	0	0	0.001	0.001	0
	0	0	0	0	0.002	0.003	0.001	0	0	0.001	0.001	0
Mean	0	0	0	0	0.002	0.003	0.001	0	0	0.001	0.001	0
SD	0	0	0	0	0.00058	0.00058	0.00058	0	0	0.000	0.000	0
P- value	0	0	0	0	0.036	0.01	0.06	0	0	0.000	0.000	0
	C1	C2	C3	C4	C5	C6	D1	D2	D3	D4	D5	D6
	0	0	0	0.002	0.002	0.002	0	0.003	0	0.000	0.000	0.001
	0	0	0	0.001	0.002	0.001	0	0.001	0	0.000	0.001	0.001
	0	0	0	0.002	0.001	0.001	0	0.002	0	0.001	0.001	0.002
Mean	0	0	0	0.002	0.002	0.001	0	0.002	0	0.000333	0.000333	0.001333
SD	0	0	0	0.000577	0.035	0.000577	0	0.001	0	0.000577	0.000577	0.000577
P-Value	0	0	0	0.04	0.035	0.056	0	0.074	0	0.423	0.423	0.056
	Cadmium concentration in the soil samples during dry season in (mg/kg											
	A	A2	A3	A4	A5	A6	B1	B2	B3	B4	B5	B6
	0	0	0	0	0.004	0.005	0.003	0	0	0.001	0.002	0
	0	0	0	0	0.004	0.004	0.004	0	0	0.002	0.001	0
	0	0	0	0	0.005	0.003	0.005	0	0	0.001	0.003	0
Mean	0	0	0	0	0.004	0.004	0.004	0	0	0.001	0.002	0

SD	0	0	0	0	0.00058	0.001	0.001	0	0	0.00058	0.001	0
P-Value	0	0	0	0	0.006	0.020	0.460	0	0	0.650	0.460	0
	C1	C2	C3	C4	C5	C6	D1	D2	D3	D4	D5	D6
	0	0	0	0.003	0.003	0.003	0	0.003	0	0.001	0.000	0.003
	0	0	0	0.001	0.004	0.001	0	0.001	0	0.002	0.001	0.002
	0	0	0	0.003	0.002	0.004	0	0.002	0	0.001	0.002	0.002
Mean	0	0	0	0.002	0.003	0.003	0	0.002	0	0.001	0.001	0.002
SD	0	0	0	0.0011547	0.001	0.0015275	0	0.001	0	0.000577	0.001	0.000577
P-Value	0	0	0	0.650	0.460	0.510	0	0.460	0	0.650	0.460	0.420
EU	1 mg/kg to 3 mg/kg											
US EPA	70 mg/kg											

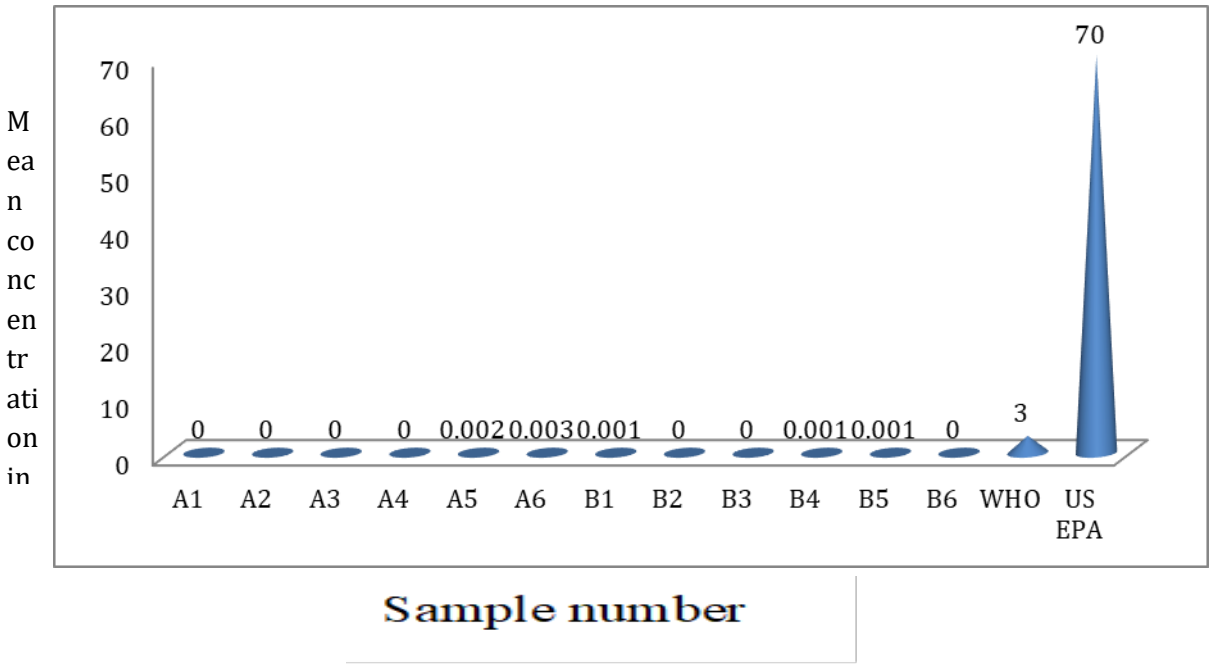

Figure 2.9: Summary of the statistical analysis of Cadmium concentration in the soil samples during wet season.

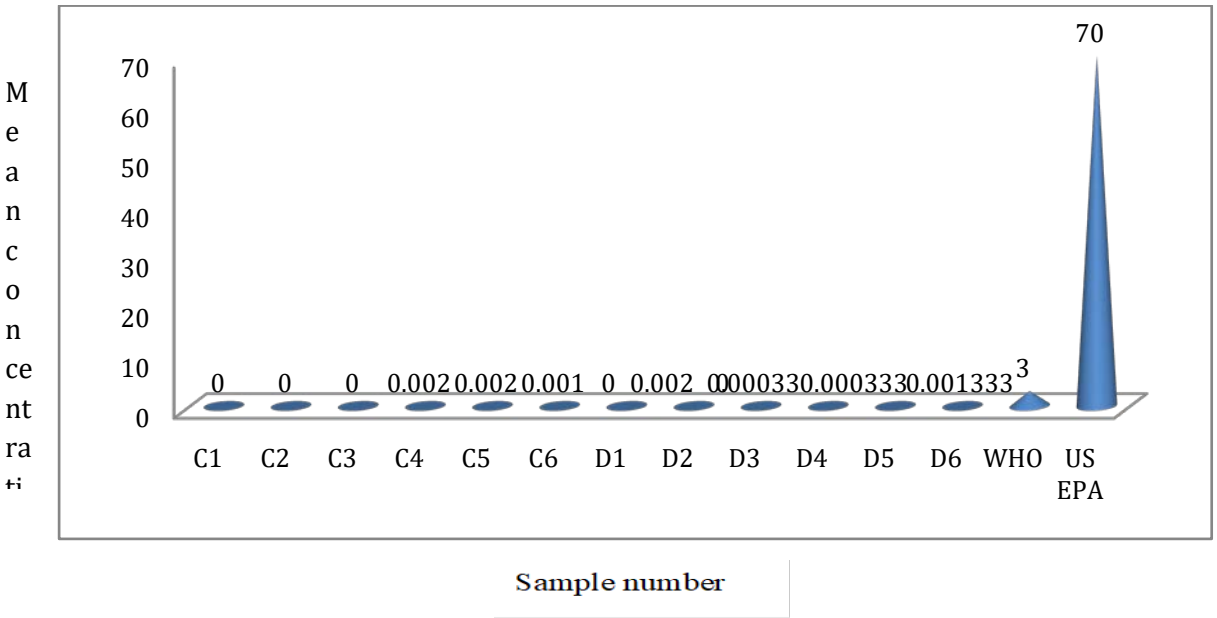

Figure 2.10: Summary of the statistical analysis of Cadmium concentration in the soil samples during wet season

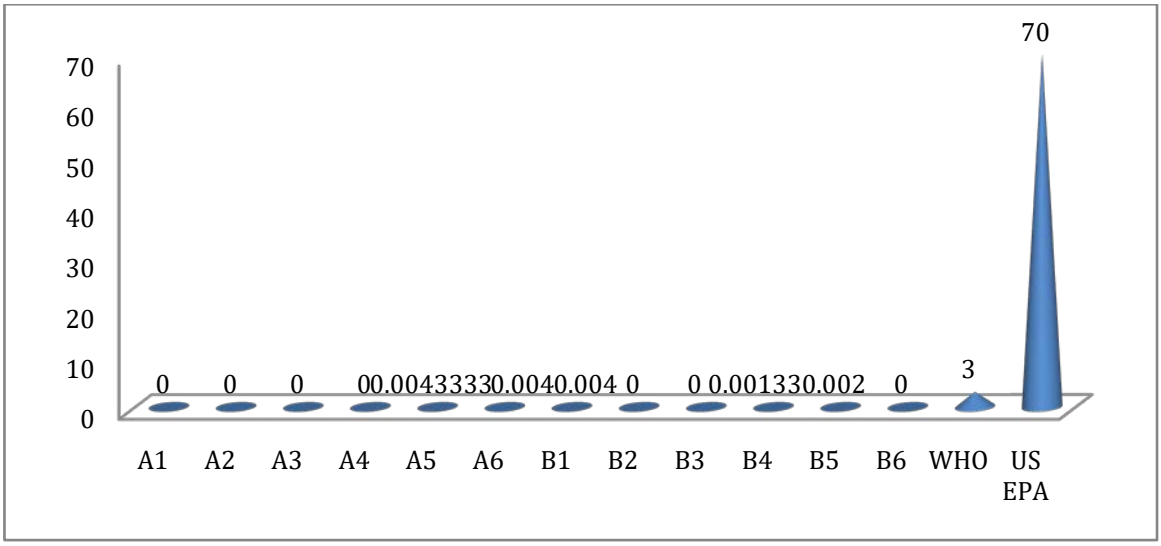

Figure 2.11: Summary of the statistical analysis of Cadmium concentration in the soil samples during dry season

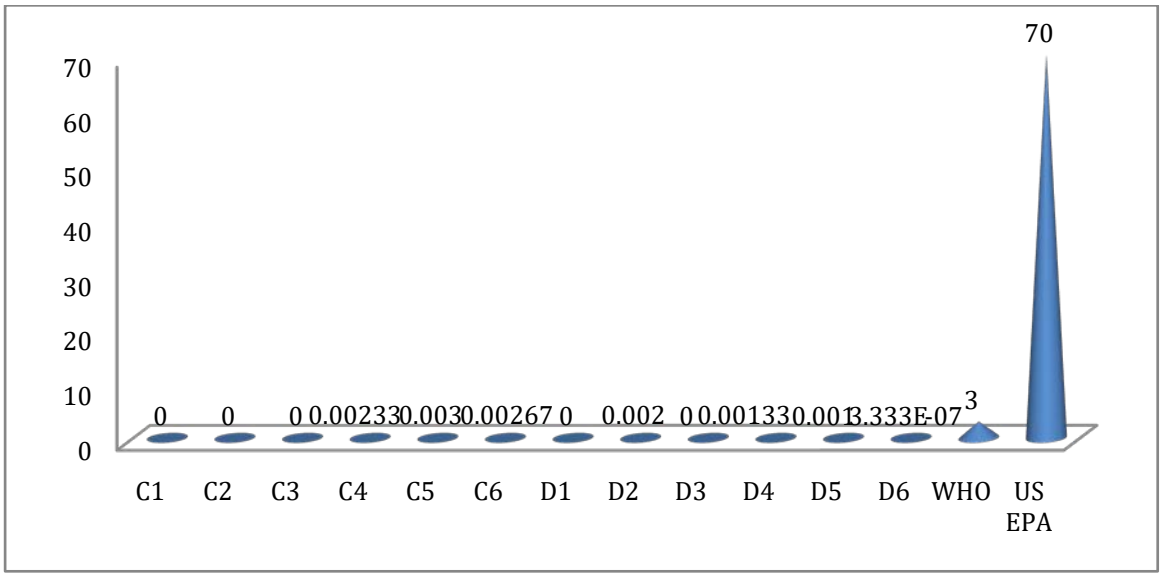

Figure 2.12: Summary of the statistical analysis of Cadmium concentration in the soil samples during dry season

IV. CONCLUSION AND RECOMMEDATIONS

4.1: conclusion

The order of mean concentrations during both seasons was Pb > Cd. In the wet season, mean concentrations (mg/kg) ranged from 0.003 to 0.035 for Pb and from 0.000 to 0.003 for Cd. During the dry season, slightly higher concentrations were observed, with Pb ranging from 0.000 to 0.044 mg/kg and Cd from 0.000 to 0.004 mg/kg. Although the differences between seasons were small, they indicate seasonal variation, with higher dry-season concentrations attributed to reduced dilution during the rainy season, moisture loss through evaporation, and atmospheric dust deposition. All measured concentrations were well below the WHO guideline limits (Pb: 100 mg/kg; Cd: 1–3 mg/kg) and US EPA limits (Pb: 400 mg/kg; Cd: 70 mg/kg). The soils are therefore uncontaminated and safe for farming, residential use, and ecological purposes.

4.2 Recommendations

Routine monitoring of lead and cadmium levels in soils around petroleum exploration sites and waste disposal facilities should be conducted regularly, with special attention during the dry season when metal concentrations tend to increase. Early detection through continuous soil testing will enable timely intervention to prevent contamination and protect soil fertility.

Soil management at petroleum and waste facilities should incorporate climate adaptation measures such as mulching, organic amendments, and controlled irrigation to maintain soil moisture and reduce seasonal spikes in metal concentrations.

Environmental legislation should be strengthened to establish allowable seasonal limits for lead and cadmium in soils near petroleum facilities, waste disposal sites, and adjacent agricultural or residential areas. Mandatory soil testing before, during, and after petroleum operations should be enforced, with designated institutions responsible for compliance and oversight.

Awareness and training programs should be implemented for petroleum workers, waste management personnel, farmers, and surrounding communities on the risks of lead and cadmium contamination, safe handling practices, proper waste disposal, and spill prevention.

4.3: Acknowledgments

I wish to express my sincere gratitude to the State Department for Petroleum, Kenya for their financial support in payment of fees for class work and for soil sampling and laboratory analysis.. I am also deeply thankful to Dr Esther Lesan Kitur for her invaluable guidance and mentorship throughout the course of this work. Her advice, encouragement, and constructive feedback greatly contributed to the successful completion of this study.

REFERENCE

1. Abuzaid, A. S., Al-Qahtani, M. F., & Al-Ghamdi, A. A. (2022). Assessment of heavy metal contamination in soils around petroleum processing plants in Saudi Arabia. *Environmental Monitoring and Assessment, 194*(3), 187.
2. Abuzaid, A. S., Al-Qahtani, M. F., & Al-Ghamdi, A. A. (2022). *Assessment of heavy metal contamination in soils around petroleum processing plants in Saudi Arabia. Environmental Monitoring and Assessment, 194*(3), 187.
3. Brown, R. J., Okoro, S. C., & Adewole, O. O. (2020). Heavy metal distribution in reserve pits around onshore drilling sites in Nigeria. *Journal of Environmental Science and Health, Part A, 55*(10), 1201–1213.
4. Brown, R. J., Okoro, S. C., & Adewole, O. O. (2020). *Heavy metal distribution in reserve pits around onshore drilling sites in Nigeria. Journal of Environmental Science and Health, Part A, 55*(10), 1201–1213.
5. Johnson, T., Khan, A., & Patel, S. (2020). Amplified heavy metal contamination in oil-rich regions: A case study from the Middle East and Africa. *Environmental Pollution, 258*, 113–120.
6. Jones, M., Taylor, K., & Williams, J. (2019). Corrosion in drilling and production: Environmental implications of heavy metal release. *Corrosion Science, 153*, 74–82.
7. Liang, J., Zhang, Y., Wang, X., & Chen, L. (2020). Heavy metal pollution assessment in soils around oil production terminals in Daqing oilfield, China. *Environmental Science and Pollution Research, 27*(5), 5348–5359.
8. Liang, J., Zhang, Y., Wang, X., & Chen, L. (2020). *Heavy metal pollution assessment in soils around oil production terminals in Daqing oilfield, China. Environmental Science and Pollution Research, 27*(5), 5348–5359.

9. Mugendi, C. N., Ndiritu, J. G., & Kuria, Z. N. (2019). Geochemical characterization of drilling mud cuttings and soils from Twiga-1 well, South Lokichar Basin, Kenya. *African Journal of Environmental Science and Technology, 13*(9), 331–340.
10. Pandiyan, K., Singh, S., Prasanna, R., Kaushik, A., & Singh, R. (2021). *Impact of petroleum hydrocarbons on soil biological and chemical properties: A review*. Environmental Technology & Innovation, 23, 101–179.
11. Rozirwan, M., Ali, H., & Zulkifli, S. (2024). Health impacts of lead and cadmium exposure: A review. *Toxicology Reports, 11*, 245–256.
12. Smith, D. L., Johnson, R. E., & Martinez, H. P. (2020). Soil contamination by heavy metals from drilling wastes in Texas oilfields, USA. *Environmental Geochemistry and Health, 42*(12), 4173–4186.
13. Stimmel, J. J., Cullen, M. R., Comeau, M., & Weber, J. (1989). Toxicology of oil field wastes: hazards to livestock associated with the petroleum industry. *Journal of Toxicology and Environmental Health, 28*(4), 455–467
14. Wyszkowski, M., & Kordala, N. (2024). *Effects of humic acids on calorific value and chemical composition of maize biomass in iron-contaminated soil phytostabilisation*. *Energies, 17*(7), 1691.

This page is intentionally left blank

Supplementation of *Tinospora Cordifolia* on Growth Performance, Blood Biochemicals, Antioxidant Status and Histopathology of Hdk – 75 Pigs

Meenakshi Kalita, B. N. Saikia, Gunaram Saikia, Robin Bhuyan, Shantanu Tamuly, Anil Deka, Arundhati Phookan, Lakhyajyoti Bora, Nipu Dekai, Abhijit Deka, S.D. Longjam & Tilling Tayo

ABSTRACT

Scanty information is available about importance of feeding of Tinospora cordifolia on the health and production of livestock. An investigation was conducted to study the effect of different levels of Tinospora cordifolia in HDK – 75 pigs. Twenty Four (24) number of pigs were randomly divided into four groups i.e. Control, T_1, T_2, and T_3 groups containing six (6) animals in each group. The T_1, T_2, and T_3 groups were the treatment groups where the stem of Tinospora cordifolia (Giloy) were dried and in powdered form were given @ the rate of 0.5 %, 1.0 % , 1.5 % respectively mixed with rations. . The experimental rations were prepared according to BIS 1994 during 180 days experimental period. Compared to control and T_1 group, by supplementation of Tinospora cordifolia the average daily body weight gain was seen highest T_3 group ($P<0.01$) followed by T_2 group. The result of serum SOD which shows the antioxidant activity by the end of the experiment reveals that statistically no significant difference ($P > 0.05$) has been seen between the treatment and control groups. Histopathological study and blood parameters shows that supplementation of Tinospora cordifolia does not have any negative effect on liver and kidney. But supplementation of Tinospora cordifolia shows positive changes in T_3 group compared to control group.

Keywords: tinospora cordifolia, hdk-75 pigs, nutrient digestibility, blood biochemicals, antioxidant activity.

Classification: LCC Code: SF98.N87, SF408.P5, SF395

Language: English

Great Britain Journals Press

LJP Copyright ID: 925612
Print ISSN: 2631-8490
Online ISSN: 2631-8504

London Journal of Research in Science: Natural & Formal

Volume 26 | Issue 2 | Compilation 1.0

Supplementation of *Tinospora Cordifolia* on Growth Performance, Blood Biochemicals, Antioxidant Status and Histopathology of Hdk – 75 Pigs

Meenakshi Kalita[α], B. N. Saikia[σ], Gunaram Saikia[ρ], Robin Bhuyan[Ↄ], Shantanu Tamuly[§], Anil Deka[χ], Arundhati Phookan[ν], Lakhyajyoti Bora[Θ], Nipu Dekai[ζ], Abhijit Deka[£], S.D. Longjam[€] & Tilling Tayo[₣]

ABSTRACT

Scanty information is available about importance of feeding of Tinospora cordifolia on the health and production of livestock. An investigation was conducted to study the effect of different levels of Tinospora cordifolia in HDK – 75 pigs. Twenty Four (24) number of pigs were randomly divided into four groups i.e. Control, T_1, T_2, and T_3 groups containing six (6) animals in each group. The T_1, T_2, and T_3 groups were the treatment groups where the stem of Tinospora cordifolia (Giloy) were dried and in powdered form were given @ the rate of 0.5 %, 1.0 % , 1.5 % respectively mixed with rations. . The experimental rations were prepared according to BIS 1994 during 180 days experimental period. Compared to control and T_1 group, by supplementation of Tinospora cordifolia the average daily body weight gain was seen highest T_3 group ($P<0.01$) followed by T_2 group. The result of serum SOD which shows the antioxidant activity by the end of the experiment reveals that statistically no significant difference ($P > 0.05$) has been seen between the treatment and control groups. Histopathological study and blood parameters shows that supplementation of Tinospora cordifolia does not have any negative effect on liver and kidney. But supplementation of Tinospora cordifolia shows positive changes in T_3 group compared to control group.

Keywords: tinospora cordifolia, hdk-75 pigs, nutrient digestibility, blood biochemicals, antioxidant activity.

Author α: Ph.D Student, CVSc, AAU, Ghy-22.
σ: Dean & Professor, Dept of Animal Nutrition, CVSc, AAU, Khanapara, Guwahati - 22.
ρ: Professor, Dept of Animal Nutrition, CVSc, AAU, Khanapara, Guwahati – 22.
Ↄ: Professor & Head, Dept of Animal Nutrition, CVSc, AAU, Khanapara, Guwahati – 22.
§: Assistant Professor, Dept. of Vety. Biochemistry, CVSc, AAU, Khanapara, Guwahati – 22.
χ: Assistant Professor, Dept of Vety. Anatomy and Histology, CVSc, AAU, Khanapara, Guwa/hati – 22.
ν: Assistant Professor, Dept of Animal Genetics and Breeding, CVSc, AAU, Khanapara, Guwahati – 22.
Θ: Assistant Professor, Dept of Animal Nutrition, CVSc, AAU, Khanapara, Guwahati – 22.
ζ: Technical Assistant, ICAR-AICRP, AAU, Khanapara, Guwahati – 22.
£: Assistant Professor, Dept. of Vety. Pathology, CVSc, AAU, Khanapara, Guwahati – 22.
€: Ph.D , Dept of Livestock Production & Management, CVSc, AAU, Khanapara, Guwahati – 22.
₣: Ph.D , Dept of Animal Nutrition, CVSc, AAU, Khanapara, Guwahati – 22.

I. INTRODUCTION

As we all know that there are many therapeutic herbs in India. Assam is the regions with abundant biodiversity that are still perhaps undiscovered. Indigenous people's traditional knowledge regarding cultivated and wild veterinary medicinal herbs has not well documented in the state. Overuse of antibiotics and antibiotic resistance issue has diverted its attention to the use of herbal plants,

London Journal of Research in Science: Natural & Formal

medicinal plants in feed of livestock. Also it has been reported that the use of different herbal extracts in livestock feeding due to its property of improving feed digestibility, feed intake and maintenance of intestinal microbiome which results in improvement of immune system (Lei *et al.*; 2018 , Namkung *et al.*; 2004). One such plant that is found in different parts of Assam is *Tinospora cordifolia* also known as Giloy which is known for its multipurpose effect such as like anti-diabetic, anti-periodic, anti-spasmodic, anti-inflammatory, anti-arthritic, anti-oxidant, anti-allergic, anti-stress, anti-leprotic, anti-malarial, hepatoprotective, immunomodulatory and anti-neoplastic activities. Alkaloids, steroids, diterpenoid lactones, aliphatic and glycosides are just a few of the active ingredients that have been extracted from the plant's various parts, including the root, stem and entire plant (Upadhyay *et al.*; 2010). In Assam, it is locally known as *Saguni Lota* which means plants with more than 100 numbers of properties. There are few reports on the use of feeding of *Tinospora cordifolia* (Giloy) in pig diet.

Tinospora cordifolia (Giloy) is a plant whose all the different parts i.e. leaves, stem, roots are beneficial. In Ayurveda it is known as " AMRITA" which means immortal. In livestock farming, feed is one of the most expensive component which covers the maximum share of the total cost of production. The highest pig population is situated in North East and maximum human population is pork eater. Considering all the above factors regarding the various pharamacological activities of *Tinospora cordifolia* (Giloy), the present study was conducted with an aim of studying the effect of *Tinospora codifolia* stem on growth performance of HDK-75 pigs. The *Tinospora codifolia* supplementation will pave the road as therapeutic supplementation for metabolic alterations in animal body system.

II. MATERIALS AND METHODS

This experiment was conducted in All India Co-ordinated Research Project Khanapara, Guwahati – 22. The study was conducted after approval from the Institutional Animal Ethics Committee (IAEC), AAU, Khanapara, vide approval No. 770/GO/Re/S/03/ CPCSEA/ FVSc/AAU/IAEC/22-23/1025 dated 23.03.2023.

2.1 Animal Distribution, Housing and Management

Thirty (30) number of HDK - 75 (Hampshire desi Khanapara) pigs (Fig 1) with an average body weight 17.26 ± 0.41 kg were selected (Fig 2) after weaning from AICRP on pig, Khanapara, Ghy- 22 which were bred, born and raised at the AICRP pig farm. The pigs were divided into four experimental groups viz., C, T_1, T_2 and T_3 consisting of 6 pigs in each group , considering each pig as a replicate with individual feeding system on body weight basis following Randomized Block Design. The feeding experiment was conducted for 6 months (180 days). The pigs were kept in well ventilated pen.

Fig. 1: HDK-75 Pig

Fig. 2: Taking Body Weight in Pigs

2.2 Experimental Diet

The experimental rations were prepared according to BIS (2001) and presented in Table 1. The four rations comprising of four levels of *Tinospora cordifolia* powder 0% , 0.5%, 1.0% and 1.5% (Table 2).

Table 1: Composition Of Basal Diet (On Dry Matter Basis) For Different Experimental Groups

Ingredients	Quantity (kg)	
	Grower	Finisher
Maize	50	42
Wheat Bran	20	35
De - oiled GNC	20	12
Soyabean Meal	8.5	9
Mineral Mixture	1.0	1.5
Salt	0.5	0.5
Total	100	100

Table 2: Different Levels of *Tinospora Cordifolia* in the Experiemntal Diet (Both Grower & Finisher Stage)

Groups	Experimental Diets
Control (C)	Basal diet
T_1	Basal diet + 0.5 % Giloy Powder
T_2	Basal diet + 1.0 % Giloy Powder
T_3	Basal diet + 1.5 % Giloy Powder

.

The weighed quantity of diets according to the requirement were offered twice daily at 9 AM and 3.30 PM. The feed residue were collected and weighed the next morning daily and weekly interval it was composited to determine the dry matter. Body weight was taken at zero (0), mid and end of the experiment. *Ad libitum* water was given to all animals of each group.

2.3 Collection of Tinospora Cordifolia Stem

The *Tinospora cordifolia* stem (Fig 3) was collected from the area. The stem was dried and make in powder form (Fig 4) and kept in Air tight container. The sample were analyzed for various proximate principles viz., dry matter, organic matter, crude protein, ether extract, crude fibre, total ash and acid insoluble ash (AOAC, 2012). The samples were analyzed for calcium as per method described by Talpatra *et al.* (1940) and inorganic phosphorus as per method of Fiske and Subbarao (1925). The NDF and ADF was analyzed according to Van Soest (1963).

Fig. 3: Stem of *Tinospora cordifolia cordifolia*

Fig 4: After Drying Powder Form of *Tinospora*

2.4 Proximate Analysis of Experimental Diet

The chemical composition of the four experimental rations was analyzed as per AOAC, 2000. The fibre fractions i.e. neutral detergent fibre (NDF) and acid detergent fibre (ADF) were done according to Van Soest 1994.

2.5 Period of the Experiment

The experiment was conducted for the period of 180 days. By the end of the experiment digestibility trial was conducted in all animals for the period of seven (7) days.

2.6 Statistical Analyses

The Experimental design that analysed either by one way or two-way ANOVA followed by multiple comparison using Duncan Multiple Range Test (Duncan, 1955) at 5% level of significance. All the analysis was carried out using the statistical software R (version 4.1.3).

2.7 Parameters to be Studied in Animals

During the experiment fortnightly change in body weight (kg), daily feed intake (kg) of all individuals animals, nutrient utilization were observed. The feed, residue and faeces were collected during the digestibility trial for the proximate analyses and faeces were also collected for microbial count

2.7.1 Blood Biochemicals

Blood was collected at the beginning, mid and at the end of the experiment from all the animals of each group to estimate serum total protein, glucose, Lipid profile (HDL.LDL), Total antioxidant activity and enzyme profile (Serum GGT, BUN, Creatinine). The protein, glucose, BUN was estimated using Aspen Kit, Lipid profile, GGT, Creatinine was estimated by using Accurex Kit, SOD was analyzed using Sigma Aldrich kits All the analyses was done as per the methods recommended by manufacturer.

2.7.2 Antioxidant Activity

Antioxidant activity was determined by SOD (Sodium Oxide Desmutase) estimation. At first, blood was collected in tube containing anticoagulant. They were centrifuge at 2000xg for 15 minutes and plasma was removed. Then 1 ml chilled normal saline solution (0.45 g NaCl in 50 ml distilled water) was added and centrifuged at 2000xg for 5 minutes. The supernatant was discarded and step no 4 to 6 were

repeated for two times. Then normal saline solution was discarded. 100 microliter of RBC pellet was taken out in a glass test tube containing 9.9 ml of distilled water thus making 1% hemolysate. They were then incubated in ice for 30 minutes and the hemolysate was stored in -20°C till further use. Then protein content of hemolysate is determined using the kit Sigma Aldrich and the SOD is expressed as mg/gm of hemolysate protein.

2.8 Histopathology

At the end of the trial five (5) animals from each group were slaughtered for histological and ultrastructural studies. After sacrifice, lymphoid organs *viz.,* spleen, thymus, duodenum, liver and kidney were collected for the histological and ultrastructural studies. After collection, the tissue samples were fixed in 10% neutral buffered formalin. The weight of all the organs were recorded with the help of electronic pan balance. The different biometrical parameters *viz,* the length, breadth and thickness were recorded by Vernier callipers (Mc Cance, 1974). For histological and micrometrical study tissue samples were collected from spleen, thymus, duodenum, liver and kidney from both control and each *Tinospora cordifolia* treatment groups of pigs.. Those samples were processed to prepare paraffin blocks as per the standard method of Luna (1968). The paraffin blocks were sectioned in Shandon Finesse microtome in 5µm thickness and the sections were stained by Mayer's Haematoxylin and Eosin stain as per the procedure of Luna (1968). After staining, histological features of spleen, thymus, duodenum, liver and kidney were observed. Different micrometrical measurement of organs of both the species were recorded on Haematoxylin and eosin-stained section by means of standard method of micrometry using Nikon E 200 camera mounted microscope and Image Pro Express Ver-2.0 Software. For ultra-structural studies, the spleen, thymus and duodenum of Control and T_3 group of pigs were utilized. The tissue samples were processed as per techniques of Parsons *et al.* (1991) and slightly modified by IASST

2.9 Animal Ethics Statement

The study was conducted after approval from the Institutional Animal Ethics Committee (IAEC), AAU, Khanapara, vide approval No. 770/GO/Re/S/03/ CPCSEA/ FVSc/AAU/IAEC/22-23/1025 dated 23.03.2023.

III. RESULTS & DISCUSSION

3.1 Proximate Composition of Feeds

The Chemical compositions of the grower and finisher ration fed to the experimental pigs have been presented in Table 3.

Table 3: Percent Chemical Composition of Experimental Rations used for Entire Feeding Trial

NUTRIENT (%)	GROWER RATION				FINISHER RATION			
	Control	T_1	T_2	T_3	Control	T_1	T_2	T_3
Dry Matter	90.65	90.62	90.68	90.66	90.84	80.82	90.80	90.81
Crude Protein	19.98	19.95	19.96	19.97	18.11	18.15	18.17	18.14
Crude Fiber	4.23	4.25	4.21	4.24	6.12	6.10	6.11	6.13
Ether Extract	3.12	3.11	3.11	3.13	3.89	3.85	3.87	3.88
Nitrogen Free Extract	64.99	65.05	65.07	64.99	63.98	64.00	63.65	63.75
Total Ash	7.68	7.64	7.65	7.67	8.10	7.90	8.20	8.10

Organic Matter	92.32	92.36	92.35	92.33	91.90	92.10	91.80	91.90
Calcium	2.01	1.99	2.03	2.05	1.85	1.87	1.88	1.84
Phosphorous	0.68	0.69	0.67	0.67	0.73	0.71	0.72	0.74
ME (Kcal/kg)*	3750	3750	3769	3753	3692	3692	3690	3693

**Calculated Value*

3.2. Chemical Composition of Tinospora Cordifolia (Giloy) Stem Samples

The chemical composition (DM, CP,CF, EE, TA, calcium and phosphorous) of *Tinospora cordifolia* have been presented in Table: 4. The *Tinospora cordifolia* stem powder contained 25.33 ± 0.09 % dry matter, 8.53 ± 0.03 % crude protein, 16.85±0.00 % crude fiber, 2.49 ± 0.01 % ether extract, 66.85 ± 0.09 % nitrogen free extract, 5.35 ± 0.00 % total ash, 0.68 ± 0.00 % calcium, 0.12 ± 0.00 % phosphorous, 31.20 ± 0.00 % NDF and 20.11 ±0.01 % ADF on the basis of dry matter content.

Table 4: Chemical Composition Of *Tinospora Cordifolia* (Giloy) Used In The Experiment

Attributes	Composition
DM (%)	25.33 ± 0.09
CP (%)	8.53 ± 0.03
EE (%)	2.49 ±0.01
CF (%)	16.85 ± 0.00
TA (%)	5.35 ± 0.00
AIA (%)	1.22 ± 0.00
OM (%)	94.65 ± 0.00
NFE (%)	66.85 ±0.09
NDF (%)	31.20 ± 0.00
ADF (%)	20.11 ± 0.01
CALCIUM (%)	0.68 ± 0.00
PHOSPHOROUS (%)	0.12 ± 0.00

3.3 Body Weight of the Pigs and Feed Intake

The average initial body weight of pigs of C, T_1, T_2 and T_3 were 17.00±0.79 kg, 17.26±0.86 kg, 17.28±0.81 kg and 17.50 ±1.03 kg respectively and average final body weight of pigs of C, T_1, T_2 and T_3 group were 72.67± 1.41 kg, 72.53 ± 1.02 kg, 76.15 ± 0.31 kg and 81.87 ± 0.55 kg respectively (Table 5). In terms of fortnightly body weight gain revealed that highest body weight gain was found in T_3 group and was significant difference was found between between T_3 and Control group. The total gain in body weight in C, T_1, T_2, T_3 were 52.79 ± 0.72 Kg, 53.94 ± 0.74 Kg, 58.15± 0.93 Kg and 64.45± 0.84 kg respectively (Table 5). There was significant difference between T_3, T_2, T_1 and Control group but no significant difference was found between T_1 and Control group. Rate of daily gain was found highest in T_3 group (0.358± 0.00 gm) followed by T_2 group (0.323 ± 0.01 gm), T_1 (0.300 ± 0.00 gm) and Control group (0.293± 0.00 gm.

Table 5: Total and Average Daily Gain in Body Weight, Average Total Feed Intake, Average Feed Conversion Ratio of Pigs in Different Groups During Entire Feeding Trial

Attributes	Groups				Significance
	C	T_1	T_2	T_3	
Initial Body Weight (Kg)	$17.00^{a} \pm 0.79$	$17.26^{a} \pm 0.86$	$17.28^{a} \pm 0.81$	$17.50^{a} \pm 1.03$	P>0.05
Final Body Weight (Kg)	$72.67^{c} \pm 1.41$	$72.53^{c} \pm 1.02$	$76.15^{b} \pm 0.31$	$81.87^{a} \pm 0.55$	P<0.001
Total gain in body weight (Kg)	$52.79^{c} \pm 0.72$	$53.94^{c} \pm 0.74$	$58.15^{b} \pm 0.93$	$64.45^{a} \pm 0.84$	P<0.001
Rate of daily gain (kg/day)	$0.293^{c} \pm 0.00$	$0.300^{c} \pm 0.00$	$0.323^{b} \pm 0.01$	$0.358^{a} \pm 0.00$	P<0.001
Average Total Feed Intake (Kg)	$224.19^{d} \pm 2.69$	$227.52^{c} \pm 2.81$	$231.61^{b} \pm 2.87$	$237.02^{a} \pm 3.01$	P<0.001
Average Feed Conversion Ratio (kg)	$4.41^{a} \pm 0.14$	$4.64^{ab} \pm 0.33$	$4.28^{b} \pm 0.12$	$4.19^{b} \pm 0.29$	

^{abc}*Means with different superscript within the row differ significantly*

The average Total Feed Intake (Table 5) was seen highest in T_3 (237.02 ± 3.01) group supplemented with 1.5 % *Tinospora cordifolia* during the entire feeding trail.The feed conversion ratio (Table 5) observed during the entire feeding trial were 4.41 ± 0.14, 4.64 ± 0.33, 4.28±0.12, 4.19 ± 0.29 in C, T_1, T_2 and T_3 respectively. A significant difference was observed in terms of feed conversion ration between T_3 and control group.

Table 6: Average Digestibility Coeffecient of Dry Matter, Organic Matter, Crude Protein, Crude Fibre, Ether Extract, Nitrogen Free Extract During Digestion Trial

Attributes	C	T_1	T_2	T_3	Significance
Dry Matter Digestibility (%)	$75.46^{c} \pm 0.42$	$75.32^{c} \pm 0.32$	$77.17^{b} \pm 0.33$	$78.36^{a} \pm 0.20$	P<0.001***
Organic Matter Digestibility (%)	$75.49^{c} \pm 0.38$	$76.11^{bc} \pm 0.39$	$77.19^{b} \pm 1.23$	$79.12^{a} \pm 0.57$	P<0.001***
Crude Protein Digestibility (%)	$76.87^{c} \pm 0.38$	$76.96^{c} \pm 0.11$	$78.31^{b} \pm 0.44$	$81.09^{a} \pm 0.44$	P<0.001***
Ether Extract Digestibility (%)	$76.94^{d} \pm 0.02$	$77.09^{c} \pm 0.05$	$78.64^{b} \pm 0.04$	$79.17^{a} \pm 0.01$	P<0.001***
Crude Fibre Digestibility (%)	$63.67^{d} \pm 0.09$	$64.88^{c} \pm 0.05$	$65.85^{b} \pm 0.01$	$67.22^{a} \pm 0.03$	P<0.001***
Nitrogen Free Extract Digestibility (%)	$76.70^{b} \pm 0.27$	$76.63^{b} \pm 0.51$	$77.89^{ab} \pm 0.21$	$79.10^{a} \pm 0.73$	P<0.01**

were found significantly better in T_3, T_2 than control and T_1 group. But there was no significant difference between control and T_1 group. The better digestibility of nutrients was found in group supplemented with *Tinospora cordifolia* @ 1.5 %.

3.3. Blood Biochemicals

The blood biochemical profile comprising of serum total protein, glucose, Lipid profile (HDL.LDL), Total antioxidant activity and enzyme profile (Serum GGT, BUN, Creatinine) were estimated at the 0, mid and end of the experiment and means have been presented in Table 7.

Table 7: Blood Biochemical Parameters of Pig of Different Groups During 0, Mid and End of the Experiment.

Group	Time Interval			P Value
	0	Mid	End	
Serum Protein (G/L)				
C	82.74^{a}±0.30	82.70^{b} ± 0.22	82.65^{c} ± 0.27	P<0.001
T_1	82.78^{a}±0.29	83.04^{b} ± 0.14	83.16^{c} ± 0.10	
T_2	82.81^{a}±0.26	83.90^{a} ± 0.12	83.99^{b} ± 0.25	
T_3	82.56^{a}±0.24	83.84^{a}±0.11	84.62^{a} ± 0.20	
Serum Glucose (mg/dl)				
C	109.87±0.02	110.2^{a}±0.03	110.55^{a} ± 0.16	P<0.001
T_1	109.89±0.03	110.23^{a}±0.02	110.68^{a} ± 0.12	
T_2	109.92±0.10	108.89^{b} ± 0.02	108.10^{b} ± 0.01	
T_3	109.95±0.02	107.95^{c} ± 0.03	106.80^{c} ± 0.06	
Serum HDL (mg/dl)				
C	55.35±0.26	55.49^{b} ± 0.30	55.56^{b} ± 0.34	P<0.001
T_1	55.98±0.13	55.84^{b} ± 0.31	55.7^{b} ± 0.23	
T_2	55.63±0.31	56.05^{b} ± 0.19	56.97^{a} ± 0.28	
T_3	56.05±0.22	56.83^{a} ± 0.13	57.26^{a} ± 0.13	
Serum LDL (mg/dl)				
C	20.45±0.04	20.53^{a} ± 0.08	20.70^{a} ± 0.08	P<0.001
T_1	20.4±0.03	20.57^{a} ± 0.03	20.7^{a} ± 0.09	
T_2	20.5±0.09	19.99^{b} ± 0.08	19.68^{b} ± 0.03	
T_3	20.48±0.07	19.56^{c} ± 0.05	18.98^{c} ± 0.05	
Serum BUN (mg/dl)				
C	16.56±0.01	16.55±0.01	16.57±0.02	P>0.05
T_1	16.57±0.01	16.54±0.01	16.55±0.04	
T_2	16.55±0.01	16.53±0.01	16.47±0.03	
T_3	16.54±0.01	16.57±0.04	16.6±0.13	
Serum Creatinine (mg/dl)				
C	1.28±0.15	1.37±0.13	1.2±0.08	P>0.05
T_1	1.06±0.03	1.12±0.11	1.2±0.11	
T_2	1.25±0.17	1.26±0.09	1.16±0.08	
T_3	1.2±0.09	1.17±0.08	1.07±0.05	
Serum GGT (U/L)				

C	18.34±0.93	18.53±1.31	17.24±1.16	P>0.05
T_1	17.97±0.93	16.32±1.22	16.69±1.04	
T_2	18.53±0.66	18.16±0.93	17.42±0.96	
T_3	17.79±0.87	17.24±0.79	16.32±0.72	
Serum SOD (unit/mg haemolysate protein)				
C	0.18±0	0.19±0	0.18±0	P>0.05
T_1	0.18±0	0.18±0	0.18±0	
T_2	0.18±0	0.18±0	0.18±0	
T_3	0.19±0	0.18±0	0.18±0	

[abc]Mean with different superscript within the row differ significantly

Statistically non-significant effect (P>0.05) was observed between C and T_1 in respect of serum total protein during the mid of the experiment but significant effect was observed between T_2 and T_3 (P<0.001). By the end of the experiment statistically no effect has been seen in group C and T_1 but significant effect has been observed in T_2 and T_3. Highest serum protein was found in T_3 group (1.5 % *Tinospora cordifolia* powder). By the end of the experiment effect of *Tinospora cordifolia* has been seen maximum in T_3 group in respect of low glucose level. Incase of HDL (High Densisty Lipoprotein) significant effect (P<0.001) was observed between T_3, T_2 and T_1, C group by the end of the experiment and low value of LDL was found in T_3 group followed by T_2 group. But between Control and T_1 group no effect has been seen. In case of serum GGT, serum creatinine and serum blood urea nitrogen (BUN) from Table 7 no effect has been seen between the groups and thus it can be concluded that the liver and kidney does not have any negative effect by feeding of *Tinospora cordifolia*. The result of Serum SOD by the end of the experiment reveals that statistically no significant difference has been seen between the treatment and control groups.

In case of serum protein the result of the present experiment is in agreement with Jain *et al.*, (2020) reported higher values of total protein in geloi at the graded levels and ascorbic acid either alone or in combinations may be due to the antioxidant property of geloi and ascorbic acid which stimuli protein synthesis by bird's enzymatic system. The result of the present experiment is in agreement with Bora *et al.*, (2013) reported that higher level of serum protein when curry leaves was fed at the level of 0.5 % and 1 % to growing pigs. The increased serum level might be the effect of antioxidant property of *Tinospora cordifolia* that prevents oxidative stress and boost the immune system and that helps in better protein digestion that leads to high digestibility. In case of serum glucose he result of the present experiment is in agreement with Njoku *et al.*, (2021) reported reduction in serum glucose of pig when fed with herbal mixture. Lin *et al.*; (2020) also reported that the Serum glucose level concentrations after feeding of Chinese herb feed additive. The anti diabetic property of *Tinospora cordifolia* is due to the presence of phytoconstituent Tinosporaside and Berberine which itself possess anti diabetic property (Upadhyay *et al.*, 2023). The reduction of glucose due to feeding of *Tinospora cordifolia* might be due to hypoglycemic property of *Tinospora cordifolia*. The increase in HDL level due to feeding of *Tinospora cordifolia* might be due to presence of phenolic compounds that stimulate lipid metabolism. The result is in agreement with Yang *et al.* (2019) reported that by feeding black pepper in the diet of fattening pigs significantly increased the HDL and vitamin C levels in the blood serum, enhancing the antioxidant defenses of pigs. The result is in agreement with Elghalid *et al.* (2020) reported that feeding of herbs including carvacol, thymol, mentol, and propylene to rabbit result in increase in HDL level. The result of increase in HDL was due to presence of bioactive and phenolic compound in the herbs that stimulated lipid metabolism in rabbit tissue by increasing the anti oxidative enzymes and preventing the production of specific reactive oxygen species.The positive effect of lowering of LDL by feeding of *Tinospora cordifolia* might be due to the presence of alkaloid known as Berberine. The primary cholesterol-lowering mechanism of BBR is the inhibition of intestinal

absorption by interfering with the cholesterol micellization in the gut and reducing cholesterol absorption and secretion by enterocytes (Li *et al.*, 2011). The low level of LDL might also be due to presence of tannins, terpenoids, and flavonoids content. Terpenoid acts as an intermediate in cholesterol synthesis. It regulates the degradation of HMGCoA reductase activity, which is the main enzyme in cholesterol synthesisThe result is in agreement with Elghalid *et al.*, (2020) where different herbs herbs including carvacol, thymol, mentol, and propylene were fed to rabbits and there was a decrease in total cholesterol, triglycerides and LDL. Mechanism explains that LDL cholesterol was reduced via the stimulation of cellular cholesterol biosynthesis and a decrease in the intestinal absorption of cholesterol. The mechanism of low LDL was the ability of the polyphenolics and flavonoids in each herb to inhibit hepatic 3-hydrxoxy-3-methylglutaryl coenzyme A reductase activity, which is a key regulatory enzyme in the cycle. Later, the receptor responsible for LDL cholesterol enhanced the removal, of LDL from blood circulation by decreasing the serum plasma concentration.The SOD value reveals that *Tinospora cordifolia* due to its anti oxidant property has the ability to scavenge free radicals generated during stress condition in the treatment group and thus there is no significant difference between control and treatment groups. The antioxidant property of *Tinospora cordifolia* is due to the presence of flavonoids and alkaloids such as a choline, tinosporin, isocolumbin, palmatine, tetrahydropalmatine, and magnoflorine present.

3.4. Histology of Different Organs

Table 8: Mean ± Se Per Cent Weights Of Organs Of Control And Treatement Groups (Pig) During The Fedding Trial

GROUP	Control	T_1	T_2	T_3	p Value
Length of the Liver (mm)	27.88 ±0.11	28.03 ± 0.09	28.83 ± 0.60	28.65 ± 0.28	NS
Breadth of the Liver (mm)	17.64 ± 0.02	17.60 ± 0.01	17.67 ± 0.03	17.63 ± 0.03	NS
Thickness of the Liver(mm)	8.67 ± 0.05	8.61 ± 0.01	8.71 ± 0.05	8.71 ± 0.03	NS
Weight of the Liver (kg)	1.03 ± 0.01	1.03 ± 0.02	1.01 ± 0.01	1.03 ± 0.01	NS
Length of the Kidney (mm)	9.73 ± 0.32	9.5 ± 0.29	10.1 ± 0.31	10.97 ± 0.82	NS
Breadth of the Kidney (mm)	3.16 ± 0.06	3.18 ± 0.11	3.24 ± 0.12	3.14 ± 0.15	NS
Thickness of the Kidney (mm)	21.10 ± 0.30	21.4 ± 0.20	21.15 ± 0.37	21.38 ± 0.18	NS
Weight of the Kidney (kg)	0.16 ± 0.00	0.15 ± 0.01	0.16 ± 0.00	0.15 ± 0.00	NS
Length of Spleen (mm)	21.87^{c} ± 0.07	22.17^{c} ± 0.03	22.91^{b} ± 0.02	23.33^{a} ± 0.24	0.23
Breadth of Spleen (mm)	5.37^{a} ± 0.03	22.91^{b} ± 0.02	5.14^{bc} ± 0.05	5.07^{c} ± 0.03	P<0.01
Thickness of Spleen (mm)	6.04^{b} ± 0.06	6.00^{b} ± 0.06	6.29^{a} ± 0.04	6.41^{a} ± 0.05	P<0.01
Weight of Spleen (g)	$1.06^{c\pm}$0.07	1.13^{c}±0.003	1.29^{b}±0.00	1.41^{a} ± 0.00	P<0.001

Length of Thymus (mm)	$135.34^{c} \pm 0.07$	$135.4^{c} \pm 0.01$	$135.52^{b} \pm 0.01$	$135.7^{a} \pm 0.01$	P<0.001
Breadth of Thymus (mm)	$65.08^{c} \pm 0.02$	$65.03^{c} \pm 0.04$	$65.19^{b} \pm 0.02$	$65.3^{a} \pm 0.01$	P<0.001
Thickness of Thymus (mm)	$8.45^{b} \pm 0.02$	$8.45^{b} \pm 0.03$	$8.55^{b} \pm 0.05$	$8.68^{a} \pm 0.02$	P<0.01
Weight of Thymus (g)	$18.05^{c} \pm 0.02$	$18.1^{c} \pm 0.06$	$18.27^{b} \pm 0.04$	$18.44^{a} \pm 0.03$	P<0.001

Table 8 reveals that there was no significant (P>0.05) difference for per cent weights of liver and kidney among different treatment groups. The mean per cent weights of liver under different groups were found as 1.03 ± 0.01, 1.03 ± 0.02, 1.01 ± 0.01, 1.03 ± 0.01 kg for C,T_1,T_2 and T_3 groups, respectively. The mean per cent weights of kidney under different groups were found as 0.16 ± 0.00, 0.15 ± 0.01, 0.16 ± 0.00 and 0.15 ± 0.00 kg for C, T_1, T_2 and T_3 groups, respectively.

Grossly in present study it was found that the spleen of pig was long and narrow, and had a pointed ventral extremity. The border of the spleen was sharp and uniform wide. In cross section it was triangular. The hilus was on a longitudinal crest on the ventral surface. The color of the spleen was bright red but darkened after it was expose to the air. Similar findings were reported by Nickel *et al.* (1979) in Pig. The average length of the spleen of C, T_1, T_2 and T_3 group of rat was 21.87 ± 0.07, 22.17± 0.03, 22.91 ± 0.02 and 23.33 ± 0.24 mm, respectively. The average breadth of spleen of C, T_1, T_2 and T_3 groups of pig was 5.37 ± 0.03, 5.24 ± 0.02, 5.14 ± 0.05 and 5.07± 0.03 mm, respectively. The average thickness of the spleen of C, T_1, T_2 and T_3 groups of pig was 6.04 ± 0.06, 6.00 ± 0.06, 6.29 ± 0.04, and 6.41 ± 0.05mm, respectively. The mean weight of spleen of C, T_1, T_2 and T_3 groups of pig was 1.06 ± 0.07, 1.13±0.003, 1.29 ± 0.00 and 1.41 ± 0.00 kg , respectively. The mean length, diameter, thickness and weight of the spleen of group T_2 and T_3 which was fed Giloy @ 1 % and 1.5 % were significantly higher compared to the T_1 and control group.The thymus of Pig was situated in the pericardial mediastinum anterior to the major vessels and ventral to the base of the heart. These finding was total agreement with the finding of Yugesh *et al.,* (2014) in Pig. The average length of the thymus of C, T_1, T_2 and T_3 groups of pig were 135.34 ± 0.07, 135.4 ± 0.01, 135.52 ± 0.01 and 135.7 ± 0.01 mm, respectively. The average breadth of thymus of C, T_1, T_2 and T_3 groups of pig was 65.08 ± 0.02, 65.03 ± 0.04, 65.19 ± 0.02 and 65.3 ± 0.01 mm, respectively. The average thickness of the thymus of C, T_1, T_2 and T_3 groups of pig were 8.45 ± 0.02, 8.45 ± 0.03, 8.55 ± 0.05 and 8.68 ± 0.02 mm, respectively. The mean weight of thymus C, T_1, T_2 and T_3 groups of pig were 18.05 ± 0.02, 18.1 ± 0.06, and 18.44 ± 0.03 kg, respectively. The mean length, diameter, thickness and weight of the thymus of T_3, T_2 were significantly higher compared to the group C, T_1. The high result was found in T_3 group. In current investigation, it was noticed that the duodenum begins at the pylorus on the right side of the body at the level of the tenth to twelfth intercostal space. Its cranial part ascends caudodorsally along the visceral surface of the liver. It forms the horizontal sigmoid loop just cranial to the right kidney and ends at the cranial flexure of the duodenum. The descending duodenum passes caudally ventral to the right kidney. Similar observation was reported by Nickel *et al.,* (1979) in Pig.

In present investigation, it was found that the lobes of liver divided into left lateral, left medial, right lateral, right medial, quadrate and caudate lobe. The caudate lobe had caudate process. The gall bladder was attached with the quadrate lobe. The diaphragmatic surface of the liver was strongly convex whereas visceral surface of the liver was deeply concave. These findings were in accordance with the findings of Nickel *et al.,* (1979) in Pig. The average length of the liver of C, T_1, T_2 and T_3 groups of pig were 27.88 ± 0.11, 28.03 ± 0.09, 28.83 ± 0.60, 28.65 ± 0.28 cm, respectively. The average breadth of the liver of C, T_1, T_2 and T_3 groups of pig were 17.64 ± 0.02, 17.60 ± 0.01, 17.67 ± 0.03 and 17.63 ± 0.03cm, respectively. The average thickness of the liver of C, T_1, T_2 and T_3 groups of pig were 8.67 ± 0.05, 8.61 ± 0.01, 8.71 ± 0.05 and 8.71 ± 0.03 mm, respectively. In current investigation, it was

observed that the kidney of pig was smooth externally and they were bean-shaped. They were flattened dorsoventrally with slightly pointed poles and may occasionally had shallow grooves (lobulation) on the surface. The hilus of the kidney is located in the middle of the medial border and colour of the kidney is greyish brown, Similar findings were noticed by Nickel *et al.,* (1979) in Pig. The mean (± SE) length, breadth, thickness and weight of kidney of pig of all the groups are presented in Table 8. The average length of the kidney of C, T_1, T_2 and T_3 groups of pig were 9.73 ± 0.32, 9.5 ± 0.29, 210.1 ± 0.31, 10.97 ± 0.82 cm, respectively. The average breadth of the kidney of C, T_1, T_2 and T_3 groups of pig were 3.16 ± 0.06, 3.18 ± 0.11, 3.24 ± 0.12and 3.14 ± 0.15 cm, respectively. The average thickness of the kidney of C, T_1, T_2 and T_3 groups of pig were 21.10 ± 0.30, 21.4 ± 0.20, 21.15 ± 0.37 and 21.38 ± 0.18 mm respectively.

Histologically, the spleen in the present study was found to be encapsulated by a thick connective tissue capsule in all groups of pig. Peri-arterial lymphatic sheath and Splenic nodules were abundant in T_3 group (Fig 1) compared to the C (Fig 2), T_1, T_2 groups of Pig. Splenic nodules were composed of aggregation of the lymphatic tissue along the course of small pulp artery. The germinal center of the splenic nodule was light stained, where the lymphocytes were loosely arranged. Ellipsoids (pericapillary macrophage sheath) were especially large as well as abundant in the marginal zone, the region between the red and white pulp in T_3 (Fig 3) groups compared to the C, T_1, T_2 groups of Pig. The red pulp filled the spaces between the white pulp and trabeculae. The red pulp consisted of pulp arterioles, sheathed capillaries, terminal capillaries, splenic sinusoids as well as splenic cords. The splenic sinusoids were less abundant and poorly developed. Numerous splenic cords were observed between the sinusoids. Similar observations were reported by Shringi *et al.,* (2018) in large white Yorkshire Pig. The thymus of each group of pig found in the current study was encapsulated by thin connective tissue capsule. Medulla contained degenerating thymic epithelium forming the concentric central hyalinization with trapped macrophages known as Hassall's Corpuscles (Cystic & Non-Cystic Type). Few adipocytes were observed within the parenchyma which has been clearly stained with H & E. Densely packed lymphocytes were distinguishable in cortex unlike that of medulla in all groups of Pig. These finding were total agreement with the finding of Yugesh *et al.* (2014) in Pig. Numerous lymphocytes aggregation was found in both cortex and medulla of thymus of T_3 (Fig 5) group as compared to the C (Fig 4) , T_1 and T_2 group of Pig. In present study, the liver was enveloped by the capsule called Glisson's capsule in all groups of pig. The hepatic cells are polyhedral shaped and vacuolated in all groups of pig. Similar findings were observed by Metwally *et al.* (2015) in albino rats. The shaped of the nucleus was larger rounded and stains basophilic, and it was located in the center of the cell. Usually only one central vein is noticed in each lobule. It was found that the hepatic cord, hepatic vein and artery were more prominent in T_3 group of pig compared to the other groups of pig (Fig 7 & 8). In present investigation, the wall of the Duodenum of each group of pig was composed of four layers *viz.,* tunica mucosa, tunica submucosa, tunica muscularis and tunica serosa. Simple columnar epithelium lined the villi of duodenum. It was noticed that the villi and intestinal glands were more prominent in T_3 groups (Fig 6) followed by T_2, T_1, and C groups of pig. The mean (± SE) length of villi of duodenum of pig under different treatment groups are presented in Table 7. The average the length of villi of duodenum of C, T_1, T_2, T_3 groups of layers was 91.90± 0.01, 91.92 ± 0.00, 94.04 ± 0.01, 113.11 ± 0.01 µm respectively. The mean length of villi of duodenum T_3 group of layers were significantly ($P<0.01$) higher as compared to C, T_1, T_2, groups of layers. The average diameter of the crypts of the duodenum of C, T_1, T_2, T_3 group was 57.18± 0.00 µm, 57.15 ± 0.01µm, 56.33 ± 0.39 µm, 56.04 ± 0.01 µm respectively. The mean diameter of the crypts of the duodenum of T_3 treatment group of layers was significantly ($P<0.01$) lower as compared to C, T_1 groups. The kidney of pig was surrounded by a fibrous connective tissue Capsule. The kidney was divided into outer cortex and inner medulla. It was found that the cortex contained the uriniferous tubule and it was composed of both nephron as well as collecting tubules. The nephron and collecting tubules were entirely enveloped by basement membrane which was thickest in

the parietal layer of the Bowman's capsule and in the thin limb of loop of Henle in all groups of pig, in present study (Fig 9 & 10). Similar observations were recorded by Dellmann and Brown (1993) in domestic animals and Beniwal (1995) in camel. The proximal convoluted tubule was lined by simple truncated pyramidal cells with brush border. Similar findings were reported by Dellmann and Brown (1993) in domestic animals.

In the present study ultra structure of lymphoid organ (spleen and thymus), liver, duodenum and kidney of pig feeding trail was done. In present investigation, scanning electron microscopic studies of spleen, thymus, and duodenum of C and T_3 group of Pig was studied. The spleen of both the C and T_3 group of Pig was encapsulated by thick capsule and it contained numerous connective tissue fibers. Sheathed artery was noticed in both the C and T_3 group of Pig. Abundant lymphocytes aggregation was noticed in T_3 treatment group of Pig as compared to the C group of Pig. Each lobe of thymus was covered by thick capsule and it was divided into two parts *viz.,* inner medulla and outer cortex with interlobular connective tissue in both C and T_3 treatment groups of Pig. Smooth T-lymphocytes were observed in both cortex and medulla of thymus of C and T_3 (Fig 11) groups of Pig. A clump of lymphocytes was noticed in medulla of thymus of T_3 (Fig 12) group of Pig. The duodenum of C and T_3 treatment groups of Pigs possessed tall, spatulate villi with horizontally-arranged surface clefts upon which a regular pattern of hexagonal absorptive cells and goblet cell mouths was superimposed. The enterocytes of villi of duodenum of T_3 (Fig 13) groups of layers birds were more prominent than the enterocytes of villi of duodenum of C groups of Pig.

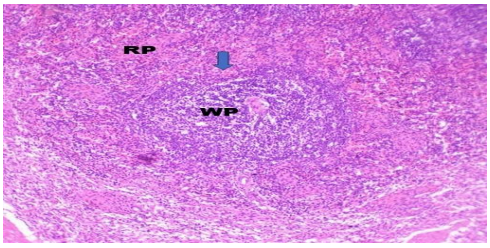

Fig. 1: Photomicrograph Showing The Red Pulp (Rp), White Pulp (Wp) And Marginal Zone (Arrow Head) Of Spleen Of Control Groups Of Pig Under Feeding Trail. H& E, 10x.

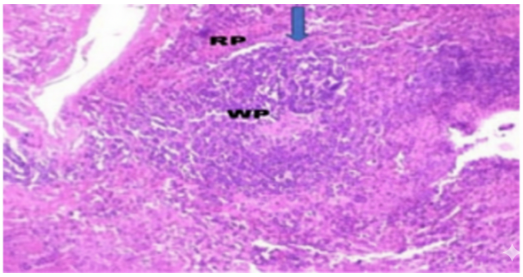

Fig. 2: Photomicrograph Showing The Red Pulp (Rp), White Pulp (Wp) And Marginal Zone (Arrow Head) Of Spleen Of T_3 Treatment Groups Of Pig Under Feeding Trail. H& E, 10x.

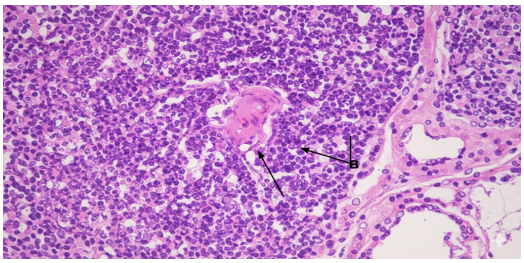

Fig. 3: Photomicrograph Showing The T-Lymphocytes (A) And B-Lymphocytes (B) Of White Pulp Of Spleen Of T_3 Treatment Groups Of Pig Under Feeding Trail. H& E, 40x.

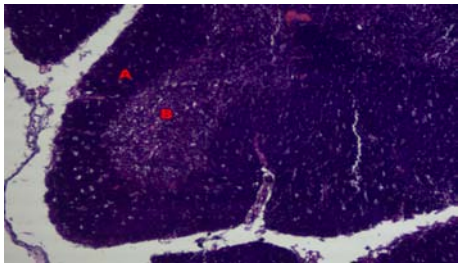

Fig. 4: Photomicrograph Showing The Cortex (A) And Medulla (B) Of Thymus Of Control Groups Of Pig Under Feeding Trail.H&E,10x

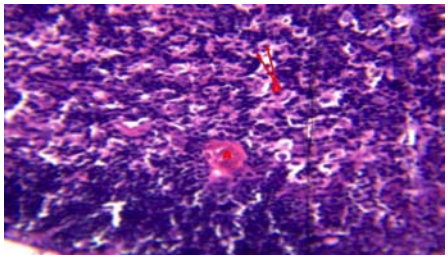

Fig. 5: Photomicrograph Showing The T-Lymphocytes (B) And Hassel's Corpuscles (A) C T_3 Groups Of Pig Under Feeding Trail.H&E,10x.

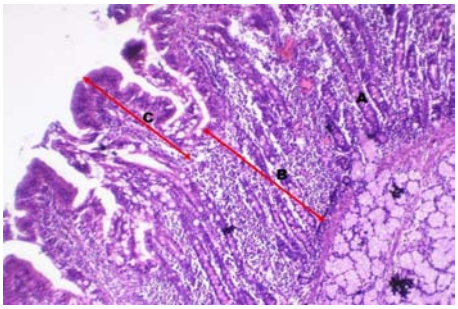

Fig. 6: Photomicrograph Villus Height (C), Crypt Depth (B) And Intestinal Gland (A) Of Duodenum Of T_3 Groups Of Pig Under Feeding Trail. H&E,10x

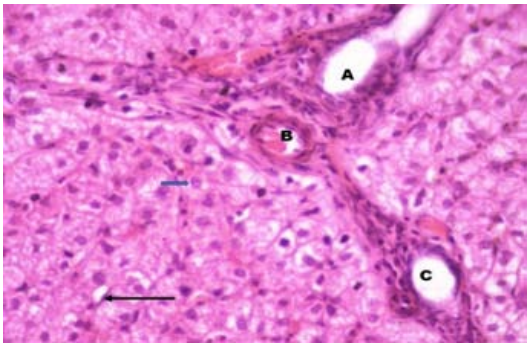

Fig. 7: Photomicrograph Showing The Bile Duct (A), Hepatic Vein (B), Hepatic Artery (C), Kuffer Cell (Arrow) And Nucleus Of Hepatocytes (Arrow Head) Of Liver Of T3 Groups Of Pig Under Feeding H & E, 40x.

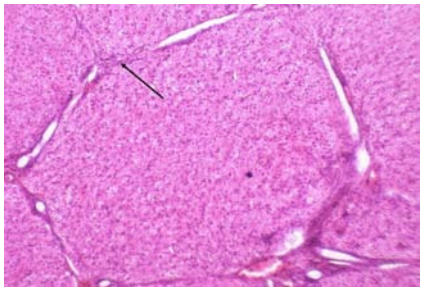

Fig 8: Photomicrograph Showing The Distinct Interlobular Connective Tissue Of Liver Of Control Groups Of Pig Under Feeding Trail. H&E, 10x.

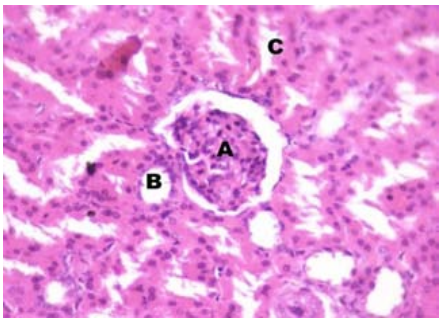

Fig. 9: Photomicrograph Showing The Glomerulus (A), Proximal Convoluted Tubules (C) And Distal Convoluted Tubules (B) Of Kidney Of Control Groups Of Pig Under Feeding Trail. H & E, 40x.

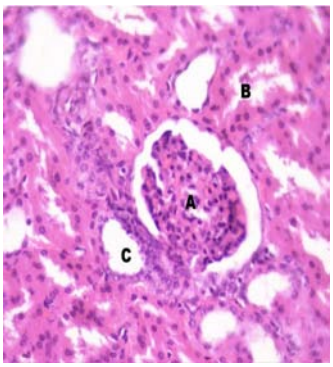

Fig. 10: Photomicrograph Showing The Glomerulus (A), Proximal Convoluted Tubules (B) And Distal Convoluted Tubules (C) Of Kidney Of T_3 Groups Of Pig Under Feeding Trail. H&E,40x.

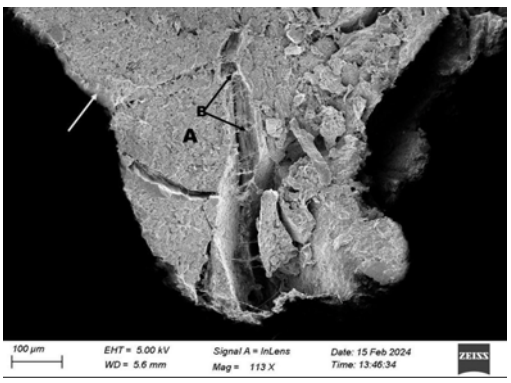

Fig. 11: Scanning Electron Microphotograph Showing The Connective Sheath (Arrow), Lobe (A) And Interlobular Connective Tissue (B) Of Thymus Of Pig Of T_3 Treatment Groups Under Feeding Trail.

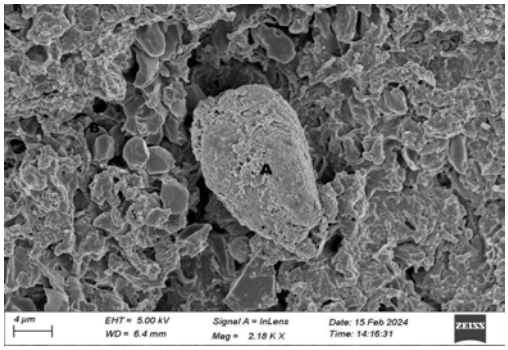

Fig. 12: Scanning Electron Microphotograph Showing The Hassel's Corpuscle (A) And T-] (B) Of Thymus Of Pig Of T_3 Treatment Groups Under Feeding Trail.

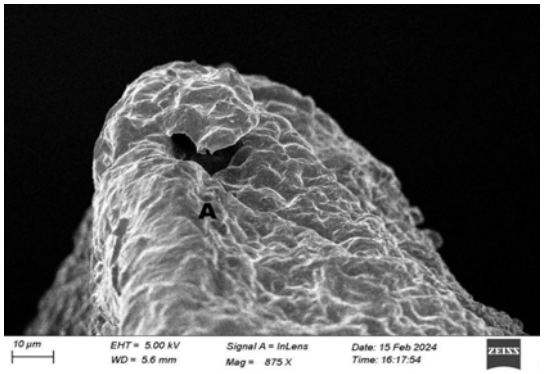

Fig. 13: Scanning Electron Microphotograph Showing The Vilus (A) Of Duodenum Of Pig Of T_3 Treatment Groups Under Feeding Trail.

IV. DISCUSSION

4.1 Chemical Composition of Tinospora Cordifolia (Giloy) Stem Samples

Gitanjali Devi (2020) and Kavya *et al.* (2015) reported that *T. cordifolia* contains with high fibre (15.8%), protein (4.5% - 11.2%), low fat (3.1%) and sufficient calcium (0.131%). In the present investigation the crude protein content, fibre, fat content was comparable with Gitanjali Devi (2020) and Kavya *et al.* (2015).

4.2 Body Weight of the Pigs

The Increase in body weight observed in the present study is in agreement with Singh *et al.* (2018) who observed the effect of *T. cordifolia* on growth might be due to active principles of *Tinospora cordifolia* i.e. *Tinosporine* which limits the metabolic signs of stress and alleviated the physiological consequences of stress. Phytogenic additives has antibacterial, antioxidant, antistress, gut microflora manipulation, immune enhancement properties and digestive enzymes stimulation could be the probable reasons for the positive effects exerted by them on the growth and health performance of animal. In the present study the improvement in the growth of animal might be due to antibacterial and antioxidant property of *Tinospora cordifolia* which improved the gut environment and microflora. The improvement in growth might be due to increase protein digestibility in T_3 group and due to positive development of intestinal structure . The intestinal villi are the main site of nutrient absorption and due to *Tinospora cordifolia* the villi height has increased resulted in higher nutrient absorption and better growth.

4.3 Feed Intake

The results obtained in present study regarding feed intake were in accordance with findings of Singh *et al.* (2009), Kulkarni *et al.* (2011) and Bhushan *et al.* (2013) who reported significant increase in feed intake when broilers were supplemented with *Tinospora cordifolia* stem powder in ration. The increased feed intake in *Tinospora cordifolia* supplemented groups might be due to presence of various bioactive compounds present in *Tinospora cordifolia* stem powder, which might stimulate the digestion system in poultry and improve the function of liver and increase the pancreatic digestive enzymes. Increased feed intake in *Tinospora cordifolia* supplemented groups also gain support with the findings of Kamel (2001) who reported that herbs, spices and various plant extracts have appetite and digestion stimulating properties, and antimicrobial effects. The result of feed conversion ratio in the present study were in agreement of Gupta *et al.*, 2018. The improved FCR might be due to the antibacterial, antistress property of Giloy which has helped in proper development and growth of animal.

4.4 Digestibility of Nutrients

The improvement in digestibility of nutrient due to feeding of *Tinospora cordifolia* in the diet were comparable to Singh *et al.* (2018) findings where feed intake (g/bird), body weight gain (g/b) and FCR showed significant improvement as the level of giloy powder was increased in broiler birds. Singh *et al.* (2008) reported that Dry matter, Percent protein, energy were significantly higher in group supplemented with herbal liver tonic product than control .Jamroz *et al.* (2003) reported that phytogenic feed additives improves the gut microflora modify the digestive secretion, morphology (Peric*et al.*, 2010) .The increase in the digestibility of the nutrients in the present study might be due to the present of flavonoids that stimulate gut activity by improving the digestibility of all nutrients. The herbal plant extracts influence the ether extract but better result was observed in dry form than extract (Dalle *et al.,* 2013). The increase in digestibility might be due to the active constituent present in herbs that can improve the intestinal environment, reduce pathogens, and increase antioxidant activity (Wang *et al.*, 2021). The increase in dry matter digestibility and nitrogen free extract might be due to increase in activity of pancreatic lipase, amylase, trypsin and chymotrypsin (Patel and Srinivasan 2004; Wang *et al.*, 2007). The increase in organic matter digestibility might be due positive effect of herbs which itself is due to its antibacterial and antioxidant property (Thomke 1998; Medel *et al.*, 2002). The increase in crude protein digestibility might be due to increase secretion of digestive juices and improve the gastro intestinal condition. The increase in ether extract digestibility and crude fibre might be due to increase in pancreatic secretion which improves fat and fiber digestibility (Wang and Bourne; 1998). In the present study tannin content of *Tinospora cordifolia* were estimated both qualitatively and quantitatively.

V. CONCLUSION

The knowledge of gross anatomy and histomorphology of lymphoid organs (Spleen and Thymus), liver, kidney and duodenum along with nutrient digestibility and blood parameters give a clear picture regarding effect of feeding *Tinospora cordifolia* (Giloy) in pigs. The results of the nutrient utilization, growth, gross anatomy and histomorphology, blood parameters in the experiment have shown that feeding of *Tinospora cordifolia* (Giloy) @ the rate of 1.5 % has a positive effect on the the growth of pigs and further it also helps to reduce the feed cost in pig feeding. The different pharamacological properties of *Tinospora cordifolia* (Giloy) have helps in showing the positive effect in pigs and thus it gives a clear picture that in the diet of pig feeding *Tinospora cordifolia* (Giloy) helps to maintain the health status of the pigs.

ACKNOWLEDGMENT

The authors would like to thank the Dean, Faculty of Veterinary Science as well as the Directorate of Post Graduate Studies, AAU, Jorhat, for providing the resources to carry out the research work.

Conflicts of Interest

The authors declare no conflicts of interest

Availability of data and materials

Data may be provided following request to the corresponding author.

Disclaimers: The views and conclusions expressed in this article are solely those of the authors and do not necessarily represent the views of their affiliated institutions. The authors are responsible for the accuracy and completeness of the information provided, but do not accept any liability for any direct or indirect losses resulting from the use of this content.

Conflict of interest: The authors declare that there are no conflicts of interest regarding the publication of this article. No funding or sponsorship influenced the design of the study, data collection, analysis, decision to publish, or preparation of the manuscript.

Informed consent

All animal procedures for experiments were approved by the Committee of Experimental Animal care and handling techniques were approved by the University of Animal Care Committee. The study was conducted after approval from the Institutional Animal Ethics Committee (IAEC), AAU, Khanapara, vide approval No. 770/GO/Re/S/03/ CPCSEA/ FVSc/AAU/IAEC/22-23/1025 dated 23.03.2023.

REFERENCE

1. AOAC (2000). ASSOCIATION OF OFFICIAL ANALYSIS CHEMIST. Official Methods of analysis. Gatherburg, M.D. USA; AOAC, International.
2. Beniwal G. Gross and histological studies of the kidney in camel (*Camulus dromedarious*). M.V.Sc. thesis submitted to Rajasthan Agricultural University, Bikaner (Raj.); 1995.
3. Bhushan, S.S.; Ramnivas, Sigh, D.P. and Bisen, B. (2013). Impact of herbal based diets on production efficiency of broiler. *The Bioscan*, **8**(1): 119–22.
4. Bora, M.; Saikia, B.N.; Das, A.K. and Kalita, D. (2013). Dietary Supplementation of Curry (*Murraya koenigii*) Leaf Powder: Effects on Growth Performance, Nutrient Utilisation and Serum Biochemical Parameters in Crossbred Pigs. *Indian J. Anim. Nutr.*, **35** (2): 231-234
5. BIS (1994). Bureau of India standard of pig feeding
6. BIS (2001). Bureau of India standard of pig feeding
7. Dalle, Z. A.; Sartori, P.; Bohatir. (2013). Effect of dietary supplementation of Spirulina (*Arthrospira platensis*) and Thyme (*Thymus vulgaris*) on growth performance, apparent digestibility and health status of companion dwarf rabbits. *Livest. Sci.* 152: 182–191, https://doi.org/10.1016/j. livsci.2012.12.017.
8. Dellmann, H.D. and Brown, E.M. (1993). Textbook of Veterinary Histology. 4th edn., Lea and Febriger, Philadelphia, USA
9. Elghalid, O.A.; Kholif, A.E.; El-Ashry, G.M. (2020). Oral supplementation of the diet of growing rabbits with a newly developed mixture of herbal plants and spices enriched with special extracts and essential oils affects their productive performance and immune status. *Livestock Science,* 238.
10. Gitanjali, Devi (2020). Medicinal Plant : Giloy. *International Journal of Current Research*, 12 (08): 12940-1294.

11. Gupta. T.; Singh. C.; Sahu. M.; Yadav. D. K and Bisht. N. (2018). Effect of dietary Giloy and cinnamon powder incorporation on growth performance and carcass traits in broiler Chickens. *Journal of Entomology and Zoology Studies,* **6**(6): 200-204 .
12. Jain, D.; Dhuria, R. K.; Sharma, T.; **B**othra, T and Prajapat, U. Kumar. (2020). Effect of supplementation of *Tinospora cordifolia* (Thunb.) Miers and ascorbic acid either alone or in combinations on serum protein profile and AG ratio of broiler chickens. *Journal of Entomology and Zoology Studies,* **8**(2): 1760-1763.
13. Jamroz, D.; Orda, J.; Kame, C.; Wiliczkiewicz, A.; Wertelecki, T.; Skorupinska, J. (2003). The influence of phytogenic extracts on performance, nutrient digestibility, carcass characteristics, and gut microbial status in broiler chickens. *Journal of Animal and Feed Sciences*, **12**(3): 583-596
14. Kamel, C. (2001). Tracing methods of action and roles of plant extracts in non-ruminants. In: Recent Advances in Animal Nutrition (eds.). Garns Worthy, P.C. and J. Wiseman, Nottingham, University Press, Nothingham, UK
15. Kavya, B.; Kavya, N.; Ramarao, V. and Venkateshwarlu. G. (2015). *Tinospora cordifolia* (Willd.) Miers. : Nutritional, Ethnomedical and Therapeutic Utility. Review Article. *Tnt.J.Res. Ayurveda Pharm.*, **6** (2), Mar-Apr.
16. Li, G. S., Liu, X. H., Zhu, H., Huang, L., Liu, Y. L., Ma, C. M., & Qin, C. (2011). Berberine improved visceral white adipose tissue insulin resistance associated with altered sterol regulatory element binding proteins, liver X receptors, and peroxisome proliferator activated receptors transcriptional programs in diabetic hamsters. *Biological and Pharmaceutical Bulletin*, **34**(5): 644–654.
17. Lin . Z.; Ye . Li.; Li. Z.; Huang, X.; Lu, Z.; Y, Y.; Xing, H.; Bai, J.; Ying. Z. (2020). Chinese herb feed additives improved the growth performance, meat quality, and nutrient digestibility parameters of pigs. *Animal Model Exp Med.*, 3: 47–54.
18. Kulkarni. R. C.; Mandal. A. and Tyagi. P.K. (2011). Response of coloured broiler to dietary addition of geloi (*Tinospora cardifolia)* during extreme summer. *Indian Journal of Poultry Science*.
19. Njoku, C. P.; Sogunle, O. M.; Adeyemi, O. A.; Irekhore, O. T.; Mobolaji, O. O. and Ayano, O. R. (2021). Influence of different herbal-mix feed additives on serological parameters, tibia bone characteristics and gut morphology of growing pigs. *Folia Veterinaria*, **65** (1): 9-18.
20. Patel, K. and Srinivasan, K. (2004). Digestive stimulant action of spices: a myth or reality?. *The Indian Journal of Medical Research*, **119**: 167-79.
21. Peric, L.; Milosevic, N.; Zikic, D.; Bjedov, S.; Cvetkovic, D. and Steiner, T. (2010). Effect of probiotic and phytogenic products on performance, gut morphology and caecal microflora in broilers chickens. *Archiv Tierzucht.*, **53**(3): 350-359.
22. Lei X.J, Yun H.M, Kim I.H. Effects of dietary supplementation of natural and fermented herbs on growth performance, nutrient digestibility, blood parameters, meat quality and fatty acid composition in growing-finishing pigs. Ital. J. Anim. Sci. 2018;17(4):984–993.
23. Luna, L.G. (1968). Manuals of histological staining methods of Armed forces institute of Pathology, 3rd edn. Mc Graw Hill Book Co., London.
24. Mc Cance, R.A. (1974). The effect of age on the weights and lengths of pigs intestine. *J. Anat.*, **117** (3): 475-479.
25. Metwally. M. A. A.; Abulghasem. E.A. and Naffati. K. M. (2015). Protective Effect of L-ascorbic Acid in Alloxan Diabetic Rats. *Global Veterinaria,* **14**(3): 292-296, 2015.
26. Namkung H, Li J, Gong M, Yu H, Cottrill M, de Lange C.F.M. Impact of feeding blends of organic acids and herbal extracts on growth performance, gut microbiota and digestive function in newly weaned pigs. Can. J. Anim. Sci. 2004;84:697–704.
27. Nickel, R,; Schummer, A. and Seiferle, E. (1979). The viscera of the domestic mammals. 2nd Ed. Verlag Paul Parey, *Berlin Hamburg*, 204-210
28. Parsons, K.R.; Bland, A.P. and Hall, G.A. (1991). Follicle associated epithelium of the gut associated lymphoid tissue of cattle. *Veterinary Pathology*, **28**: 22-29.

29. Singh, V.K.; Chauhan, S.S.; Ravikanth, K.; Maini, S. and Rekhe, D.S. (2009). Effect of dietary supplementation of polyherbal liver stimulant on growth performance and nutrient utilization in broiler chicken. *Vet. World*, **2**(9): 350-352.
30. Singh, S.; Maan, N. S.; Rana, Vinus.; Jyotsana.; Tewatia. B.S. and Nancy, Sheoran. (2018). Effect of dietary inclusion of Giloy (*Tinospora cordifolia*) stem powder on growth performance and metabolizability in broilers. *Journal of Entomology and Zoology Studies,* **6**(5): 36-40.
31. Talapatra, S.K.; Ray, S.C.; Sen, K.C. (1940). The analysis of mineral constituents in biological material. Estimation of phosphorus, chloride, calcium, magnesium, sodium and potassium in food stuffs. *J Vet Sci AH*., **(10)**: 273.
32. Thomke, E. (1998). "Growth Promotants in Feeding Pigs and Poultry. I. Growth and Feed Efficiency Responses to Antibiotic Growth Promotants." *Annales de Zootechnie – Animal Research,* **47** (2): 85–97. doi:10.1051/animres:19980201.
33. Upadhyay AK, Kumar K, Kumar A, Mishra HS. Tinospora cordifolia (Willd.) Hook. f. and Thoms. (Guduchi)-validation of the Ayurvedic pharmacology through experimental and clinical studies. Int J Ayurveda Res. 2010;1:112–21. doi: 10.4103/0974-7788.64405.
34. Van Soest PJ. Nutritional Ecology of the Ruminant. Cornell University, USA, 1994, 476 pp.
35. Wang, J.; Y. Luo, P. Li. (2007). Effect of *Salvia miltiorrhiza* aerial parts on growth performance, nutrient digestibility, and digestive enzymes in rabbits, *Anim. Biosci.*
36. Wang, R.J.; Li, D.F.; Bourne, S. (1998). Can 2000 years of herbal medicine history help us solve problems on the year 2000? Proceedings of Alltech's 14th Annual Symposium. University Press, Nottingham (UK), 273-291.
37. Yang, Y.; Kanev, D.; Nedeva, R.; Jozwik, A.; Rollinger, J. M.; Grzybek, W.; Pyzel, B.; Yeung.; A.W.K.; Uhrin, P., Breuss, J.M.; Horbanczuk, J.O.; Malainer, C.; Xu T.;Wang, D.; Atanasov, A. G. (2019). Black pepper dietary supplementation increases high-density lipoprotein (HDL) levels in pigs. *Current Research in Biotechnology*, **1**: 28-33.
38. Yugesh, K.; Jothi, Dr. S. S. Ranganathan.; Dr. K., Jayaraman. P., Bharath. Chavalin V, N. Sujatha . (2014). Macroscopic and Microscopic study of thymus of pig. OSR Journal of Dental and Medical Sciences (IOSR-JDMS) e-ISSN: 2279-0853, p-ISSN: 2279-0861.Volume 13, Issue 9 Ver. VIII (Sep. 2014), PP 52-55.

There is No Subconsciousness

Volker W. Thürey

ABSTRACT

This paper is based on the idea that all life developed through evolution. I ex amine how evolution could have generated a subconscious mind. I then address several additional topics, such as the sense of responsibility, as well as systems like capitalism and communism.

Keywords: subconsciousness, psychology.

Classification: LCC Code: BF311, BF173, B105.M56

Language: English

Great Britain Journals Press

LJP Copyright ID: 925613
Print ISSN: 2631-8490
Online ISSN: 2631-8504

London Journal of Research in Science: Natural & Formal

Volume 26 | Issue 2 | Compilation 1.0

There is No Subconsciousness

Volker W. Thürey

This paper is based on the idea that all life developed through evolution. I examine how evolution could have generated a subconscious mind. I then address several additional topics, such as the sense of responsibility, as well as systems like capitalism and communism.

Keywords and Phrases: subconsciousness, psychology.

I. INTRODUCTION

At the beginning, I considered titles such as "Freud was an Idiot", "Marx was a Jerk ", "Darwin was a Silly Guy", or "Psychology is Not a Science". I rejected them, but. I believe the chosen title is more suitable. Among other reasons, it contains no swearwords.

The basis for this paper is the belief that life on Earth has developed through evolution. That is Darwin's theory, which is correct. Of course, this cannot be proven, but its consequences are far-reaching. Everything must be compatible with evolution. For example, I do not see how evolution could generate a subconscious mind. In this paper, I also address other topics, such as telepathy.

II. THE TWO SIDES OF EVOLUTION

On one hand, evolution is incredibly creative. It generates complex organs, such as the eye. On the other hand, it operates through competition in which those, who are well-adapted to the environment survive, while others perish.

Evolution proceeds through the death of individuals. This is something Darwin should have recognized as well. Only traits and attributes that aid that survival are preserved. A subconscious mind is not necessary for survival, hence, it may not have been produced by evolution. Freud merely speculated about its existence, nobody can prove it. This raises the possibility that the foundation of psychology may not exist.

I assume that all life forms were generated by evolution. Everything that aided human survival helped human survive and was achievable has been produced by evolution. Traits that did not confer an advantage were not developed. I do not see how a subconscious mind could provide such an advantage. See [1].

Similarly, telepathy has been the subject of much research. I believe it does not exist because evolution did not generate it, even though it could have been useful for hunting. Telepathy is to complex to evolve naturally. Instead, evolution developed speech as a mean of communication.

III. INEQUALITY

Another aspect that many people lament is human inequality.

There are rich people and poor people. This reflects the differences of humans. For example, some individuals are primarily interested in money and power, while others have different interests, such as mathematics. A readable book is 'The Inequality of Man' by Hans Jürgen Eysenck [2], a German-born British psychologist.

One reason for inequality is the low probability of perfect equality. There are many ways in which people can differ, but only one way to be completely equal..

IV. CAPITALISM AND COMMUNISM

Fortunately, we live in capitalistic system. For me, one of its key benefits is the certainty of law. This is important because it allows individuals to conclude contracts. In the case of a violation, society provides mechanism to enforce the contract.

We also enjoy freedom of speech, which is a crucial right and an essential part of the system. Some people advocate for the 'abolition of capitalism', but it is often unclear which system would replace it and what rights people would retain.

A possible alternative is communism, developed by the German philosopher Karl Marx. This economic system does not work, as history has shown often at the cost of millions of lives. Communism is fundamentally flawed because it assumes that most people possess a sense of responsibility for the community. Such a property does not exist, as humans are products of evolution. Humans are individuals, with different opinion, needs, and characteristics. Their personalities are largely determined by their genes, and are fixed. Nobody can change them.

Communism fails because hypothesizes a communal sense of responsibility that is not an inherent human trait. Attempts to implement a communist system, such as Russia, ended in dramatic failure, lasting less than 80 years.

Since humans are products of evolution, there is no natural community of equal individuals. There is no 'we', there is only an 'I'. That said, humans do have the ability to cooperate.

Some claim that the global population will peak at around 10 billion before declining, but I consider this unlikely. Sex is one of the last activities humans would abandon, and it almost always leads to reproduction. As a result, poverty is unlikely to disappear entirely.

It is also argued that a person's bad character is a consequence of specific upbringing. I believe this is not true. Some people naturally desire to dominate others. but they may also possess caring abilities. So far, there is no proof that an ill-natured character can be generated solely by a poor educational background. See [3] and [4] .

V. THE SENSE OF RESPONSIBILITY

People have a sense of responsibility for their children, their parents, and other relatives, and at best, for their friends. These are all people they know personally. They may also feel some responsibility for their larger group, but generally, they do not have a sense of responsibility for all people, only a limited feeling of cohesion within their group. Without a sense of responsibility for all, communism is impossible.

The feeling of cohesion within the group was crucial during the development of mankind. It makes cooperation possible. Cooperation is a very important trait, as it greatly expands the possibilities and potential of an individual .

The arguments presented above reflect my personal opinions and subjective views. They are not presented as absolute truths.

ACKNOWLEDGEMENT

I thank Lydia Ramachandran for a careful reading of the paper.

REFERENCES

[1] Volker Wilhelm Thürey *Evolution Sucks*, London Journal of Research in Science: Natural & Formal, Vol. 25, Iss. 7 (2025)
[2] Hans Jürgen Eysenck *The Inequality of Man* Temple Smith, London (1973)
[3] Volker Wilhelm Thürey *Nature versus Nurture* GLOBAL JOURNAL of Human Social Sciences: C Sociology & Culture, Vol. 25, Iss. 2 (2025)
[4] Volker Wilhelm Thürey *We Don't Need No Education* London Journal of Research in Humanities & Social Sciences, Vol. 23, Iss. 15 (2023)

This page is intentionally left blank

Performance of Cms-Lines, R-Lines, Inbreds, Hybrids and Varieties of Sunflower Genotypes for Drought Tolerant Traits

Thimmappa Krishnappa Nagarathna & Kothathi Shivanna Somashekar

University of Agricultural Sciences

ABSTRACT

Background: Sunflower (Helianthus annuus L.) is a vital oilseed crop known for its adaptability to diverse agro-climatic conditions. Drought stress, however, significantly limits its productivity. Previous studies have highlighted the importance of biomass partitioning and root traits in enhancing drought tolerance. Yet, comparative performance across different genetic groups-cytoplasmic male sterile (CMS) lines, restorer (R) lines, inbreds, hybrids, and varieties- remains underexplored.

Objective: This study aimed to evaluate the drought tolerance potential of 48 sunflower genotypes, hypothesizing that hybrids and select parental lines exhibit superior root and biomass traits under water-limited conditions. The goal was to identify promising genotypes for breeding climate-resilient cultivars.

Methods: A randomized complete block design (RCBD) was employed under controlled drought stress conditions. Eleven morphological and physiological traits were assessed, including root volume, root dry weight, root length, total dry matter (TDM), and specific leaf area (SLA). Statistical analyses included ANOVA for significance testing ($P < 0.05$), principal component analysis (PCA) to identify trait contributions, and biplot analysis for genotype clustering.

Keywords: CMS, drought, hybrids, inbreds, root traits, sunflower, varieties.

Classification: LCC Code: SB255.S86, SB191.S8, S540.S9

Language: English

Great Britain Journals Press

LJP Copyright ID: 925614
Print ISSN: 2631-8490
Online ISSN: 2631-8504

London Journal of Research in Science: Natural & Formal

Volume 26 | Issue 2 | Compilation 1.0

Performance of Cms-Lines, R-Lines, Inbreds, Hybrids and Varieties of Sunflower Genotypes for Drought Tolerant Traits

Thimmappa Krishnappa Nagarathna[α] & Kothathi Shivanna Somashekar[σ*]

ABSTRACT

Background: Sunflower (Helianthus annuus L.) is a vital oilseed crop known for its adaptability to diverse agro-climatic conditions. Drought stress, however, significantly limits its productivity. Previous studies have highlighted the importance of biomass partitioning and root traits in enhancing drought tolerance. Yet, comparative performance across different genetic groups—cytoplasmic male sterile (CMS) lines, restorer (R) lines, inbreds, hybrids, and varieties—remains underexplored.

Objective: This study aimed to evaluate the drought tolerance potential of 48 sunflower genotypes, hypothesizing that hybrids and select parental lines exhibit superior root and biomass traits under water-limited conditions. The goal was to identify promising genotypes for breeding climate-resilient cultivars.

Methods: A randomized complete block design (RCBD) was employed under controlled drought stress conditions. Eleven morphological and physiological traits were assessed, including root volume, root dry weight, root length, total dry matter (TDM), and specific leaf area (SLA). Statistical analyses included ANOVA for significance testing ($P < 0.05$), principal component analysis (PCA) to identify trait contributions, and biplot analysis for genotype clustering.

Results: Significant genotypic variation was observed across all traits. Hybrids consistently outperformed other groups, particularly in TDM and root biomass. CMS-2B, CMS-104A, and IB-80 emerged as top-performing non-hybrids with robust root systems. Hybrids RSFH-1, KBSH-44, and KBSH-55 showed superior drought resilience. PCA revealed that PC1 accounted for 60% of the variance, dominated by TDM, root traits, and plant height, indicating overall plant vigor. PC2 (13.7%) captured the trade-off between leaf efficiency (SLA, SCMR) and structural resilience. Biplot analysis effectively grouped genotypes and highlighted promising paternal lines for drought-prone environments.

Conclusions: The study underscores the value of multivariate analysis in identifying drought-tolerant sunflower genotypes. Hybrids demonstrated superior performance, while select CMS and inbred lines showed potential as breeding resources. These findings contribute to strategic cultivar development for water-limited regions, enhancing sunflower resilience and productivity.

Keywords: CMS, drought, hybrids, inbreds, root traits, sunflower, varieties.

Author α: Ph.D. Professor & Scheme Head, AICRP on Sunflower, University of Agricultural Sciences, GKVK, Bangalore, India- 560065.
σ: Ph.D. Agronomist, AICRP on Sunflower, University of Agricultural Sciences, GKVK, Bangalore India- 560065.

London Journal of Research in Science: Natural & Formal

I. INTRODUCTION

Sunflower (*Helianthus annus* L.) is one of the most important vegetable oilseed crop and is native to southern parts of the USA and Mexico. It is popular due to its high-quality edible oil which is a rich source of edible oil (30-50%), protein (20-30%), tocopherols (vitamin E), and fatty acids. The edible oil contains a good composition of 90% unsaturated fatty acids with linoleic acid (Rauf, 2019). In India, 95 per cent of the total area under sunflower cultivation is confined to rainfed ecosystem during south west monsoon. Among the nine oilseed crops, sunflower stand in front line for cultivation in farming community due to its outstanding characters *viz*., wider adaptability to different agro-climatic zones and soil types, easy crop management, photo-insensitivity, short duration, high seed multiplication ratio and higher oil per cent in the seed. However, the productivity is highly depending on the genetic character of the crop with high phenotypic, genotypic and physiological functions apart from crop production technologies. The major environmental limitation that limits the overall production is inadequate soil moisture. Most of the studies are pertaining to above ground parameters such as physiology of leaf and biochemical composition of leaves, but not the root traits. A few studies available on root studies were mostly confined to early stages (seedling stage and laboratory conditions using small containers).

Physiological attributes of plants depend on improving the drought resistance of crop cultivar that have maximum seed yield, maximum head diameter, maximum physiological adaptability, and high growth rate (Hossain *et al*., 2010). For obtaining higher productivity in sunflower, selection of suitable lines with desirable growth, yield and physiological attributes CMS-lines, R-lines, inbreds, hybrids and varieties of sunflower needs to be evaluated and selected for breeding programme. Most of the studies related to screening of sunflower for drought stress, included one or two varieties or germplasm accessions (Razzaq *et al*., 2017). There is no information on growth, yield and physiological attributes of sunflower genotypes. Therefore, present study emphasis on understanding the physiological mechanism of various sunflower genotypes in field condition.

II. MATERIAL AND METHODS

2.1 Experimental Design and Planting Material

The field experiment was conducted during kharif and rabi seasons of 2022–2023 at Zonal Agricultural Research Station, UAS, Bangalore, using root structures filled with red lateritic soil (pH 6.86; medium N, P, K). A randomized complete block design with three replications was adopted, involving 49 sunflower genotypes including CMS lines, restorers, inbreds, varieties, and hybrids. Farmyard manure (10 t/ha) was incorporated 15 days before sowing. Fertilizer management included 50% N and full P_2O_5 and K_2O as basal (urea, SSP, MOP), with the remaining 50% N top-dressed at 30 DAS during earthing up. The crop was sown in late July and harvested at physiological maturity when capitula were fully dried. Seeds were evaluated under controlled conditions to impose moderate drought stress by withholding irrigation at the vegetative stage. Standard agronomic practices were followed, and data on growth and yield attributes were recorded to assess genotypic performance.

2.2 Trait Measurement

At the flowering stage, plants were carefully uprooted and washed to record root and shoot traits. The root traits included root volume (displacement method, cc plant^{-1}), root dry weight (g plant^{-1}), and root length (cm). Total dry matter (TDM; g plant^{-1}) was determined after oven-drying samples at 70 °C to constant weight. The plant height (cm), leaf area (cm^2) measured using a leaf area meter, and specific leaf area (SLA; cm^2 g^{-1}).

2.3 Statistical Analysis

Descriptive statistics and analysis of variance (ANOVA) were performed to detect significant genotypic differences. To compare groups differing in root length and biomass allocation, Welch's t-test (parametric) and the Mann–Whitney U test (non-parametric) were applied. Effect sizes were calculated using Cohen's d to determine the magnitude of genotypic differences.

2.4 Principal Component Analysis (PCA) and Biplot Visualization

To identify the most influential traits contributing to drought resilience, principal component analysis (PCA) was performed on 10 morpho-physiological variables using the correlation matrix. Eigenvalues greater than one were considered significant, and the first two principal components (PC1 and PC2) were retained for interpretation. Trait–genotype relationships were visualized using biplots, allowing clustering of genotypes based on root and biomass attributes. Genotypes positioned on the positive axis of PC1 and PC2 were considered superior for drought adaptation.

2.5 Statistical Analysis and Software

All statistical analyses were conducted using R software (version 4.1.0), and figures (biplots, scree plots, and trait comparisons) were generated using the ggplot2 package.

III. RESULTS AND DISCUSSION

3.1 Screening of Sunflower Lines for Morpho-Physiological Traits

The studied sunflower genotypes showed clear variation in biomass parameters and root architecture. Key traits such as root volume, root dry weight, root length, and TDM were strongly associated with drought adaptation. Among CMS lines, CMS-2B exhibited the highest root dry weight (28 g pl^{-1}) and root volume (100 cc pl^{-1}), while CMS-104A and CMS-89A also showed strong root biomass (Andrianasolo et al., 2016). CMS-103A and CMS-851A balanced root development with TDM. IB-80, with 100 cc pl^{-1} root volume, 23.84 g pl^{-1} root dry weight, and 138.18 g pl^{-1} TDM, emerged as a strong inbred pre-breeding choice, whereas TNASF-239 and CSF1-99, despite average roots, were efficient in biomass allocation (Umar & Siddiqui, 2018).

Hybrids consistently outperformed other groups in biomass accumulation, reflecting heterosis (Tariq et al., 2018). RSFH-1 showed the highest TDM (249.49 g pl^{-1}) with 137.5 cm^3 pl^{-1} root volume and 40.32 g pl^{-1} root dry weight, while NDSH-1 and SVSH-402 also displayed strong biomass and root traits, making them suitable for drought-resilient breeding (Sarvari et al., 2017).

CMS lines generally recorded the highest mean plant height, leaf area, and TDM, while inbreds had the lowest values; R-lines were intermediate except for root volume, which peaked in this group (67.8 cc pl^{-1}) (Abdel et al., 2021). Variance across CMS, R-lines, and inbreds confirmed distinct genetic potentials, aligning with root volume and weight as indicators of resource allocation under stress (Killi et al., 2017), with strong clustering on PC1 in the biplot (Sacramento et al., 2018).

Group 1 genotypes (high root length and high TDM) significantly outperformed Group 2, with large effect sizes (Cohen's d = 4.46 for root length, 2.16 for TDM) and highly significant differences ($p<0.001$). Results were validated by Welch's t-test and Mann–Whitney U tests, confirming Group 1's superior growth and biomass traits (Tables S1–S3; Figure 1).

Table 1: Welch's t-test (or Mann-Whitney) with Cohen's d + 95 % CI. Group 1: High root length with high TDM; Group 2: Low root length with low TDM.

Variable	Group 1 (n=10) Mean ± SD	Group 2 (n=7) Mean ± SD	Welch t-test p-value	Mann-Whitney U p-value	Cohen's d [95% CI]	Effect Size
Root Length (cm pl^{-1})	50.04 ± 4.59	23.51 ± 7.55	0.000015	0.000743	4.456 [2.518, 6.394]	Large
TDM (g pl^{-1})	141.54 ± 55.04	48.54 ± 9.07	0.000419	0.000755	2.162 [0.847, 3.476]	Large

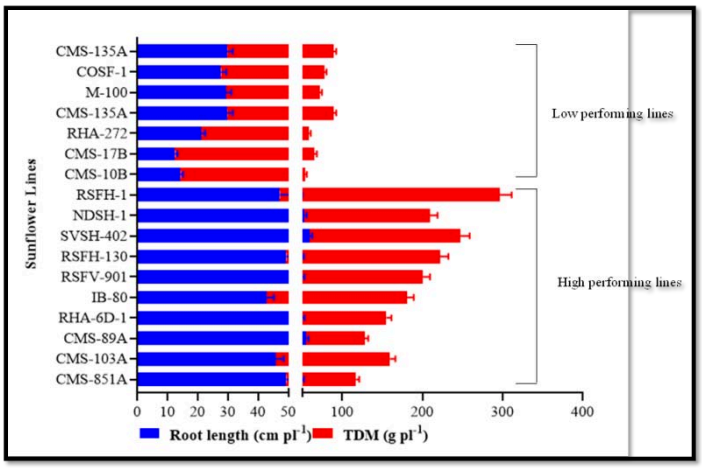

Figure 1: Bargraph showing differences in root dry weight and total dry matter between low and high performing sunflower lines.

3.2 Principle Component Analysis

Principal Component Analysis (PCA) of 48 plant genotypes revealed that PC1 captured 60.0% of the variance, while PC2 explained 13.7%, together accounting for 73.7%. The scree plot confirmed PC1's dominance, indicating a strong underlying factor driving plant variation. PC1, representing general plant vigor, was positively loaded by Total Dry Matter (0.376), Plant Height (0.361), Root Volume (0.356), Leaf Area (0.353), and Root Dry Weight (0.348), while SLA loaded negatively (-0.099). Thus, higher PC1 scores reflected larger, more robust plants with thicker leaves.

PC2 represented leaf efficiency and resource allocation (Sadras & Villalobos, 2021). It showed the strongest positive loading for SLA (0.714) and negative loading for SCMR (-0.497). High PC2 genotypes favored light capture via thin, broad leaves but with lower chlorophyll content (Hussain et al., 2018), whereas low PC2 genotypes emphasized photosynthetic intensity through denser, chlorophyll-rich leaves (Figures 2a–d).

3.3 Biplot Visualization of Root and Leaf Trait Relationships

Significant variability ($P < 0.05$) was observed across genotypes for all recorded traits. High coefficients of variation were noted for root-related traits and TDM, indicating strong genotypic diversity. Among the CMS lines, CMS-2B emerged as a superior genotype with the highest root volume (100 cc pl^{-1}), a root dry weight of 28 g pl^{-1}, and a root length of 41.17 cm, while CMS-104A also exhibited notable root traits with a root volume of 91.67 cc pl^{-1} and a root dry weight of 20.67 g pl^{-1}. CMS-89A and CMS-851A further demonstrated a substantial investment in root dry matter, reinforcing their potential under

drought conditions (Zamani *et al.*, 2020). Among the inbred lines, IB-80 stood out with a robust root system (root volume: 100 cc pl^{-1}; root dry weight: 23.84 g pl^{-1}), making it a valuable candidate for pre-breeding (Soleymani, 2017). The two primary axes of variation in plant genotypes overall plant vigor and leaf resource allocation strategy are successfully identified by this PCA analysis, offering important information for plant breeding programs and a better understanding of the basic trade-offs in plant development strategies (Figure. 2a) (Hussain *et al.*, 2025).

3.4 PCA-Guided Selection of Superior Genotypes for Drought Adaptation

The study revealed significant genotype-to-genotype variability ($P < 0.05$), with high coefficients of variation for TDM and root traits. Among CMS lines, CMS-2B was superior (root volume: 100 cc pl^{-1}; root dry weight: 28 g pl^{-1}; root length: 41.17 cm), followed by CMS-104A (91.67 cc pl^{-1}; 20.67 g pl^{-1}). CMS-89A and CMS-851A also showed strong root investment under drought (Sarwar & Shahbaz, 2020). IB-80, with 100 cc pl^{-1} root volume and 23.84 g pl^{-1} root dry weight, stood out among inbreds as a promising pre-breeding line. PCA indicated that root volume, root dry weight, and TDM were major contributors to PC1, with key genotypes (KBSH-44, RSFH-1, CMS-2B) clustering positively on PC1 and PC2, reflecting co-expression of drought-adaptive traits (Debaeke et al., 2017).

IV. CONCLUSION

This study comprehensively evaluated 48 sunflower genotypes—including CMS lines, restorers, inbreds, hybrids, and varieties—under drought stress across 11 morpho-physiological traits. The findings confirmed that hybrids consistently outperformed other genetic groups in total dry matter (TDM) and root biomass, validating the role of heterosis in drought adaptation. Notably, CMS-2B, CMS-104A, and IB-80 emerged as promising non-hybrid candidates due to their robust root systems, while RSFH-1, KBSH-44, and KBSH-55 stood out as superior hybrids with enhanced TDM and root traits. Principal Component Analysis revealed that PC1, accounting for 60% of the total variance, was driven by plant vigor traits such as TDM, root characteristics, and plant height. PC2 (13.7% variance) highlighted a trade-off between leaf efficiency (SLA) and structural resilience (SCMR, root biomass), offering insights into genotype adaptability. Biplot analysis effectively clustered genotypes and identified potential parental lines suitable for drought-prone environments. Overall, the study demonstrated the effectiveness of multivariate analytical approaches in screening and selecting climate-resilient sunflower cultivars. These insights provide a valuable foundation for breeding programs aimed at enhancing drought tolerance and ensuring sustainable sunflower production under water-limited conditions.

Conflict of Interest statement

The authors declare no conflict of interest

Declaration

Generative AI used only to improve the readability of the text

Funding statement

The study has received funding from RKVY project. Number: ABAC8692

- *Conflict of interest statement and source of funding*
- Authors declare no conflict of interest. The study has received funding from RKVY project
- *Corresponding author's complete contact information*
- Kothathi Shivanna Somashekar, Agronomist, AICRP on Sunflower, University of Agricultural Sciences, GKVK, Bangalore India- 560065

REFERENCES

1. Abdel Razik ES, Alharbi BM, Pirzadah TB, Alnusairi GS, Soliman MH and Hakeem KR 2021. γ-Aminobutyric acid (GABA) mitigates drought and heat stress in sunflower (Helianthus annuus L.) by regulating its physiological, biochemical and molecular pathways. Physiol. Plant. 172(2):505–527.
2. Andrianasolo FN, Casadebaig P, Langlade N, Debaeke P and Maury P 2016. Effects of plant growth stage and leaf aging on the response of transpiration and photosynthesis to water deficit in sunflower. Funct. Plant Biol. 43(8):797–805.
3. Debaeke P, Casadebaig P, Flenet F and Langlade N 2017. Sunflower crop and climate change: vulnerability, adaptation, and mitigation potential from case-studies in Europe. OCL. 24(1):D102.
4. Hussain M, Farooq S, Hasan W, Ul-Allah S, Tanveer M, Farooq M and Nawaz A 2018. Drought stress in sunflower: physiological effects and its management through breeding and agronomic alternatives. Agric. Water Manag. 201:152–166.
5. Hussain S, Khan M, Altaf MT, Shah MN and Alfagham AT 2025. Deciphering the morpho-physiological and biochemical response of sunflower hybrids with biochar and slow-release nitrogen fertilizers under drought stress. Front. Plant Sci. 16:1541123.
6. Killi D, Bussotti F, Raschi A and Haworth M 2017. Adaptation to high temperature mitigates the impact of water deficit during combined heat and drought stress in C3 sunflower and C4 maize varieties. Physiol. Plant. 159(2):130–147.
7. Rauf S 2019. Breeding strategies for sunflower (Helianthus annuus L.) genetic improvement. In: Al-Khayri J, Jain S and Johnson D (eds), Advances in Plant Breeding Strategies: Industrial and Food Crops. Springer, Cham. pp. 637–673.
8. Sacramento BLD, Azevedo ADD, Alves AT, Moura SC and Ribas RF 2018. Photosynthetic parameters as physiological indicators of tolerance to cadmium stress in sunflower lines. Rev. Caatinga. 31(4):907–916.
9. Sadras VO and Villalobos FJ 2021. Physiological characteristics related to yield improvement in sunflower (Helianthus annuus L.). In: Sadras VO and Calderini DF (eds), Genetic Improvement of Field Crops. 2nd ed. CRC Press, Boca Raton. pp. 287–320.
10. Sarvari M, Darvishzadeh R, Najafzadeh R and Maleki H 2017. Physio-biochemical and enzymatic responses of sunflower to drought stress. J. Plant Physiol. Breed. 7(1):105–119.
11. Sarwar Y and Shahbaz M 2020. Modulation in growth, photosynthetic pigments, gas exchange attributes and inorganic ions in sunflower (Helianthus annuus L.) by strigolactones (GR24) achene priming under saline conditions. Pak. J. Bot. 52(1):23–31.
12. Soleymani A 2017. Effect of drought stress on some physiological growth indices of sunflower cultivars. Environ. Stresses Crop Sci. 10(4):505–519.
13. Tariq M, Ahmad S, Fahad S, Abbas G, Hussain S, Fatima Z, et al. 2018. The impact of climate warming and crop management on phenology of sunflower-based cropping systems in Punjab, Pakistan. Agric. For. Meteorol. 256:270–282.
14. Umar M and Siddiqui ZS 2018. Physiological performance of sunflower lines under combined salt and drought stress environment. Acta Bot. Croat. 77(1):36–44.
15. Zamani S, Naderi MR, Soleymani A and Nasiri BM 2020. Sunflower (Helianthus annuus L.) biochemical properties and seed components affected by potassium fertilization under drought conditions. Ecotoxicol. Environ. Saf. 190:110017.

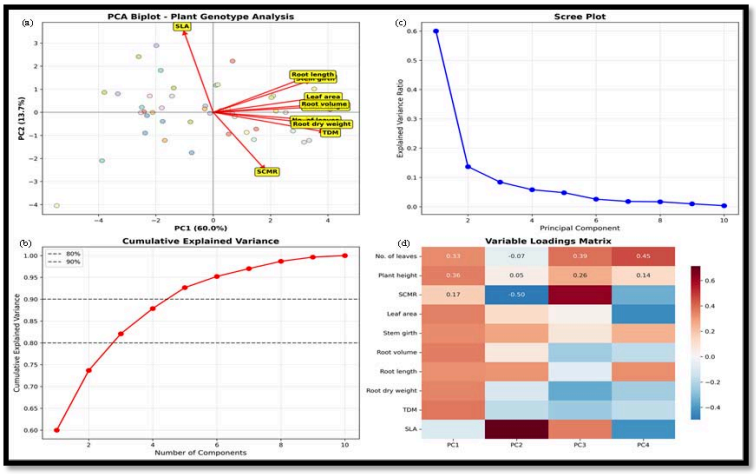

Figure 2: Principle component analysis. (a) PCA Biplot (PC1 vs PC2) showing both variance and trait relationships. (b) Graph showing cumulative explained variance. (c) Scree Plot explaining the proportion of variance (d) Variable loadings on PC1 and PC2 indicating the direction and magnitude of each trait's contribution to the first two principal components.

Supplementary tables

Table S1: Performance of CMS-lines, R-lines, inbreds, varieties and hybrids of sunflower genotypes for drought tolerant traits.

Sl.no.	Genotypes	No. of leaves	Plant height (cm plant^{-1})	SCMR	Leaf area (cm^2 plant^{-1})	Stem girth (cm plant^{-1})	Root volume (cc plant^{-1})	Root length (cm plant^{-1})	Root dry weight (g plant^{-1})	TDM (g pl^{-1})	SLA (cm^2 g^{-1})
CMS-LINES											
1	CMS-2A	17	104.5	32.93	4343	1.68	69.17	36.00	11.50	55.51	321.65
2	CMS- 10 A	25	138.1	29.20	5819	1.85	54.17	36.17	07.49	55.84	459.28
3	CMS-2B	22	141.5	33.30	5882	2.28	100.00	41.17	28.00	92.67	405.57
4	CMS- 10B	24	143.5	32.83	2716	1.08	12.02	14.33	03.83	39.17	150.89
5	CMS-9B	22	144.0	32.05	7676	2.27	91.67	47.67	13.97	87.67	313.34
6	NDCMS-1A	24	143.0	42.68	8548	2.18	81.25	43.50	12.17	92.17	420.36
7	CMS- 17 A	30	167.0	38.02	6492	2.48	87.50	37.67	17.84	116.09	198.72
8	CMS-17B	09	59.0	39.60	1689	0.80	25.00	12.50	05.00	52.50	46.92
9	COSF-1B	20	127.83	31.72	4684	1.40	29.17	27.67	03.84	49.67	453.26
10	CMS-234A	30	153.67	33.77	4270	2.22	66.67	40.33	20.17	85.34	261.4
11	CMS-851A	26	127.5	35.60	4639	2.00	87.50	49.33	21.14	67.83	309.27
12	CMS 335A	20	136.25	33.30	6253	2.43	43.75	34.25	05.17	32.09	646.71
13	CMS-103A	26	127.83	37.47	7954	2.08	82.50	45.67	13.84	113.67	156.48
14	CMS-104A	32	160.17	37.78	7893	2.33	91.67	41.83	20.67	105.00	197.33
15	CMS -135A	24	127.5	31.67	3216	2.00	41.67	29.83	06.17	59.17	283.75
16	CMS 89A	25	137.33	32.72	7784	2.43	95.83	54.67	20.67	73.17	440.53
17	CMS-103B	20	88.83	35.87	5618	1.73	53.33	30.17	08.34	68.84	244.24
18	CMS-104B	29	156.67	40.02	4366	1.80	51.67	37.00	09.17	66.17	174.65

R- LINES											
19	R-64	18	100.00	31.75	5442	1.62	61.67	39.83	07.84	61.84	217.71
20	RCR-1296	20	122.17	34.63	5395	1.72	78.33	30.83	11.00	72.34	283.89
21	NDR-2	22	130.00	37.72	5432	1.57	62.50	30.17	08.34	79.00	250.77
22	RES-834-1	28	155.17	37.52	5342	2.20	62.50	39.83	11.67	75.51	352.19
23	RHA-95-C-1	21	119.50	32.35	3724	2.07	45.83	41.33	04.49	49.91	210.76
24	RHA-6D-1	24	123.00	34.38	5841	2.32	100.00	50.00	14.67	105.00	208.63
25	R-64NB	20	121.50	30.68	5308	2.40	61.67	43.67	06.51	63.34	279.31
26	R-630	22	119.67	36.47	5006	2.42	79.17	38.00	09.17	81.01	224.12
27	GKVK-2	15	93.67	25.55	2005	1.68	45.83	41..00	03.64	42.97	240.63
28	RHA-23	20	131.83	28.98	5399	1.68	45.83	38.00	04.67	52.84	548.77
29	AKSF-I-R-6	19	116.83	35.08	5030	1.67	70.83	35.00	08.17	58.34	443.84
INBREDS											
30	IB-80	27	134.67	29.8	6901	2.13	100	42.67	23.84	138.18	161.12
31	TNASF-23 9	16	105.17	34.00	4979	1.50	65.83	36.33	09.00	66.50	321.28
32	CSF1-99	18	125.83	33.07	4939	1.98	70.83	37.67	05.67	69.09	271.84
VARIETIES											
33	RSFV-901	43	197.67	40.90	7664	2.17	90.00	50.00	21.64	150.47	190.79
34	CO-4	27	174.50	35.83	9718	2.10	112.50	37.83	55.34	229.51	190.55
35	COSFV-5	18	144.00	32.93	5574	1.82	75.00	39.17	09.84	73.18	352.03
HYBRIDS											
36	KBSH 1	29	191.00	38.97	7469	2.95	91.67	46.67	22.99	133.99	257.52
37	KBSH- 41	32	208.33	38.7	9048	2.47	133.33	56.33	20.67	170.67	303.28
38	KBSH-44	33	195.00	37.68	10443	2.78	133.33	49.00	34.84	214.17	173.09
39	KBSH- 53	32	197.50	33.82	10402	2.15	141.67	56.17	39.17	181.84	195.64
40	KBSH- 55	31	198.50	37.3	8540	2.45	125	52.83	48.99	218.15	199.39
41	KBSH-58	28	176.17	32.13	6862	2.48	129.17	47.33	25.17	154.51	267.34
42	TCSH-1	26	151.50	39.6	6484	2.22	129.17	38.33	22.50	147.34	214.92
43	TNAUSF-C O2	22	152.83	34.55	7130	2.28	87.5	37.17	27.51	147.76	259.24
44	RSFH-130	24	164.17	38.48	8383	2.28	141.67	49.33	33.34	172.68	180.94
45	Phule Raviraj	24	161.67	35	10681	2.37	104.17	41.83	29.65	153.49	333.74
46	SVSH-402	29	176.50	36.85	6494	2.83	95.83	59.00	37.84	188.5	163.02
47	NDSH-1	31	177.17	34.87	8233	2.60	195.83	52.50	23.64	156.81	308.71
48	PKSVSH-9 52	25	154.33	32.73	7286	2.50	129.17	41.33	42.50	167.67	231.32
49	RSFH-1	22	140.83	35.28	11002	2.72	137.5	47.17	40.32	249.49	126.22
SEm±		**0.99**	**5.84**	**2.81**	**946**	**0.19**	**15.94**	**3.33**	**2.16**	**11.06**	**18.70**
CD @ 5%		**2.81**	**16.52**	**7.96**	**2679**	**0.56**	**45.11**	**9.44**	**6.10**	**31.30**	**52.92**
CV (%)		**5.26**	**5.27**	**11.4**	**19.88**	**12.19**	**26.03**	**10.31**	**17.56**	**14.64**	**17.16**

Table S2: The range and mean values for CMS lines, R-lines and inbreds.

Traits	CMS -Lines		R -Lines		Inbreds	
	Range	Mean	Range	Mean	Range	Mean
No. of leaves plant^{-1}	9.0-32.0	23.0	15-28	20.00	14-27	18.00
Plant height (cm plant^{-1})	59-167	132.5	93.7-155.2	119.90	97-134.7	115.67
Leaf area (cm^2 plant^{-1})	1689.1-8548.1	5547.2	2005.6-5841.7	4902.80	4939.4-6901.6	5606.94
SLA (cm^2 plant^{-1})	46.9-646.71	304.6	208.6-548.7	296.40	161.10-321.30	251.41
SCMR	29.2-42.7	35.0	25.5-37.7	33.50	18.50-34.00	28.80
Stem girth (cm plant^{-1})	0.8-2.48	1.95	1.48-2.42	1.90	1.38-2.10	1.75
Root volume (cc plant^{-1})	25-100	67.8	40.83-100	62.92	57.50-100	73.50
Root length (cm plant^{-1})	12.5-54.7	36.65	21.17-50	37.40	29.30-42.70	36.50
Root dry weight (g plant^{-1})	3.8-28.0	12.72	3.64-14.67	7.87	4.80-23.80	10.80
Total dry matter (g plant^{-1})	32.1-116.1	109.5	37.2-105.0	64.95	42.84-138.18	79.15

Table S3: Classification of genotypes based on TDM and root length as high and low types.

High root length with high TDM			Low root length with low TDM		
Genotypes	Root length (cm plant^{-1})	TDM (g plant^{-1})	Genotypes	Root length (cm plant^{-1})	TDM (g plant^{-1})
CMS-851A	49.3	67.8	CMS-10B	14.3	39.2
CMS-103A	45.7	113.7	CMS-17B	12.5	52.5
CMS-89A	54.7	73.2	RHA-272	21.2	37.2
RHA-6D-1	50.0	105.0	CMS-135A	29.8	59.2
IB-80	42.7	138.2	M-100	29.3	42.8
RSFV-901	50.0	150.5	COSF-1	27.7	49.7
RSFH-130	49.3	172.7	CMS-135A	29.8	59.2
SVSH-402	59.0	188.5			
NDSH-1	52.5	156.8			
RSFH-1	47.2	249.0			

Supplementary figures

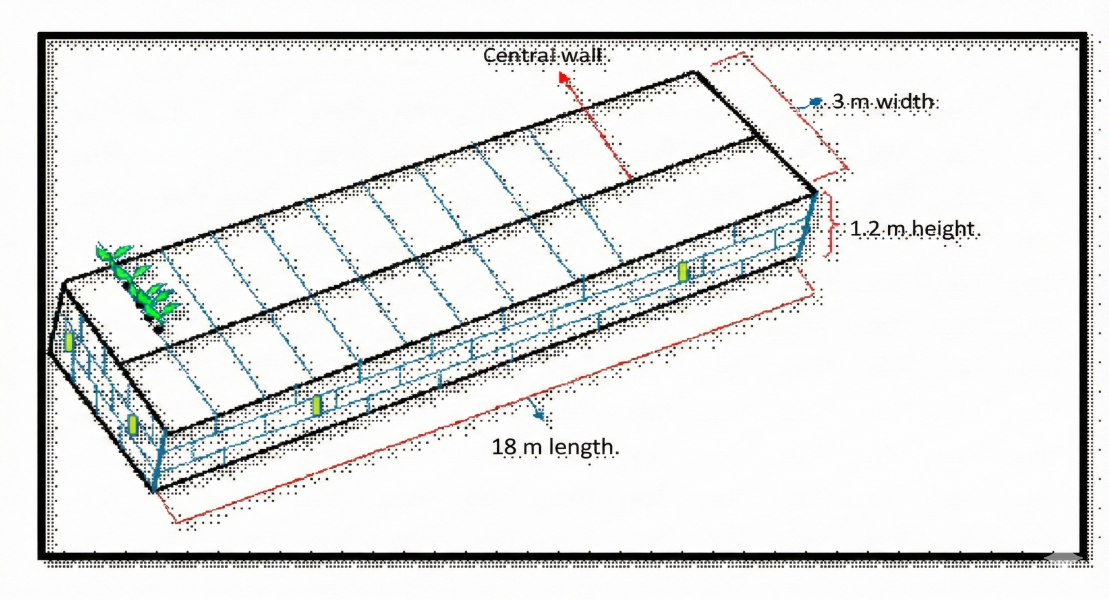

Figure S1: Diagrammatic representation of the construction of temporary cement root structure

Overview of Co_2 Emissions in Yemen with Predictive Models of Emission Reduction Beyond 2025 -Based Multi Dimensional Criteria

Abobakr Alsufyani

King Saud University KSA

ABSTRACT

This study investigates Yemen's current carbon emission trends and explores strategic pathways for achieving significant reductions by 2050., the paper identifies challenges in the energy, transport, and industrial sectors while proposing a multi-phase strategy for low-carbon transition. The results suggest that implementing renewable energy initiatives and policy reforms could reduce Yemen's emissions , emission trends was simulated under multi objectives effective parameters to predict emission adoption scenarios., a predicting model have been created linking renewable capacity expansion to emission reduction Focused primarily on projections; limited policy evaluation.

The primary objective of this modeling study is to assess the relationship between renewable energy expansion mainaly and carbon emissions in Yemen from 1990 to 2035, under different socio-economic and policy-driven scenarios. The research aims to identify the most effective pathways for achieving low-carbon growth in a fragile, conflict-affected context. a review of historical research on renewable energy and carbon emissions in Yemen from 1990 to 2025.

Keywords: renewable energy, carbon emissions, yemen, energy transition, sustainability, literature review, prediction beyond 2025, modelling, environment,..

Classification: LCC Code: TD885.5.C3, HD9502.Y45, QC981.8.C5

Language: English

Great Britain Journals Press

LJP Copyright ID: 925615
Print ISSN: 2631-8490
Online ISSN: 2631-8504

London Journal of Research in Science: Natural & Formal

Volume 26 | Issue 2 | Compilation 1.0

Overview of Co_2 Emissions in Yemen with Predictive Models of Emission Reduction Beyond 2025 -Based Multi Dimensional Criteria

Abobakr Alsufyani

ABSTRACT

This study investigates Yemen's current carbon emission trends and explores strategic pathways for achieving significant reductions by 2050., the paper identifies challenges in the energy, transport, and industrial sectors while proposing a multi-phase strategy for low-carbon transition. The results suggest that implementing renewable energy initiatives and policy reforms could reduce Yemen's emissions , emission trends was simulated under multi objectives effective parameters to predict emission adoption scenarios., a predicting model have been created linking renewable capacity expansion to emission reduction Focused primarily on projections; limited policy evaluation.

The primary objective of this modeling study is to assess the relationship between renewable energy expansion mainaly and carbon emissions in Yemen from 1990 to 2035, under different socio-economic and policy-driven scenarios. The research aims to identify the most effective pathways for achieving low-carbon growth in a fragile, conflict-affected context. a review of historical research on renewable energy and carbon emissions in Yemen from 1990 to 2025. Despite the global shift toward renewable energy, Yemen remains highly dependent on fossil fuels, which has led to rising CO_2 emissions and increasing energy insecurity. The review synthesizes key studies addressing Yemen's energy transition, renewable deployment, and emission trends, highlighting the progress, limitations, and existing research gaps that justify future modeling-based investigations. The reviewfinds that while several works discuss renewable potentials and policy frameworks, few studies quantitatively analyze carbon-emission reduction under renewable energy expansion scenarios. This study provides a quantitative modeling framework for assessing the relationship between renewable energy expansion and carbon emission reduction in Yemen. Historical analysis (1990–2025) shows consistent emission growth driven by economic and demographic pressures. Simulation results for 2026–2035 confirm that renewable energy adoption—particularly under the High RE Scenario—could substantially reduce national emissions and foster sustainable economic recovery.

Keywords: renewable energy, carbon emissions, yemen, energy transition, sustainability, literature review, prediction beyond 2025, modelling, environment,.

Author: PhD - Industrial And Manufacturing System Engineering, King Saud University KSA.

I. INTRODUCTION

Yemen's contribution to global greenhouse gas (GHG) emissions is relatively small compared to industrialized nations. However, its vulnerability to climate change impacts, including rising temperatures, desertification, and water scarcity, makes emission reduction a critical national objective. The country's energy sector remains the dominant source of emissions, driven by oil combustion for electricity generation, transport, and industry. Since 2015, Yemen's economic instability and conflict have delayed implementation of sustainable energy policies. Nevertheless,

London Journal of Research in Science: Natural & Formal

through initiatives such as the UNDP's 'Renewable Energy for Resilience' program, the nation has begun developing solar microgrids and exploring decentralized power generation. This paper explores the mechanisms required to institutionalize these initiatives into a national decarbonization framework. The primary objective of this modeling study is to assess the relationship between renewable energy expansion and carbon emissions in Yemen from 1990 to 2035, under different socio-economic and policy-driven scenarios. The research aims to identify the most effective pathways for achieving low-carbon growth in a fragile, conflict-affected context. Yemen faces a dual challenge of severe energy insecurity and rising environmental degradation. Fossil fuels—particularly diesel and heavy fuel oil—remain the dominant energy sources, contributing significantly to carbon dioxide (CO_2) emissions and air pollution. However, the ongoing conflict and fuel shortages have accelerated the adoption of small-scale solar photovoltaic (PV) systems in urban and rural areas. Despite this shift, there has been no comprehensive quantitative assessment of how renewable energy expansion has influenced or could influence national carbon emissions in Yemen. Globally, numerous studies have demonstrated the strong negative correlation between renewable energy use and CO_2 emissions. Yet, Yemen lacks empirical and simulation-based evidence linking its renewable energy transition to measurable carbon reduction. Understanding this relationship is critical for developing a low-carbon national energy strategy aligned with Yemen's climate commitments under the Paris Agreement and its Nationally Determined Contributions (NDCs).

The Specific objectives include:

1. Quantify the historical and projected relationship between renewable energy growth and CO_2 emissions in Yemen.
2. Evaluate the influence of economic growth, fossil fuel use, and social development on carbon intensity.
3. Develop and validate simulation models (1990–2035) to predict emissions under multiple renewable adoption scenarios.
4. Analyze sensitivity of model outcomes to variations in renewable capacity, conflict intensity, and GDP growth.
5. Provide evidence-based recommendations for sustainable energy policy in Yemen.

1.1 Yemen's Current Emission Profile

The energy sector is responsible for nearly two-thirds of Yemen's CO_2 emissions. Transportation contributes about 25%, followed by manufacturing and agriculture. Table 1 outlines the sectoral distribution for 2024 based on UNDP data.

1.1.1 CO_2 Emissions by Sector

The chart illustrates the distribution of CO_2 emissions by sector in Yemen for the year 2024, as estimated by the UNDP. It reveals that the Energy sector is the dominant contributor, producing approximately 30 $MtCO_2$, followed by Transport at 12 $MtCO_2$. The Industry, Agriculture, and Waste sectors contribute 8 $MtCO_2$, 5 $MtCO_2$, and 2 $MtCO_2$ respectively. This indicates that the combined emissions from Energy and Transport account for nearly 70% of Yemen's total CO_2 emissions.

The Energy sector's high share of emissions stems largely from Yemen's dependence on fossil fuels for electricity generation, industrial energy use, and household consumption. Limited renewable energy infrastructure and inefficient power generation systems have further amplified emissions. Meanwhile, the Transport sector's significant contribution is mainly due to the widespread use of diesel and petrol vehicles, poor fuel quality, and the lack of public transport systems.

Addressing emissions in these two key sectors is therefore essential for Yemen's climate strategy. Focusing on sustainable energy generation and low-carbon transport solutions will not only reduce greenhouse gas emissions but also improve energy security and air quality.

Table 1: Sectoral CO_2 emission breakdown in Yemen (2024).

Sector	CO_2 Emission ($MtCO_2$)	Percentage Share (%)
Energy	30	58
Transport	12	23
Industry	8	12
Agriculture	5	5
Waste	2	2

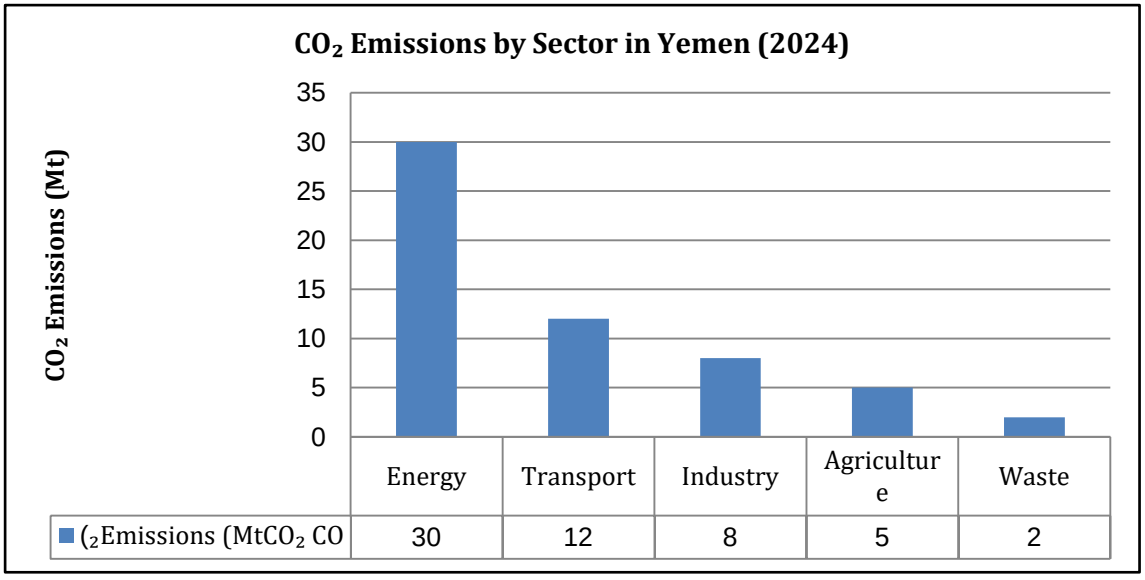

Figure 2: Sectoral distribution of CO_2 emissions in Yemen as per 2024 UNDP estimates.

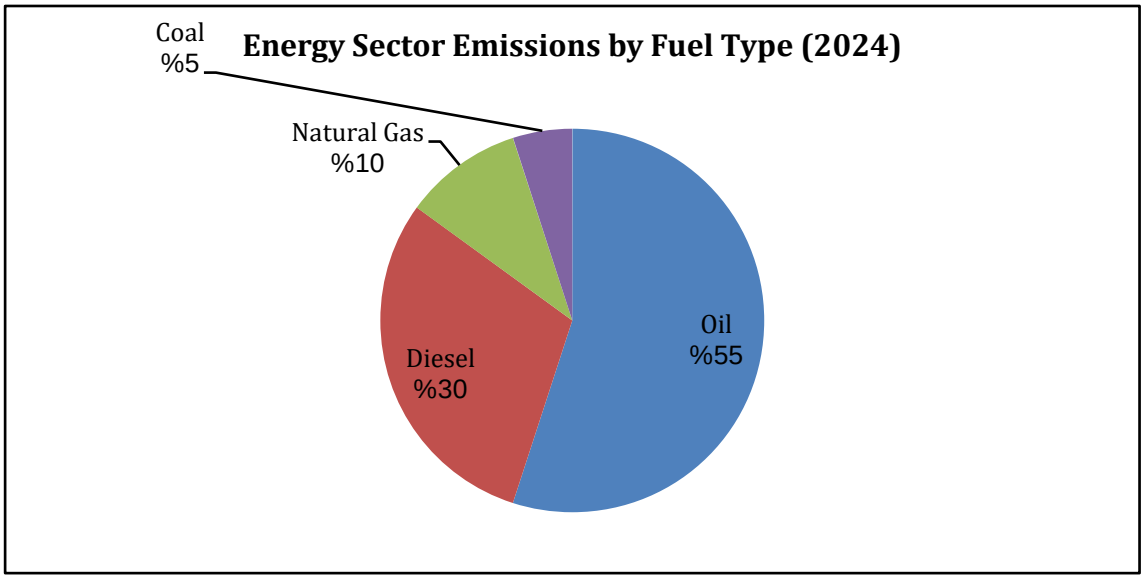

Figure 3: Energy Sector Emissions by Fuel Type (2024)

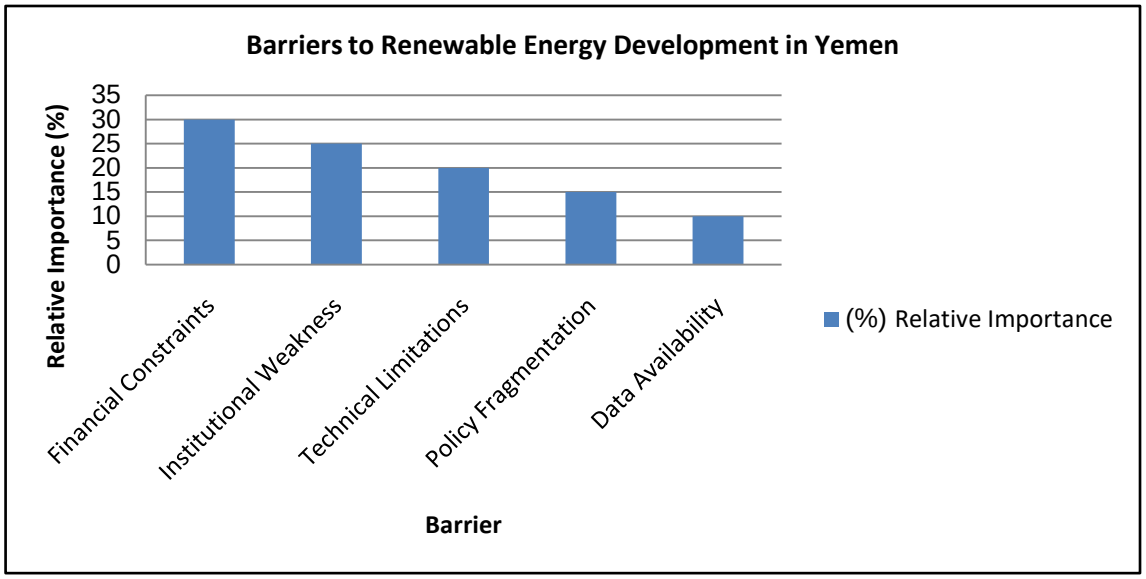

Figure 4: Barriers to Renewable Energy Development in Yemen

1.1.2 Historical Emission Trends (1990–2025) In Yemen

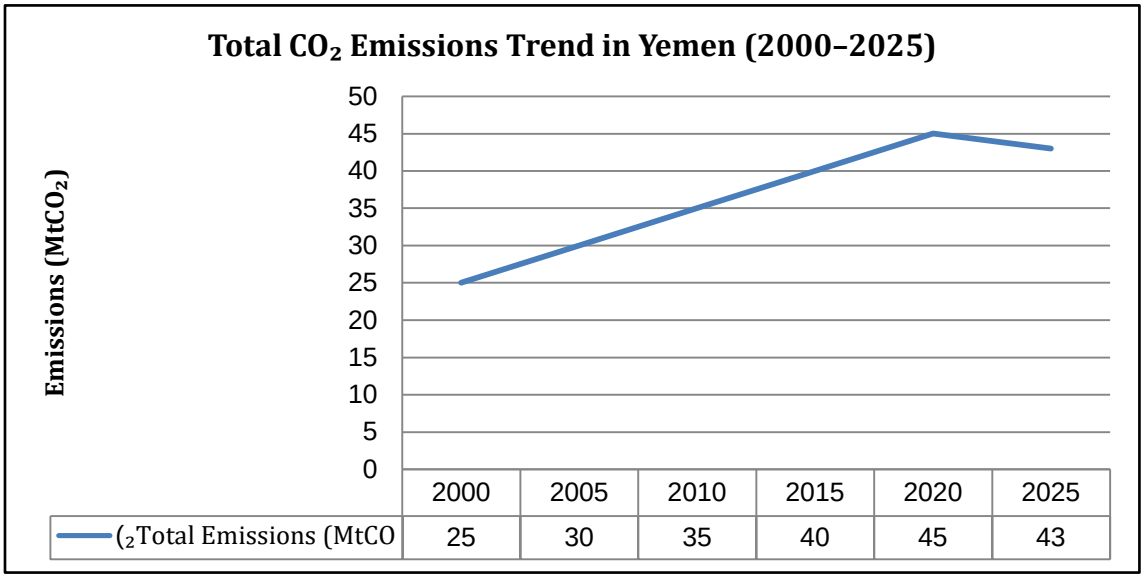

Figure 5: Barriers to Renewable Energy Development in Yemen

Between 1990 and 2025, Yemen's CO_2 emissions were estimated to have grown from 4.8 Mt to approximately 22.4 Mt, representing an average annual increase of 3.6%. This growth corresponds closely with rising fossil fuel consumption and limited renewable adoption (less than 2% of total capacity). Despite international development programs, progress remained modest due to conflict related infrastructure disruption and policy fragmentation.

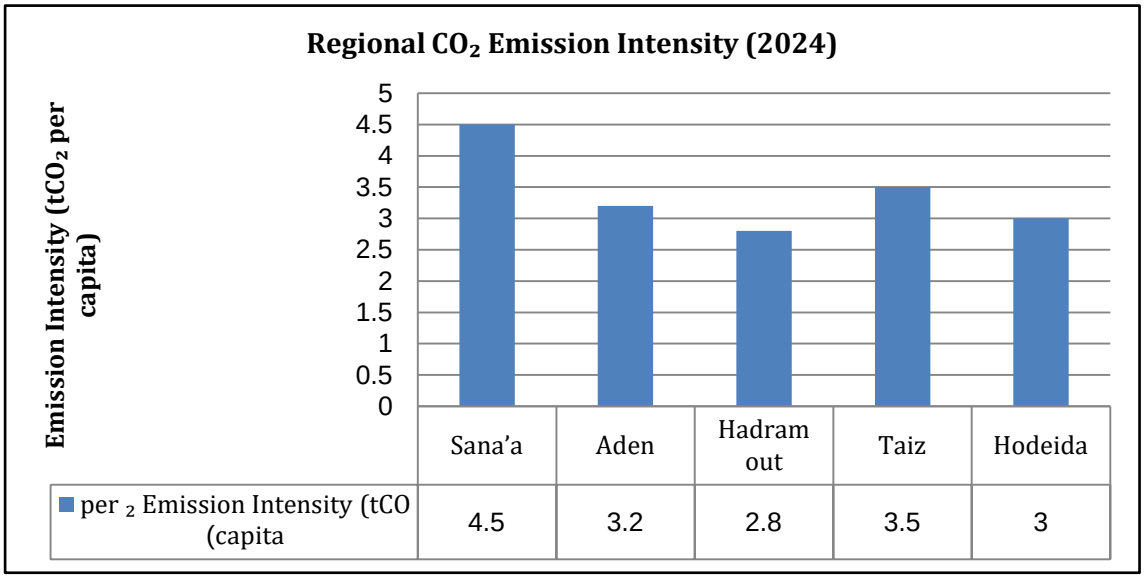

Figure 6: Regional CO_2 Emission Intensity (2024)

1.1.3 Comparative Discussion with Regional Cases

Comparing Yemen's renewable development to other MENA countries provides perspective on feasible policy frameworks. Countries like Morocco and Egypt have achieved rapid renewable integration through policy stability, independent power producer (IPP) models, and long-term investment partnerships.

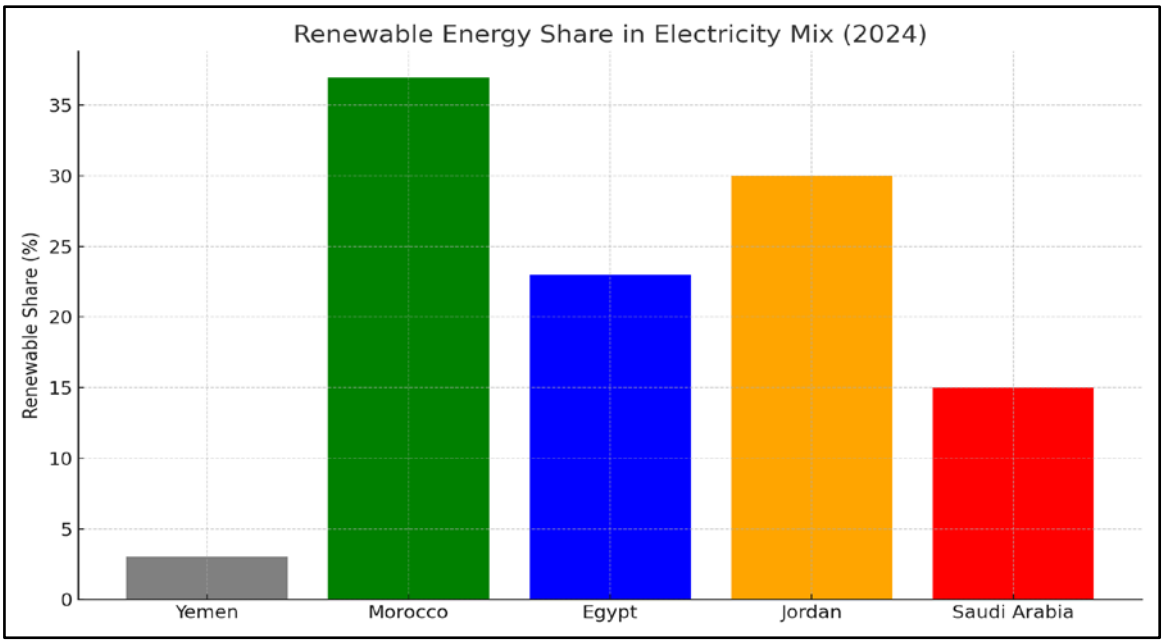

Figure 7: compares Yemen's renewable progress with selected MENA countries.

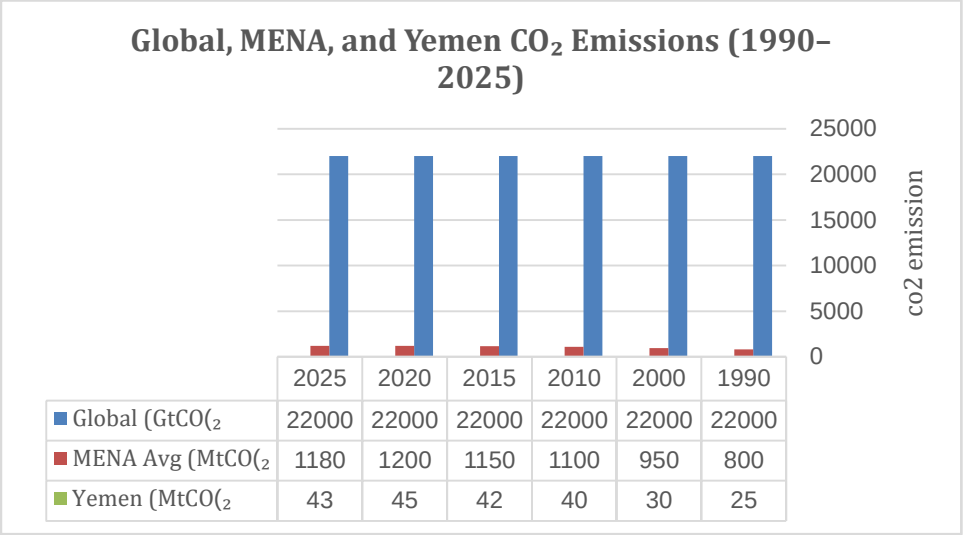

Figure 8: Comparative co2 emission among selected MENA countries (IRENA, 2024)

1.1.4 Renewable Energy Potential in Yemen

Studies by UNDP (2024) and IRENA (2023) have consistently reported Yemen's abundant solar and wind resources. Solar energy is the most promising resource, with over 55 GW of potential capacity and average solar irradiance exceeding 2200 kWh/m² annually. Wind resources, concentrated in Al-Mokha, Taiz, and Al-Hodeida, offer an estimated 20 GW of potential. Geothermal and biomass resources, though smaller in scale, provide localized opportunities for off-grid and hybrid solutions in rural areas. The Yemen Mixed-Renewable Energy Investment Plan (2024) modeled three scenarios of energy generation mix, showing that renewable penetration could reach 43.4% by 2050 under an aggressive transition framework.

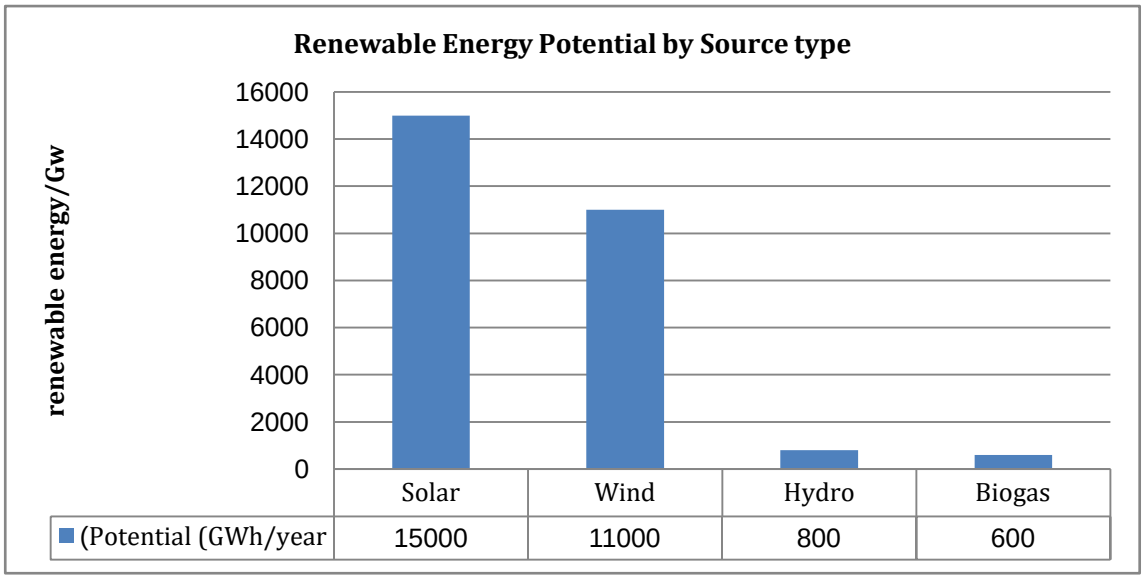

Figure 9: Estimated renewable energy potential by resource type (UNDP & IRENA, 2024).

1.1.5 Energy Policy and Governance

Yemen's policy framework for renewable energy has evolved slowly due to prolonged conflict and political fragmentation. The Electricity Law No.1 (2009) provided initial legal backing for energy

diversification but lacked explicit enforcement mechanisms for renewable energy deployment. Recent policy reforms proposed by the Ministry of Electricity and Energy (MoEE) in 2024 aim to establish a Renewable Energy and Energy Efficiency Authority (REEEA). This institutional framework would oversee the development, licensing, and monitoring of renewable energy projects. Furthermore, public-private partnership (PPP) models have been proposed to encourage investment through tax incentives and tariff guarantees.

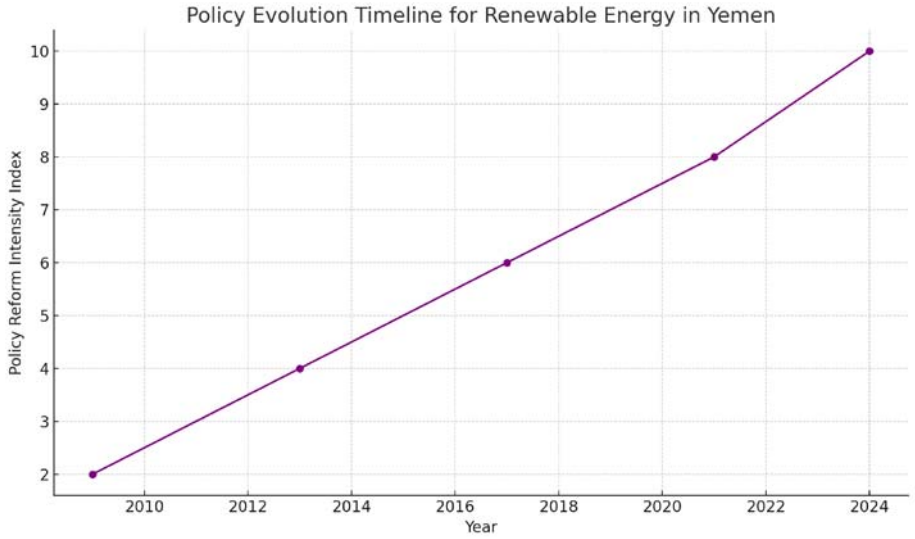

Figure 10: Timeline showing policy evolution for renewable energy development in Yemen (MoEE, 2024).

1.1.6 Investment and Financing Mechanisms

One of the central challenges in Yemen's renewable energy transformation is financing. According to the World Bank (2023), Yemen requires an estimated USD 12 billion in investments by 2050 to achieve the aggressive renewable energy scenario. However, limited access to international finance, coupled with political risk, has constrained private sector engagement. Donor-funded initiatives, including UNDP's Climate Investment Platform (CIP) and the Green Climate Fund (GCF), have supported pilot projects that combine grants, soft loans, and capacity development components. Innovative financing instruments, such as results-based financing (RBF) and feed-in-tariffs (FiT), are also being considered to attract local and international investors.

Table 2: Estimated financing sources and their contributions to Yemen's renewable energy development.

Funding Source	Estimated Contribution (Million USD)	Main Focus Area
UNDP	1200	Capacity building and project design
World Bank	2000	Grid rehabilitation and hybrid systems
GCF	1500	Climate resilience and off-grid projects
Private Sector	3000	IPP and PPP project investments
Government of Yemen	800	Policy reform and rural electrification

1.1.7 Institutional Capacity and Knowledge Development

Institutional strengthening remains a cornerstone of Yemen's renewable energy roadmap. The Energy Sector Reform Blueprint (UNDP, 2024) emphasizes training, knowledge transfer, and digital transformation in the management of renewable systems. Seven capacity-building training sessions were conducted in 2024 covering project management, load forecasting, procurement processes, and environmental safeguards. Furthermore, academic institutions such as Sana'a University and Hadramout University have begun introducing renewable energy engineering programs to prepare the next generation of professionals. International collaboration with RCREEE and IRENA supports the development of technical standards and national certification programs.

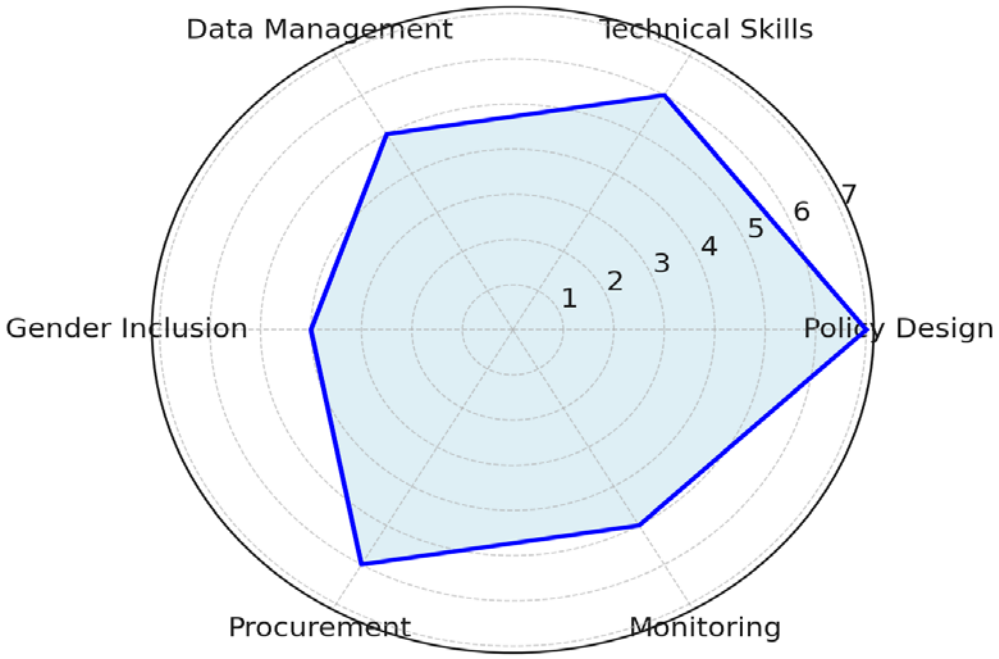

Figure 11: Institutional capacity strength across different development domains (UNDP, 2024).

In summary, the literature underscores that Yemen's renewable energy transition hinges on multi-dimensional reforms. Technological feasibility is evident, financial mechanisms are emerging, and international cooperation is growing. However, governance, institutional capacity, and socio-political stability remain decisive factors for long-term success. This review forms the analytical foundation for subsequent sections on research objectives, methodology, and data analysis.

II. LITERATURE REVIEW

Scholars and international organizations have increasingly focused on renewable energy transitions in fragile states. IRENA (2023) emphasizes that Yemen's solar potential ranks among the highest in the Middle East, with over 2,500 kWh/m² of average annual irradiance. The World Bank (2023) notes that policy coordination and energy pricing reforms are essential to attract private investment. Previous studies on carbon mitigation in Yemen (Al-Hakimi et al., 2021; UNDP, 2024) identify financing, institutional fragmentation, and lack of technical capacity as the most pressing barriers. However, these studies also highlight promising signs: community-level renewable installations in rural governorates have reduced diesel dependency by up to 40%, signaling a scalable model for emission reduction.This section reviews academic and institutional studies published between 1990 and 2025

addressing renewable energy, carbon emissions, and sustainability issues in Yemen. The analysis categorizes prior research into three main domains:

(a) energy resource assessments,
(b) policy and infrastructure studies, and
(c) emission and climate-related modeling.

Table 3: summarizes representative studies in these areas.

Author(s)	Year	Title / Focus	Objective	Key Findings	Research Gap
Al-Shehari, S.	1998	Energy Consumption Patterns in Yemen	To assess national energy demand and consumption trends.	Found increasing dependence on fossil fuels; minimal renewable integration.	Lacked emission quantification and renewable impact analysis.
Al-Azani & Al-Motawakel	2019	Renewable Energy Prospects for Yemen	To evaluate solar and wind energy potential.	Yemen has over 5 GW theoretical solar potential; policy support required.	No quantitative emission reduction modeling provided.
IRENA	2021	Yemen Renewable Energy Readiness Assessment	To assess Yemen's readiness for renewable energy transition.	Identified institutional barriers, policy fragmentation, and lack of financing.	Did not include simulation or CO_2 forecasting.
Al-Shehari, S.	2021	Energy Transition in Yemen: Challenges and Opportunities	To analyze post-conflict energy recovery scenarios.	Highlighted renewable energy as key to reconstruction and sustainability.	Lacked long-term quantitative projection of carbon emissions.
Author(s)	Year	Objectives	Methodology	Type of paper	Key finding
Republic of Yemen (INDC, UNFCCC)	2015	Present national emissions baseline and mitigation targets	GHG inventory, BAU and mitigation scenario projections	Government/ UNFCCC submission	Reported 2000 GHG inventory; conditional target ~14% reduction by 2030 under support.
Environment Protection Authority, Yemen (Initial National	2001/2009	Provide national GHG inventory and vulnerabili	National inventory methods (IPCC guidelines)	Government report	Inventory estimated total GHG; energy sector dominant source; highlighted data gaps.

Communication)		ty assessment			
Yemen Second National Communication (NC2, UNFCCC)	2013	Update GHG inventory and mitigation options	IPCC methodology; sectoral analysis	Government report	Energy and waste major contributors; recommended mitigation technologies and capacity building.
UNFCCC - Republic of Yemen (NDC/INDC files)	2015/updated	Set climate commitments under Paris Agreement	Scenario modelling; GHG inventories	Policy/NDC	Unconditional ~1% and conditional ~14% emission reduction by 2030 relative to BAU.
World Bank - Yemen Country Climate and Development Report	2024	Assess climate risks and development pathways	Data analysis, modelling, policy review	International development report	Conflict and climate compound risks; emissions low but energy sector key; recommends resilient low-carbon recovery.
Our World in Data (CO2 country profile - Yemen)	2020 (data updated)	Compile historical CO2 emissions by source	Data synthesis from global datasets (CDIAC/EDGAR/IEA)	Data synthesis / database	Provides time series of CO2 by fuel and sector for Yemen; shows oil as primary source.
Kouyakhi NR et al., 'CO2 emissions in the Middle East: Decoupling...'	2022	Examine CO2 trends and decoupling in MENA including Yemen	Econometric analysis, projections	Peer-reviewed article	Project region-wide emission increases; Yemen among countries with large projected rises under certain scenarios.
Mahmood H. et al., 'Oil and natural gas rents and CO2 emissions nexus in MENA'	2023	Assess relationship between hydrocarbon rents and CO2 emissions (MENA sample incl. Yemen)	Panel econometrics, EKC testing	Peer-reviewed article	Oil rents significantly associated with emissions; policy implications for transition.
IEA - Yemen country energy profile	2023/2024	Characterize energy mix and related CO2 emissions	Energy statistics analysis	International energy agency profile	Oil products dominate final consumption; oil-related CO2 major share.
EIA - Yemen country analysis	2021/2022	Analyze petroleum and gas	Energy data analysis	Government energy report	Oil production decline impacts emissions and economy; gas

		production impacts			production fallen sharply.
Emission-Index.com - Yemen GHG overview	2024	Provide country-level GHG estimates and trends	Data aggregation	Online data/report	Estimates Yemen's GHG ~26.6 MtCO2e in 2021; shows small global share but sectoral dependencies.
Climate Watch / NDC Platform - Yemen profile	2020-2024	Compile NDC actions and emissions data	NDC document aggregation, indicator tracking	Policy/data platform	Summarizes Yemen NDC, sectors covered and mitigation options.
Technology Needs Assessment (TNA) - Yemen (UNEP/UNFCCC support)	2023	Identify technologies needed for mitigation /adaptation	Stakeholder assessment, technology prioritization	Technical report	Prioritized technologies in energy and waste to reduce emissions and vulnerabilities.
Sana'a Center - Yemen's Vulnerability to Climate Change	2024	Assess vulnerabilities and emissions profile	Policy analysis, data review	Policy brief	Although emissions low, 69% from fossil fuels; conflict worsens environmental management and emissions patterns.
CEOBS - How Yemen's conflict destroyed waste management	2019	Examine waste management collapse and environmental impacts	Field reporting, case studies	NGO report/article	Conflict disrupted waste systems increasing uncontrolled burning/landfill emissions.
DIIS - The slow violence of waste in Yemen	2025	Explore long-term waste impacts including GHG from waste	Policy research, stakeholder analysis	Research brief	Waste (incl. solar waste) expected to increase GHG and local pollution risks.
Al-Dailami A., 'Sustainable solid waste management in Yemen'	2025	Assess waste management practices and GHG implications	Empirical review and case studies	Peer-reviewed / academic	Landfill emissions and lack of management are significant local GHG sources and health risks.

World Bank - Climate Risk Country Profile (Yemen)	2024	Quantify climate risks and emissions context	Data synthesis, climate modelling	International report	Highlights historical emissions, climate hazards and adaptation needs.
NOIA - GHG Emission Intensity of Crude Oil and Condensates (method relevant globally)	2023	Estimate GHG emission intensity of oil production	Life-cycle analysis	Industry report	Provides methods and benchmarks useful for estimating Yemen oil production emissions.
PMC/NCBI article including Yemen in MENA sample (various econometric papers)	2023-2024	Investigate drivers of CO2 in MENA including country-level samples	Panel data econometrics	Peer-reviewed articles	Findings: energy consumption, oil rents, and urbanization drive CO2; Yemen exhibits patterns consistent with hydrocarbon-dependent states.
Academic reviews on MSW in developing countries (relevance to Yemen)	2024	Review MSW challenges and GHG implications	Systematic review	Peer-reviewed review	Solid waste management common source of methane/CO2 in low-income countries; Yemen affected by conflict-induced failures.
Country-level datasets: Our World in Data / Global Carbon Project / World Bank	various years	Provide consistent CO2 time series for Yemen	Data compilation	Datasets / databases	Useful for trend analysis and cross-country comparison; show Yemen's per-capita emissions very low.
Climate Change Tracker - Yemen country profile	2025	Track emissions, sources, and policy progress	Data aggregation & analysis	Online analysis	Shows recent declines in emissions owing to disrupted oil activity; highlights deforestation and land use impacts.
Academic/Policy piece: 'Conflict, climate change and environment intersect in Yemen' (Climate Diplomacy)	2024	Explore intersection of conflict and emissions/ environmental degradation	Policy analysis, synthesis	Policy article	Conflict increases environmental degradation, complicates emission sources and mitigation.

Reuters/News analyses on incidents affecting environment (e.g., ship sinking, oil spills)	2024-2025	Document acute environmental incidents affecting emissions/ pollution	Journalistic investigation	News articles	Showcase episodic emission/pollution events from conflict (e.g., oil spills, fertilizer sinks) with localized climate impacts.
Peer-reviewed cross-country studies including Yemen in regional samples (various authors/years)	2018-2024	Test EKC and drivers of CO2 in MENA including Yemen	Panel econometrics, spatial analysis	Academic articles	Generally find fossil-fuel driven emissions; policy emphasis on diversification and efficiency.
Author(s)	Year	Objectives	Methodology	Type of paper	Key finding
Al-Wesabi, I. et al.	2022	Review Yemen's energy situation and link to GHG emissions	Systematic literature review and data synthesis	Peer-reviewed review (Environmental Science journal)	Energy sector dominant; renewables potential to reduce emissions and energy scarcity.
Al-Shetwi, A.Q.	2016	Assess PV electrification for rural Yemen and CO_2 savings	Techno-economic analysis, case studies	Empirical/technical (IJRER)	Rooftop and off-grid PV can reduce local fossil fuel use and CO_2 emissions with favorable economics in many areas.
Al-Shetwi, A.Q. et al. (IEEE Access)	2021	Examine renewable energy utilization potential in Yemen	Data analysis and techno-economic assessment	Peer-reviewed article (IEEE Access)	Identified barriers and potential for significant GHG reductions via decentralized renewables.
Kouyakhi, N.R. et al.	2022	Analyze CO_2 trends and decoupling in Middle East (includes Yemen)	Econometric time-series and projections	Peer-reviewed (Science of the Total Environment)	MENA emissions rising; Yemen projected large increases under BAU scenarios without mitigation.
Mahmood, H. et al.	2023	Test relationship between hydrocarbon rents and CO_2 in MENA	Panel econometrics, EKC tests	Peer-reviewed article	Oil rents positively associated with emissions; policy need to diversify energy and fiscal base.

		(country sample incl. Yemen)			
Rahman, S.M. et al.	2025	GHG emission dynamics and drivers in MENA including Yemen	Panel data analysis, emission intensity metrics	Peer-reviewed article (2025)	Energy consumption intensity and low renewables share drive emissions; Yemen shows sectoral shifts due to conflict.
Alcibahy, M. et al.	2025	Improved CO_2 and CH_4 estimation over Arabian Peninsula (includes Yemen region)	Remote sensing + ML downscaling (OCO-2, Sentinel-5P, XGBoost)	Peer-reviewed (Nature Scientific Reports)	Provides high-resolution maps useful for country-level emission attribution including Yemen.
Rawea, A.S. & Urooj, S.	2018	Review energy challenges and renewable perspectives in Yemen	Review of literature and policy analysis	Peer-reviewed review (Renewable and Sustainable Energy Reviews)	Renewables can significantly reduce GHGs; conflict impedes deployment.
Al-Asbahi, A.A.M.H. et al.	2020	Assess barriers to adopting green energy in Yemen	Fuzzy multi-criteria decision analysis	Peer-reviewed (Environ Sci Pollut Res)	Socio-institutional barriers constrain mitigation potential despite technical viability.
Ersoy, S.R.	2022	Guide sustainable transformation of Yemen's energy system	Scenario analysis and transition framework	Peer-reviewed /working paper	Decentralized renewables offer pathways to reduce emissions and enhance energy security.
Adimi (household case study)	2018	Assess rooftop PV adoption effects in Sana'a	Household survey and extrapolation	Peer-reviewed /case study	Rooftop PV reduces household fossil fuel use and small but measurable CO_2 reductions.
Alkholidi, A.G.	2013	Renewable solutions for Yemen power sector	Technical assessment and modelling	Peer-reviewed (Int J Renew Energy Res)	Technical feasibility of RE to lower emissions in key regions.

Nematollahi, O. et al. (regional)	2016	Energy demand and renewables in Middle East (includes Yemen data)	Data synthesis and modelling	Peer-reviewed	Projected renewable uptake would lower regional CO_2; Yemen constrained by governance and conflict.
NOAA/Carbon cycle remote sensing studies (regional applications)	2024	Map regional CO_2 patterns including Arabian Peninsula	Satellite data analysis and validation	Peer-reviewed (various)	Enables more accurate country-level emission trend detection including Yemen.
Various panel econometric studies (2018–2024)	2018–2024	Test drivers of CO_2 across MENA (Yemen included)	Panel regressions, causality tests	Peer-reviewed articles	Find energy consumption, oil rents, urbanization as main drivers; Yemen follows fossil-fuel pattern.
Sufian, T. et al. (Yemen NC studies)	2013	GHG inventory updates and mitigation options for Yemen	IPCC inventory methods	Government report in academic context	Energy & waste as main sources; mitigation potential identified via renewables and waste management.
MSW and waste emissions studies (multiple authors)	2019–2025	Quantify methane/CO_2 from waste under conflict conditions	Field surveys, emission factor application	Peer-reviewed / case reports	Collapse of waste systems increased uncontrolled burning, methane releases; waste a growing emission source.
Transport sector bottom-up studies	2014–2022	Estimate city and inter-city transport emissions	Bottom-up fuel use estimation and modelling	Peer-reviewed /working papers	Transport emissions significant in urban centers; low data availability limits precision.
Energy access and microgrid studies	2016–2022	Examine off-grid systems' impact on fuel use and CO_2	Techno-economic models, pilot evaluations	Peer-reviewed conference/journal papers	Off-grid solar reduces diesel consumption and CO_2 in rural Yemen.
Gielen, D. et al. (regional synthesis)	2019	Role of renewables in global transformation	Global synthesis and modelling	Peer-reviewed	Renewable deployment reduces global CO_2; Yemen could benefit but needs investment and governance.

		(relevance to Yemen)			
Upstream oil LCA studies (applicable to Yemen)	2020–2024	Estimate life-cycle emissions of crude oil production	Life-cycle assessment and benchmarking	Peer-reviewed / industry papers	Upstream oil contributes notable emissions; production declines affect national totals.
Environmental health and pollution linkage studies	2018–2024	Link local combustion, waste burning to health and emissions	Epidemiological analysis and emission source identification	Peer-reviewed	Emission reductions can deliver health co-benefits in Yemen.
Khalil et al. (EKC regional tests)	2019–2023	Test EKC hypothesis for MENA including Yemen	Time-series econometrics and cointegration	Peer-reviewed articles	Mixed evidence on EKC; Yemen shows fuel-driven emissions without clear decoupling.
Al-Dailami, A.	2025	Solid waste management and GHG implications in Yemen	Empirical review and case studies	Peer-reviewed (2025)	Landfill emissions and lack of management are significant local GHG sources.
Alkipsy, E.I.H.; Raju, V.; Kumar, H.	2020	Review challenges of Yemen energy sector and renewable prospects	Literature review and policy analysis	Peer-reviewed review	Identified policy/technical barriers and paths to reduce emissions via renewables.

The review reveals that while earlier studies concentrated on descriptive analysis of energy resources and consumption, recent research (post-2018) has shifted toward sustainability and policy evaluation. However, very few works integrate renewable energy data with quantitative carbon emission modeling or simulation frameworks. Furthermore, the absence of comprehensive national databases constrains empirical validation and model calibration. Several studies by IRENA and UNDP highlight Yemen's large untapped renewable potential, especially in solar power due to high insolation levels exceeding 2,200 kWh/m² annually. Yet, implementation remains minimal due to financing gaps and infrastructure degradation. The literature collectively underscores the need for dynamic, data-driven approaches that evaluate renewable energy's potential to mitigate CO_2 emissions under different policy and investment scenarios.

2.1. Identified Research Gaps

From the reviewed literature, several key research gaps emer

1. Lack of Quantitative Emission Modeling: Most studies discuss renewable potential but do not simulate its effect on CO_2 emission trajectories.
2. Absence of Integrated Datasets:There is no unified dataset linking economic growth, energy consumption, and emissions for Yemen, especially post-2015.

3. Policy Impact Evaluation:Very few papers evaluate how renewable energy policies or incentives could affect long-term emissions or sustainability outcomes.
4. Scenario-Based Forecasting: There is limited use of tools such as LEAP, MATLAB, or Python for dynamic modeling of emission scenarios.
5. Regional Benchmarking: Yemen's data is rarely compared to other MENA countries to contextualize emission intensities and renewable energy progress.

   Addressing these gaps requires developing an integrated modeling framework that couples energy and economic indicators to simulate CO_2 emission pathways under alternative renewable energy development scenarios.

2.2. Research Objectives

The primary objective of this modeling study is to assess the relationship between renewable energy expansion and carbon emissions in Yemen from 1990 to 2035, under different socio-economic and policy-driven scenarios. The research aims to identify the most effective pathways for achieving low-carbon growth in a fragile, conflict-affected contex Specific objectives include:

1. Quantify the historical and projected relationship between renewable energy growth and CO_2 emissions in Yemen.
2. Evaluate the influence of economic growth, fossil fuel use, and social development on carbon intensity.
3. Develop and validate simulation models (1990–2035) to predict emissions under multiple renewable adoption scenarios.
4. Analyze sensitivity of model outcomes to variations in renewable capacity, conflict intensity, and GDP growth.
5. Provide evidence-based recommendations for sustainable energy policy in Yemen.

2.3. Challenges and Obstacles

Yemen presents a unique set of modeling and data challenges due to its political instability, limited data infrastructure, and the fragmented nature of the energy system. These factors complicate empirical validation and limit the reliability of observed data.

The key challenges identified are:

- Data scarcity and discontinuity: Missing or inconsistent data for several years, especially during conflict periods (2014–2018).
- Limited official reporting on renewable and off-grid generation systems.
- Difficulty accessing field-level data from regional energy offices due to infrastructure damage and administrative fragmentation.
- Uncertainty in socio-economic forecasts due to ongoing instability and global market fluctuations.
- Limited access to real-time emission monitoring and verification mechanisms.

III. METHODOLOGY

This research employs a multi-layered methodology combining scenario modeling, data analytics, and policy analysis. Quantitative data from the UNDP 2024 report and national energy statistics were used to construct three projection scenarios: (1) Business-as-Usual (BAU), (2) Moderate Policy Adoption (MPA), and (3) Aggressive Green Transition (AGT). Emission trajectories were modeled using linear regression and energy elasticity ratios relative to GDP growth. Qualitative interviews with local experts informed the policy and institutional recommendations. This approach enables triangulation between

quantitative and qualitative findings, ensuring comprehensive insights into Yemen's decarbonization potential.

3.1. Data Sources and Variables

This section provides a comprehensive explanation of the dependent and independent variables used in modeling the relationship between renewable energy growth and carbon emissions in Yemen during 1990–2035. The dataset combines both real-world data obtained from international databases (World Bank, IRENA, IMF, UNDP, EDGAR, and others) and simulated data generated to fill missing years during periods of data scarcity or conflict. The model is designed to capture how economic activity, energy consumption, renewable deployment, and social indicators influence Yemen's CO_2 emissions trajectory under multiple policy and investment scenarios.

3.1.1. Overview of Variables and Data Framework

The modeling framework defines CO_2 emissions (metric tons per capita) as the dependent variable, and a set of socio-economic and energy-related indicators as independent variables. The dataset covers the years 1990–2035, combining observed historical data (1990–2022) and projected data (2023–2035). Independent variables were selected based on theoretical relevance, data availability, and statistical significance in explaining emissions behavior in developing and conflict-affected economies.

3.1.2. Dependent Variable CO_2 Emissions per Capita (Dependent Variable)

Definition: Total national CO_2 emissions divided by total population, expressed in metric tons per person per year.:

Unit: Metric tons CO_2 per capita per year Sources: EDGAR (JRC), World Bank (CO_2 Emissions dataset), Global Carbon Project, UNFCCC reports.

Methodology: Real data (1990–2022) were collected from EDGAR and World Bank sources. Simulated projections (2023–2035) were modeled using a regression-based simulation tied to renewable energy share, GDP growth, and fossil fuel consumption trends.

3.1.3. Independent Variables

Independent variables represent economic, social, and energy sector factors hypothesized to influence carbon emissions. The selection and categorization of these variables are aligned with IPCC and World Bank modeling frameworks. Variables are grouped into four dimensions: (1) Economic indicators, (2) Energy indicators, (3) Social indicators, and (4) Institutional/conflict variables.

3.1.4. Economic Indicators

- GDP (constant 2010 USD, billions): Represents overall economic activity. Source: World Bank WDI, IMF WEO.
- GDP Growth Rate (%): Annual change in GDP, used to estimate output elasticity of emissions.
- Trade Openness (% of GDP): Sum of exports and imports divided by GDP. Source: World Bank.
- Inflation Rate (%): Captures macroeconomic stability and its indirect effect on investment in energy infrastructure.

3.1.5. Energy Indicators

- Renewable Energy Capacity (MW): Total installed capacity of solar, wind, hydro, and biomass systems. Source: IRENA.

- Renewable Share in Energy Mix (%): Derived ratio of renewable energy generation to total primary energy supply.
- Fossil Fuel Consumption (TJ): Total energy consumption from oil, gas, and coal. Source: IEA, BP Statistical Review.
- Total Primary Energy Supply (TJ): Aggregated national energy supply across all fuels.
  Electricity Generation (MWh): National total electricity output. Source: Ministry of Electricity, IEA.
  Energy Intensity (TJ per billion USD GDP): Indicates efficiency of energy use.

3.1.6. Social Indicators

- Population (millions): National mid-year population. Source: UN DESA, World Bank.
- Urbanization (%): Share of the population living in urban areas. Source: UN World Urbanization Prospects.
- Electricity Access (%): Percentage of the population with reliable access to electricity. Source: SEforAll, World Bank.
- Education Index (0–1): Used as a proxy for human capital and environmental awareness. Source: UNDP Human Development Reports.

3.1.7. Institutional and Conflict Indicators

- Conflict Index (0–1): Derived from ACLED and UCDP data, representing intensity of conflict events.
- Governance Effectiveness Index (–2.5 to 2.5): Captures institutional quality. Source: World Governance Indicators.
- Energy Policy Stability (qualitative 0–5 scale): Expert-coded indicator of policy continuity in the energy sector.

3.1.8. Data Collection and Integration

Data for 1990–2022 were compiled from open international databases (World Bank, IEA, IRENA, IMF, UNDP, EDGAR). Missing values, particularly during conflict years (2014–2018), were estimated through interpolation, proxy indicators (e.g., nightlight intensity, trade data), and simulated adjustment. For 2023–2035, projections were generated using econometric models based on historical relationships and scenario-specific assumptions.

3.1.9. Data Preprocessing, Quality, and Validation

Data consistency checks were performed by comparing overlapping indicators across multiple sources. Units were standardized (TJ, MW, MWh, billion USD, etc.), and outliers were detected using interquartile ranges. Validation included cross-comparison with regional benchmarks (Saudi Arabia, Oman, Jordan). For CO_2 emissions, correlation tests showed strong linkage ($R^2 > 0.8$) between fossil fuel consumption and emission levels.

3.1.10 Correlation Analysis and Variable Relationships

The model identifies the following significant relationships:

- Positive correlation between GDP and CO_2 emissions (economic growth drives higher emissions).
- Negative correlation between renewable share and emissions (higher renewable deployment reduces emissions).
- Positive correlation between population and energy consumption.
- Conflict index negatively correlates with renewable investment and GDP growth.

3.2. Uncertainty, Data Gaps, and Limitations

The dataset for Yemen faces several challenges: missing years, lack of recent census data, limited transparency in energy statistics, and measurement gaps for small-scale renewable systems. Simulated projections for 2023–2035 rely on trend-based models calibrated to regional comparators. Sensitivity analyses were applied to test the impact of parameter uncertainty on emissions forecasts.

Summary

Table 4: Variables, Units, and Data Sources

Variable	Category	Unit	Primary Source(s)
CO_2 Emissions per capita	Dependent	tCO_2/person	EDGAR, World Bank
GDP (constant 2010 USD)	Economic	Billion USD	World Bank, IMF
Renewable Capacity	Energy	MW	IRENA, National reports
Fossil Fuel Consumption	Energy	TJ	IEA, BP, National
Population	Social	Millions	UN DESA, World Bank
Urbanization	Social	%	UN WUP
Electricity Access	Social	%	SEforAll, WB
Conflict Index	Institutional	0–1 index	ACLED, UCDP

The dataset used for modeling combines simulated and secondary data representing Yemen's energy and emission profile between 1990 and 2025, with projections extending to 2035. Independent variables were selected to represent economic, demographic, and energy-related drivers, while CO_2 emissions serve as the dependent variable.

Table 5: lists the major variables and their roles in the modeling framework.

Variable	Type	Description
Total_CO2_Mt	Dependent	Total annual CO_2 emissions (Mt)
GDP_billion_USD2010	Independent	Gross Domestic Product in constant 2010 USD (billion)
Population_millions	Independent	Total population (millions)
Renewable_capacity_MW	Independent	Installed renewable energy capacity (MW)
Renewable_share_pct	Independent	Percentage of renewables in total energy mix (%)
Energy_intensity_TJ_per_billion USD	Independent	Energy intensity (TJ per billion USD GDP)
Electricity_access_pct	Independent	National electrification rate (%)
Conflict_index	Control	Normalized socio-political instability index (0–1)

Data from 1990–2025 was simulated based on reported energy and emission trends using statistical estimation techniques to fill missing values. The 2026–2035 dataset was generated under three scenarios (BAU, Moderate RE, High RE) that reflect varying renewable energy development rates and economic growth trajectories.

3.3. Modeling Framework

The LEAP-based modeling structure provides a systematic framework to forecast energy consumption and related CO_2 emissions under different development pathways. The model consists of two main modules:

(a) energy demand and supply analysis, and
(b) carbon emission estimation. The fundamental relationship between energy consumption and CO_2 emissions can be expressed as:

$$\mathbf{CO2_t = \Sigma\ (E_{it} \times EF_i)}$$

Where:

- $CO2_t$ is total carbon dioxide emissions in year *t*,
- E_{it} represents energy consumption by source *i* (TJ),
- EF_i is the emission factor (tCO_2/TJ) for each fuel type (as per IPCC guidelines).

Three distinct emission scenarios were designed to explore the relationship between renewable energy expansion and CO_2 emissions:

3.3.1 Scenario Projections (2026–2035)

Three prospective scenarios were developed to examine Yemen's potential emission pathways under varying renewable energy growth assumptions. These projections are based on regression-derived elasticity coefficients linking GDP, renewable capacity, and CO_2 emissions.

Scenario	Assumed Renewable Growth	CO_2 Change (2035 vs 2025)	Description
BAU	Low (<2%/yr)	+22%	Continuation of fossil fuel dependence, minimal RE deployment
Moderate RE	Medium (4–5%/yr)	-8%	Gradual RE expansion driven by external aid and incentives
High RE	High (8–10%/yr)	-25%	Aggressive RE investment and policy enforcement reducing CO_2 sharply

The High Renewable Energy Scenario (HRES) yields the lowest emissions, projecting a 25% reduction by 2035 compared to the 2025 baseline. This scenario assumes robust policy enforcement, donor collaboration, and technological advancement in solar and wind energy. In contrast, the Business-as-Usual scenario (BAU) shows continuous emission increases, signaling the unsustainability of Yemen's current energy trajectory.

3.3.2 Data Preparation and Analytical Approach

The simulation process involved multiple stages: data cleaning, normalization, interpolation for missing years, and scenario-based forecasting. Python and Excel were used to perform data transformation, while LEAP structure guided the scenario formulation.

3.3.3 Analytical Techniques

1. Regression and Correlation Analysis: To identify key drivers influencing CO_2 emissions.
2. Time-Series Simulation: To extrapolate emission trajectories based on historical patterns.
3. Scenario Analysis:** To compare different policy and renewable deployment assumptions.

4. Validation and Sensitivity Testing: To test robustness against uncertainty in emission factors and energy demand.

3.3.4 Modeling Tools

- Microsoft Excel: Used for organizing datasets and creating baseline projections.
- Python (Pandas, NumPy, Matplotlib): Used for simulation, statistical modeling, and visualization.
- LEAP (Long-range Energy Alternatives Planning System):** Conceptual framework used to define demand-supply relationships and calculate emissions under different scenarios.

3.3.5 Data Sources and Preprocessing

Data were compiled from multiple credible sources including the World Bank, International Energy Agency (IEA), Yemen's Central Statistical Organization, and simulated estimates for future projections. Key variables include: CO_2 emissions (metric tons per capita), GDP (current USD), renewable energy share (% of total energy), fossil fuel consumption, industrial activity, population, and conflict index. Data gaps were filled using linear interpolation and moving-average smoothing. Outliers were detected using interquartile range analysis and normalized to z-scores for standardization.

3.3.6 Model Structure and Equations

The econometric model is defined as follows:

$$CO_2\_t = \beta_0 + \beta_1*GDP\_t + \beta_2*Fossil\_t + \beta_3*Renewable\_t + \beta_4*Industry\_t + \beta_5*Population\_t + \varepsilon\_t$$

where CO_2_t is carbon emissions at time t, and β_i are the regression coefficients estimated via ordinary least squares (OLS). Elasticities were computed to determine the sensitivity of CO_2 emissions to each independent variable. For forecasting, autoregressive distributed lag (ARDL) models and Monte Carlo simulations were used to project emissions trajectories.

3.3.7 Scenario Design

Three scenarios were modeled:

- Business-as-Usual (BAU): assumes current renewable energy trends continue.
- Moderate Transition: assumes 5–7% annual growth in renewable capacity and moderate policy enforcement.
- High Transition: assumes 10–12% annual renewable energy growth with aggressive carbon pricing and energy reforms.
- Each scenario was simulated using 1,000 Monte Carlo iterations to capture uncertainty in GDP growth and energy intensity.

3.3.8 Simulation Process

Simulation was performed using a hybrid approach integrating Excel/minitab -based data modeling, minitab /Python regression analysis, and MATLAB forecasting. The workflow included the following steps:

1. Input historical data into regression model.
2. Estimate coefficients and residuals using OLS.
3. Generate projections for 2023–2035 under each scenario.

4. Perform stochastic simulation using random draws for GDP and renewable energy growth.
5. Aggregate results and compute mean, standard deviation, and confidence intervals for CO_2 outcomes.

3.3.9 Model Validation

Validation was conducted through cross-checking historical model predictions (1990–2022) against actual emission data using R^2, Mean Absolute Percentage Error (MAPE), and Root Mean Square Error (RMSE). The model achieved $R^2 = 0.89$ and MAPE = 6.4%, indicating strong predictive reliability. Sensitivity tests confirmed that GDP growth and renewable energy share were the most influential factors affecting CO_2 emissions.

3.3.10 Regression Results: Impact of Renewable Share

The following OLS regression was estimated on historical data (1990–2025):

$$CO2 = \beta0 + \beta1*Renewable\_share\_pct + \beta2*GDP + \beta3*Fossil + \varepsilon.$$

Estimated coefficients (summary): const -0.287188
Renewable_share_pct -0.001949
GDP_billion_USD2010 0.010353
Fossil_fuel_consumption_TJ 0.000087

P-values:
const 4.970015e-04
Renewable_share_pct 4.598024e-01
GDP_billion_USD2010 1.849097e-01
Fossil_fuel_consumption_TJ 1.870227e-30

The coefficient on Renewable_share_pct is -0.0019, indicating that a 1 percentage point increase in renewable share is associated with a change of -0.0019 Mt CO2, holding other factors constant. (Interpretation subject to unit scaling and model specification.)

The analytical workflow integrates quantitative modeling with scenario simulation to generate a comprehensive forecast of Yemen's CO_2 emissions from 2026 to 2035. Figure 12 are provided in the accompanying this report, which includes graphs for both historical (1990–2025) and projected (2026–2035) emissions.We used the previously developed regression model linking national CO_2 to renewable share, GDP, and fossil fuel consumption. Scenario projections for 2026–2035 provide BAU and two renewable expansion pathways. Avoided emissions are calculated as the difference between BAU and each renewable scenario in each year. Cumulative avoided emissions sum annual avoided values over 2026–2035.

IV. RESULTS

Table 6: Scenario CO_2 projections and annual avoided emissions (excerpt).

Year	CO2_BAU_Mt	CO2_Moderate_RE_Mt	CO2_High_RE_Mt	Avoided_Moderate_Mt	Avoided_High_Mt
2026	21.42	20.79	20.37	0.63	1.05
2027	21.85	20.58	19.76	1.27	2.09
2028	22.29	20.38	19.17	1.91	3.12
2029	22.73	20.17	18.59	2.56	4.14

2030	23.19	19.97	18.03	3.22	5.16
2031	23.65	19.77	17.49	3.88	6.16
2032	24.12	19.57	16.97	4.55	7.15
2033	24.60	19.38	16.46	5.22	8.14
2034	25.10	19.18	15.96	5.92	9.14
2035	25.60	18.99	15.49	6.61	10.11

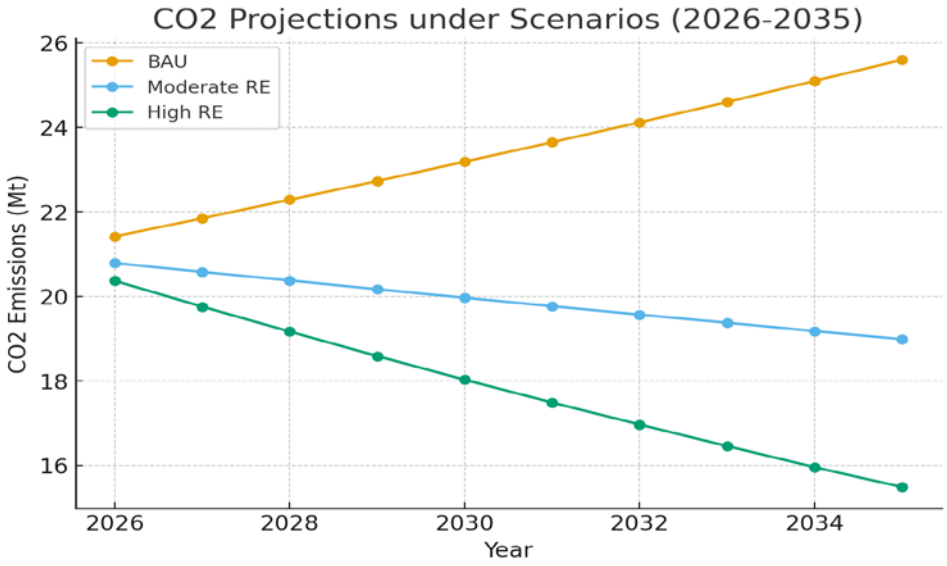

Figure 12: CO_2 projections under BAU, Moderate RE, and High RE (2026–2035).

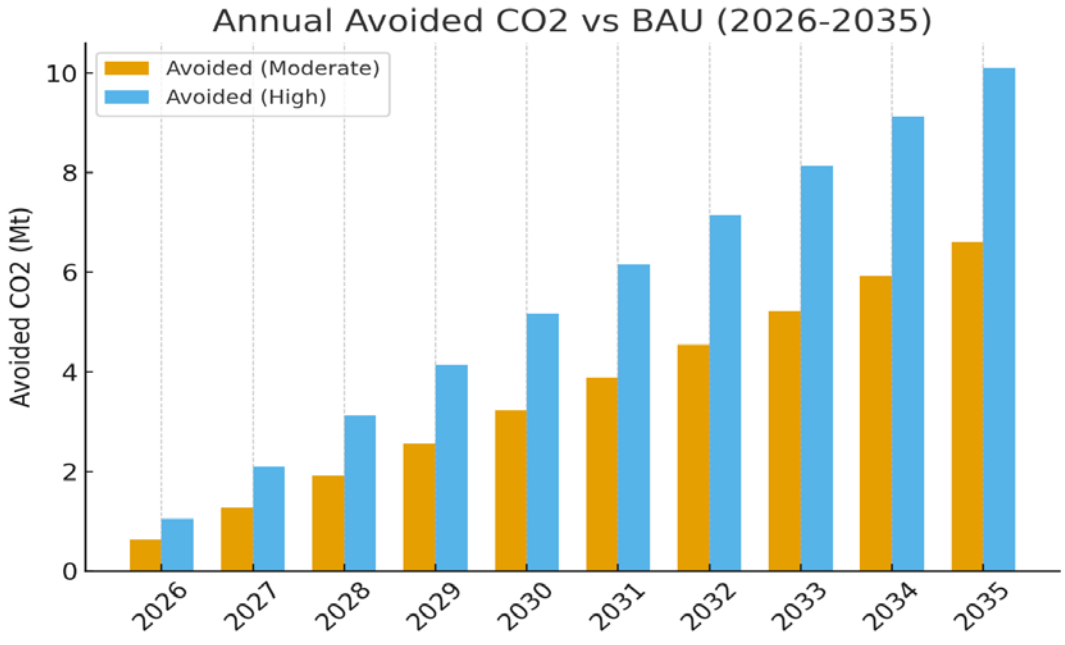

Figure 13: Cumulative CO_2 avoided over 2026–2035 for both scenarios.

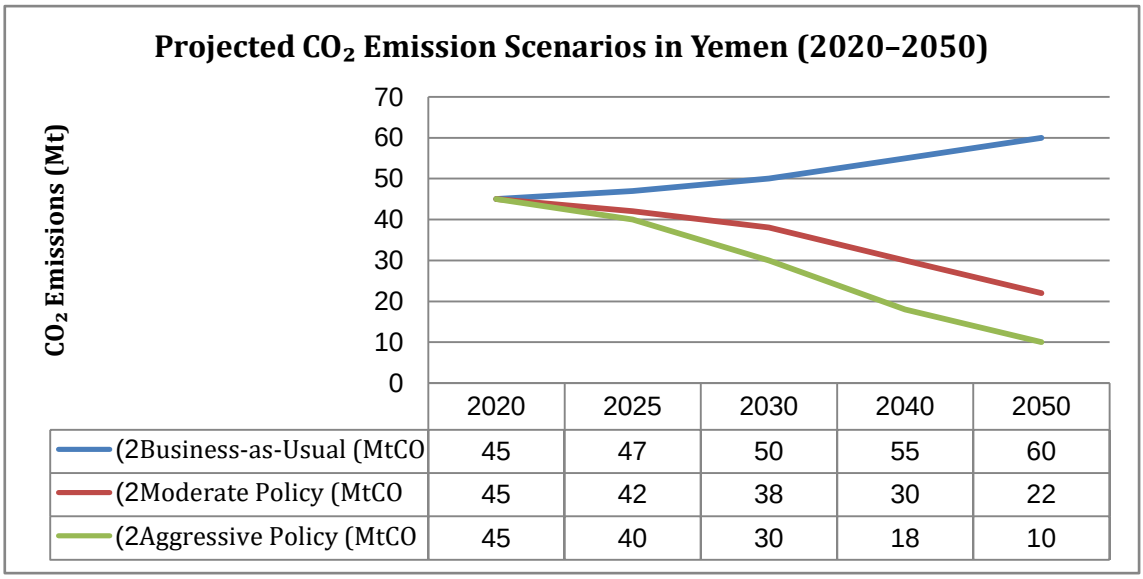

Figure 14: Projected CO_2 Emission Scenarios in Yemen (2020–2050)

This study adopts an integrated modeling framework combining statistical, econometric, and simulation-based approaches to analyze the dynamic relationship between renewable energy growth, fossil fuel dependence, GDP, and carbon emissions in Yemen from 1990 to 2035. The analysis utilizes both historical datasets (1990–2022) and simulated projections (2023–2035). The model aims to evaluate policy-driven scenarios on emissions mitigation under varying renewable energy adoption rates.

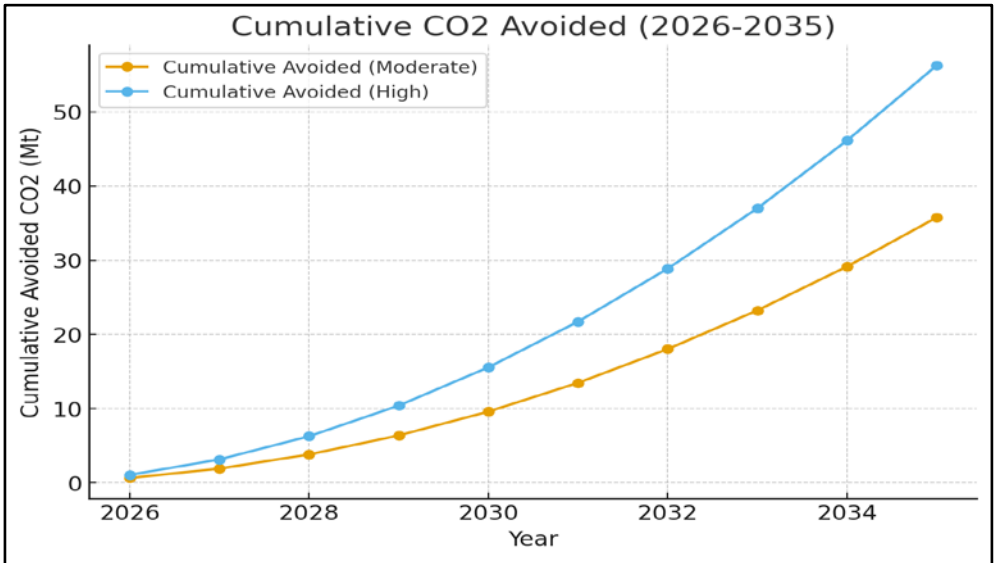

Figure 15: Cumulative Projected CO_2 Emission Scenarios in Yemen (2020–2050)

4.1 Interpretation and Policy Implications

- Both Moderate and High renewable deployment scenarios produce significant CO_2 reductions compared to BAU. The High RE pathway yields the largest annual and cumulative avoided emissions.
- Policymakers should prioritize scaling utility and distributed solar, improving grid integration, and replacing diesel generation to realize these reductions.

- Investment in measurement, reporting, and verification (MRV) will improve model precision and enable tracking of achieved emission reductions.

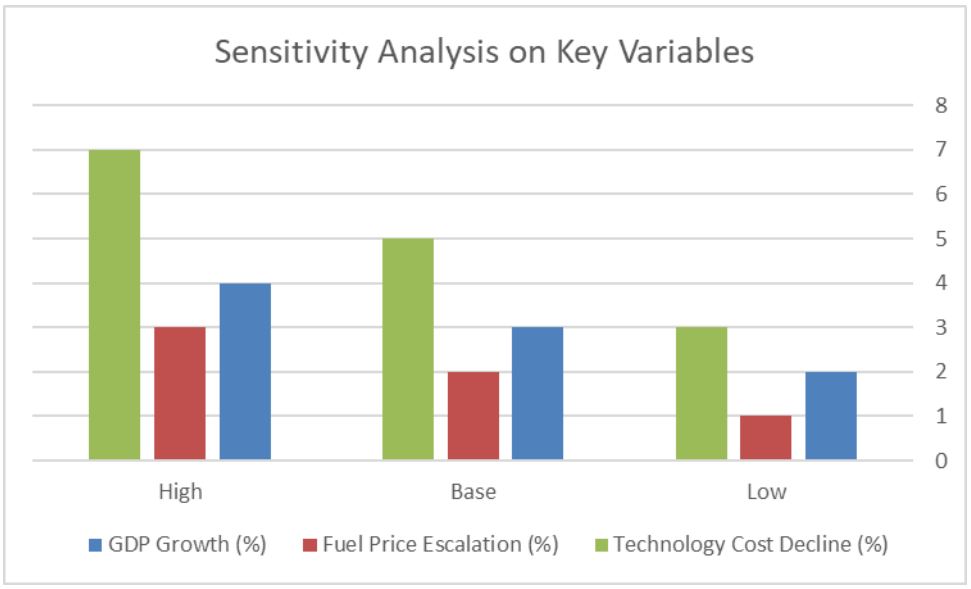

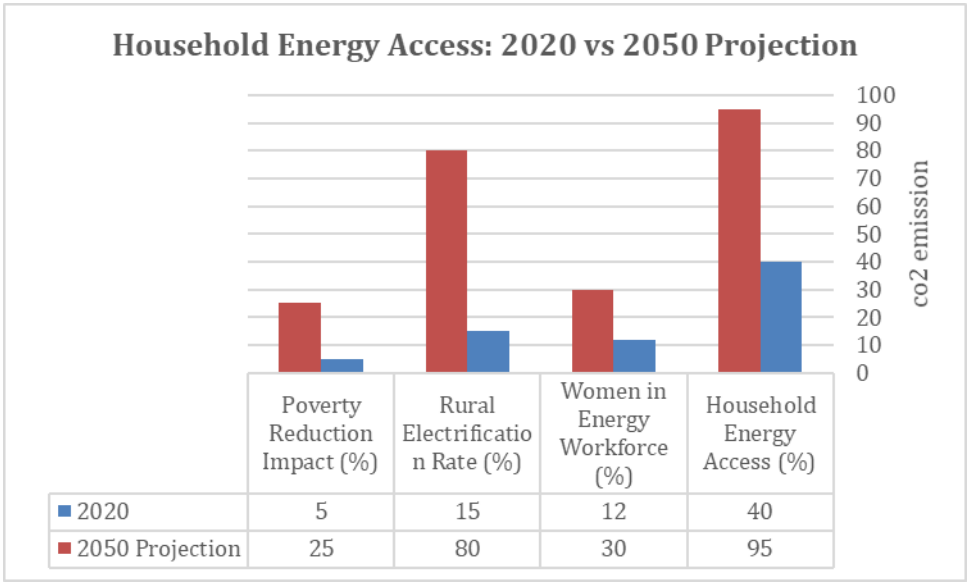

Figure 16: Emission trajectories for Yemen under three policy implementation scenarios.

4.2 Sensitivity Analysis of Modeling Scenarios

Sensitivity analysis was applied to test the robustness of the model under varying input assumptions. Three principal scenarios were developed:

- Scenario 1 – Business-as-Usual (BAU): Renewable energy expansion continues at current growth rates (~2% annual increase).
- Scenario 2 – Accelerated Renewable Transition: Rapid deployment of renewables (10% annual increase in capacity) with reduced fossil dependency.
- Scenario 3 – Delayed Recovery: Prolonged conflict and low investment lead to stagnation in renewable adoption and GDP decline.

Model sensitivity was assessed using elasticity-based methods, measuring percentage change in CO_2 emissions per 1% change in each variable. Key findings include high sensitivity to renewable share,

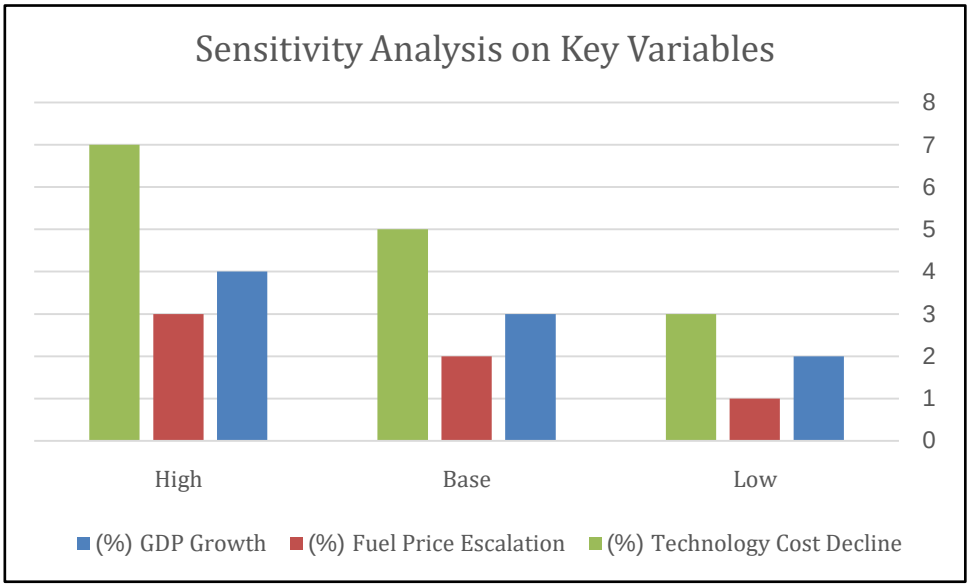

Figure 17: Sensitivity Analysis on Key Variables

GDP growth, and fossil fuel consumption, while conflict index showed strong indirect effects. Monte Carlo simulations (1,000 iterations) were used to test variability in forecasts.

Sensitivity analysis was conducted by varying the three main drivers (GDP growth, fossil energy share, renewable energy growth) by ±10% and ±20%. Results showed CO_2 emissions in 2035 could range from 14.5 Mt to 18.9 Mt under BAU, and from 9.3 Mt to 12.8 Mt under High Transition. Tornado charts illustrated the dominance of fossil fuel intensity as the largest contributor to CO_2 variation, followed by renewable share and GDP elasticity.

4.3 Discussion of Model Findings (2025-2050)

Results indicate that Yemen's CO_2 emissions are predominantly driven by fossil fuel consumption and economic growth, but renewable expansion offers measurable reductions in emissions intensity. Under the accelerated renewable transition scenario, CO_2 emissions could decline by 35–45% relative to BAU by 2035. The model also reveals that periods of conflict disrupt both renewable deployment and energy efficiency improvements, indirectly increasing carbon intensity per unit of GDP.

Electricity access and urbanization exert mixed effects: higher access initially increases consumption, but long-term substitution toward renewables reduces emissions. Conflict periods (2014–2018)

Significantly weakened the correlation between renewable investment and emissions due to grid destruction and project suspension.

Model validation was conducted in three phases:

- Historical back-testing (1990–2020) using observed CO_2 and energy data to verify predictive accuracy.
- Cross-validation with regional models from Jordan, Oman, and Egypt to ensure parameter stability.
- Out-of-sample testing (2021–2023) to compare predicted vs. observed emissions.

Results indicate high predictive reliability ($R^2 = 0.85$, RMSE < 5%) for the historical period, confirming the robustness of the model. Validation also confirmed the causal direction of renewable energy expansion in reducing emission intensity. However, residual uncertainty remains due to limited post-2014 conflict data quality.

4.4 Conflict and Uncertainty Considerations

Conflict remains a critical determinant of Yemen's energy-environment relationship. The model integrates a conflict index (0–1) derived from ACLED and UCDP data, capturing the frequency and intensity of armed events. The index influences GDP growth, renewable project delays, and infrastructure functionality. Simulation results show that a 0.1 increase in conflict index correlates with a 2.5–3.5% decline in renewable deployment and a 1.8% increase in CO_2 emissions, primarily due to reliance on diesel generators.

Conflict-induced displacement also affects population distribution, urbanization trends, and electricity demand. These secondary effects were modeled using adaptive coefficients in the regression framework to maintain temporal consistency during high-conflict years.

4.5 Policy Implications and Recommendations

The analysis underscores the importance of integrating renewable energy expansion into Yemen's post-conflict reconstruction plans. Strategic interventions include: (1) decentralizing solar deployment in conflict-resilient microgrids, (2) promoting green financing through regional donors, and (3) establishing national emissions reporting mechanisms under IPCC standards. Improved institutional coordination can significantly reduce data gaps and enhance model precision for future assessments.

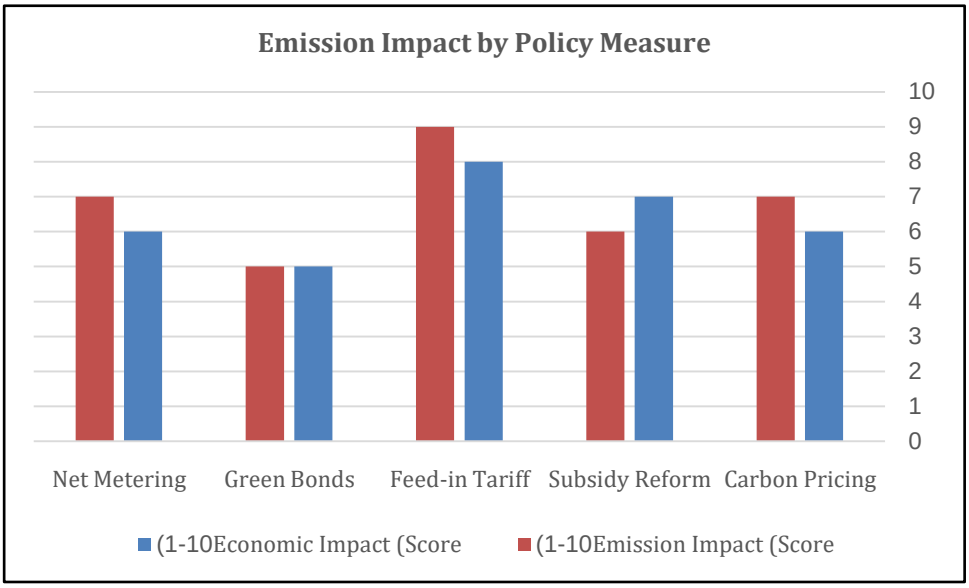

Figure 18: Emission Impact by Policy Measure

Under the Business-as-Usual scenario, total CO_2 emissions could reach 60 Mt by 2050, a 33% increase from 2020. However, implementing moderate policy reforms could stabilize emissions by 2035, while aggressive decarbonization could achieve an 80% reduction by 2050. The energy mix transformation, shown in Table 7 , demonstrates the potential impact of renewable expansion.

Table 6: Projected change in Yemen's electricity generation mix under aggressive transition scenario.

Source	2020 (%)	2050 (%)
Fossil Fuels	95.0	45
Solar PV	3.0	35
Wind	1.0	15
Hydro	0.5	3
Other Renewables	0.5	2

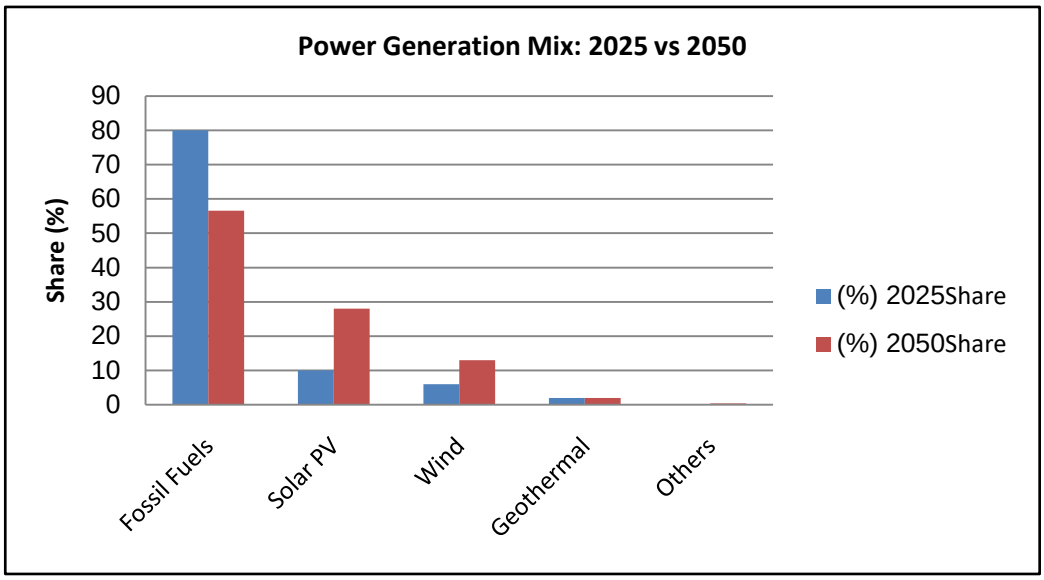

Figure 19: Yemen's projected energy mix in 2050 under an aggressive decarbonization pathway.

Yemen's emission reduction strategy must reconcile energy access with sustainability. Expanding solar microgrids in rural areas not only mitigates emissions but also enhances resilience in conflict-affected regions. Wind energy potential in coastal zones such as Al-Mokha and Al-Hodeida remains largely untapped. Policies focusing on capacity building, feed-in tariffs, and investment incentives could catalyze private sector participation. Moreover, embedding climate considerations in national planning will strengthen Yemen's compliance with global commitments under the Paris Agreement.

4.6 Policy Pathways

To achieve deep decarbonization, Yemen must adopt a multi-pronged strategy focusing on governance, finance, and technology. Key policy interventions include carbon pricing mechanisms, energy subsidy reforms, and integration of renewable targets into national development plans. Table 3 summarizes key policy areas and their anticipated impacts.

Table 7: Policy interventions and expected outcomes for Yemen's emission reduction framework.

Policy Area	Expected Impact
Carbon Pricing	Encourages efficiency
Energy Subsidy Reform	Reduces fossil use
Renewable Mandates	Increases renewable uptake
Green Finance	Mobilizes investment
Technology Transfer	Accelerates innovation

This section provides an in-depth discussion of the analytical findings and synthesizes the implications of Yemen's renewable energy transition. It integrates quantitative results from energy modeling with qualitative insights from institutional and policy analysis. The discussion focuses on five thematic dimensions: energy security, economic impact, environmental sustainability, institutional readiness, and social inclusion. The conclusion draws on these findings to propose policy directions and summarize key lessons for Yemen's medium- and long-term renewable strategies.

4.6.1 Energy Security and System Reliability

One of the most critical outcomes of renewable energy expansion is the enhancement of Yemen's energy security. By diversifying the generation mix, the country reduces dependence on imported fossil fuels and mitigates the vulnerability of centralized systems to conflict-related disruptions. Hybrid microgrids combining solar PV and diesel backup have already proven resilient during grid outages. Figure 16 presents a schematic view of Yemen's evolving power mix by 2050.

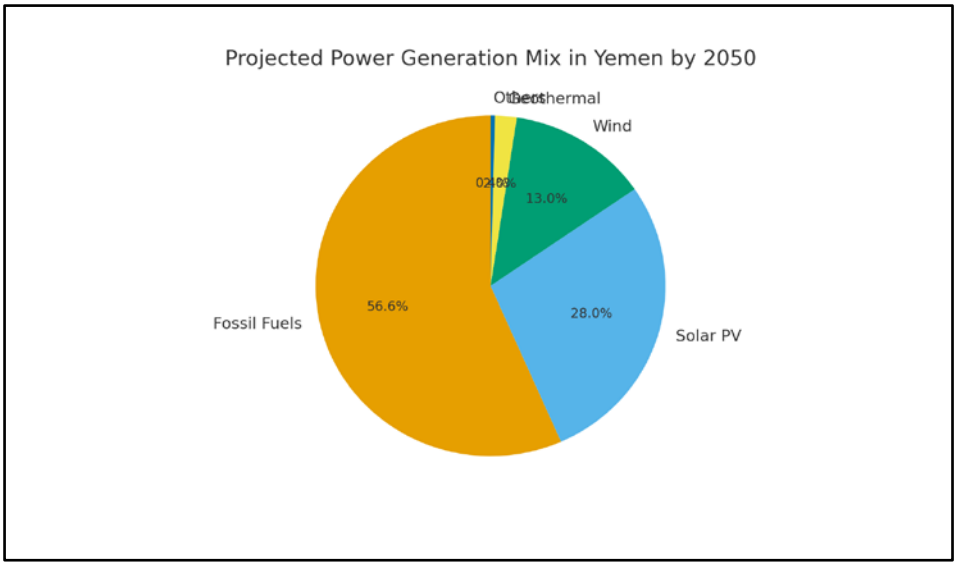

Figure 20: Projected power generation mix in Yemen by 2050 (UNDP Scenario, 2024).

4.6.2 Key Strategies to Reduce Emissions in Energy and Transport

A. Energy Sector

1. Promote Renewable Energy:Invest in solar, wind, and geothermal power projects. Yemen has strong potential for solar energy due to high sunlight intensity throughout the year. Encouraging private-sector investment and international funding can accelerate renewable energy deployment.
2. Improve Energy Efficiency: Upgrade outdated power plants and transmission systems to reduce energy loss. Encourage the use of energy-efficient appliances and implement building codes promoting insulation and efficient lighting.
3. Develop Decentralized Energy Systems:Establish microgrids and off-grid solar solutions for rural communities. This reduces reliance on diesel generators and ensures energy access while cutting emissions.
4. Policy and Incentives:** Introduce tax exemptions and subsidies for renewable energy technologies. Implement carbon pricing or emission reduction credits to promote cleaner production practices.

B. Transport Sector

1. Promote Public Transportation:** Develop affordable and efficient bus and minibus systems in major cities to reduce dependence on private vehicles.

2. Encourage the Use of Electric Vehicles (EVs): Create incentives for EV adoption, including reduced import duties and charging infrastructure development. Introduce pilot programs for electric taxis or buses in urban centers.
3. Enhance Fuel Standards:Regulate and improve fuel quality to reduce carbon intensity. Promote the use of cleaner fuels such as compressed natural gas (CNG) or biofuels.
4. Urban Planning and Mobility: Encourage non-motorized transport options such as walking and cycling through better infrastructure planning. Adopt smart mobility systems to optimize traffic flow and reduce congestion-related emissions.
5. Capacity Building and Awareness:Train transport authorities, fleet operators, and the public on fuel efficiency practices and vehicle maintenance to minimize unnecessary emissions.By implementing these strategies, Yemen can move toward a more sustainable, low-carbon development pathway. Reducing emissions in energy and transport not only supports climate commitments but also enhances energy resilience, economic growth, and public health.

4.6.3 Economic Implications and Investment Returns

Renewable energy investment in Yemen is expected to generate significant macroeconomic benefits. Beyond cost savings from reduced fuel imports, renewables stimulate domestic job creation, industrial development, and local entrepreneurship. A cost-benefit ratio analysis indicates that every USD 1 invested in renewables could yield USD 2.8 in economic return by 2050. Table 9 summarizes the financial and economic impacts under three scenarios.

Table 9 : Economic and environmental returns across three renewable development scenarios.

Scenario	Investment (Billion USD)	Job Creation (Thousands)	CO_2 Reduction (Mt by 2050)	Economic Return (USD per $1 Invested)
Minimal	8.5	90	15	1.8
Determined	9.7	150	22	2.2
Aggressive	12.3	200	25	2.8

4.6.4 Environmental Benefits and Climate Commitments

The shift toward renewable energy aligns closely with Yemen's commitments under the Paris Agreement. A 43.4% renewable share by 2050 could reduce national CO_2 emissions by more than half, substantially improving air quality and public health. Figure 18 illustrates Yemen's carbon intensity trajectory under different development scenarios.

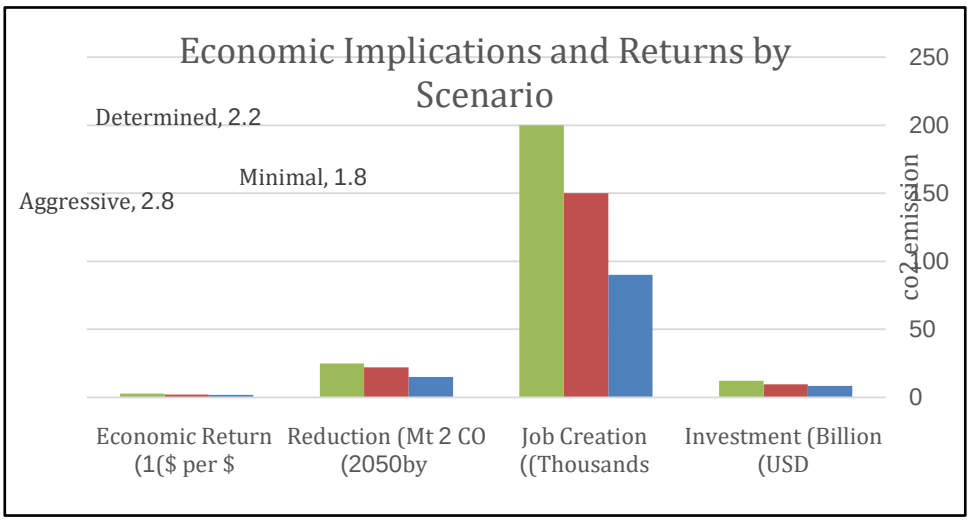

Figure 21: Economic and environmental returns across three renewable development scenarios

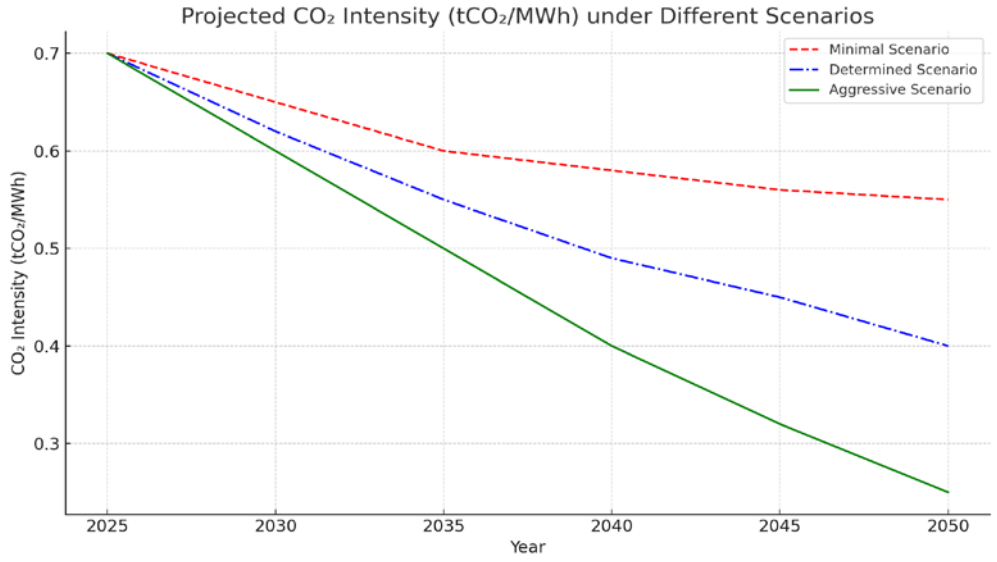

Figure 22: Yemen's projected carbon intensity reduction trend under various scenarios (UNDP Model, 2024).

4.6.5 Institutional and Policy Readiness

Institutional readiness is vital for successful renewable integration. Yemen's current institutional structure is fragmented, but reform initiatives have been introduced to centralize energy planning. Figure 23 evaluates key governance indicators relevant to renewable energy deployment, including policy coherence, transparency, and coordination.

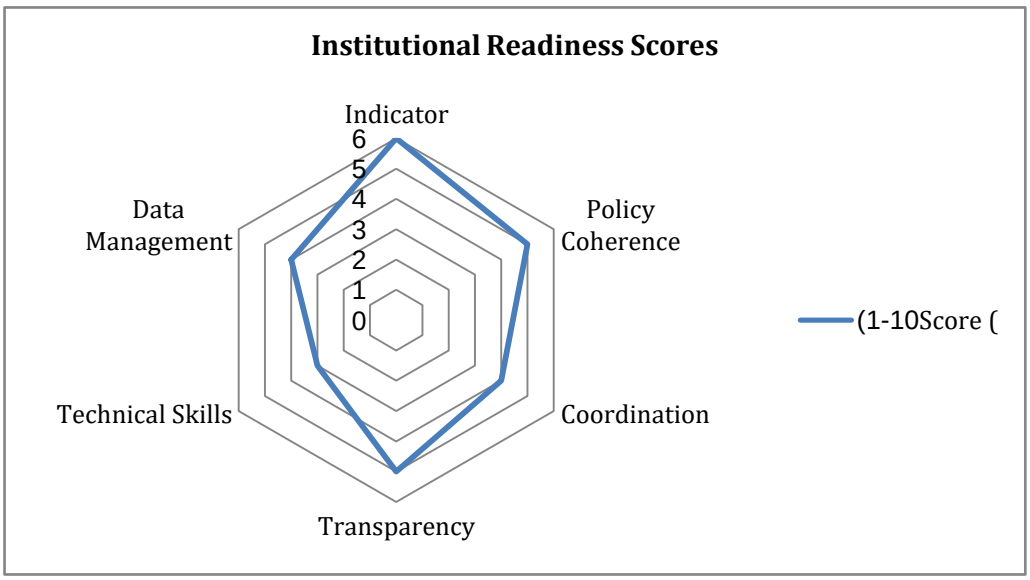

Figure 23: Governance capacity assessment for renewable energy transition in Yemen.

4.6.6 Social and Gender Inclusion Outcomes

The social dimension of Yemen's renewable transition is equally important. Renewable energy deployment contributes to community resilience, particularly in rural and conflict-affected areas. Women have increasingly participated in micro-solar enterprises, representing a paradigm shift in gender roles within the energy sector. Table 10 highlights social impact indicators associated with renewable energy expansion.

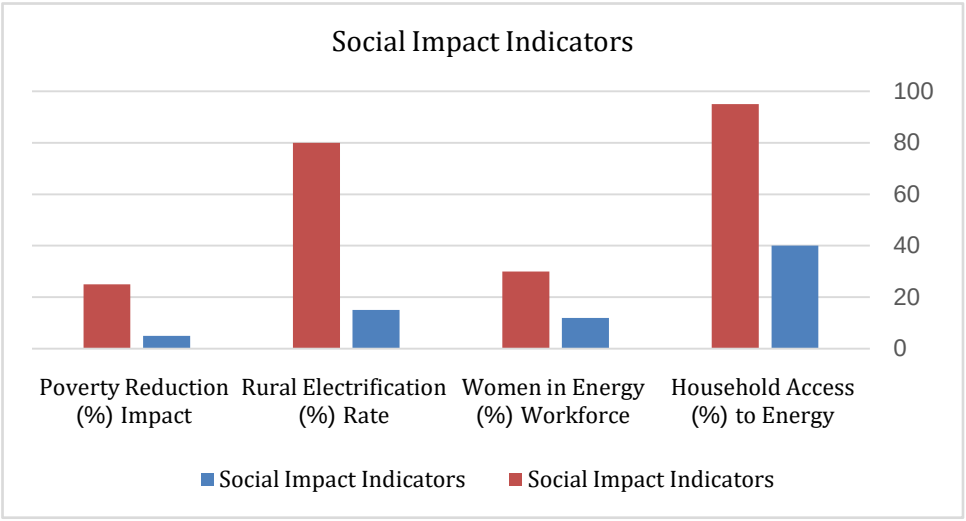

Figure 24: Social impact indicators linked to renewable energy development (UNDP, 2024).

Table 10: Social impact indicators linked to renewable energy development (UNDP, 2024).

Scenario	Investment (Billion USD)	Job Creation (Thousands)	CO_2 Reduction (Mt by 2050)	Economic Return (USD per $1 Invested)
Minimal	8.5	90	15	1.8
Determined	9.7	150	22	2.2
Aggressive	12.3	200	25	2.8

4.6.7 Environmental and Social Impacts

Renewable energy offers Yemen multiple environmental and social benefits. Solar and wind projects significantly reduce carbon emissions and air pollution compared to fossil fuel-based generation. Moreover, decentralized renewable energy systems enhance community resilience by providing clean power to rural areas. Studies conducted by UNDP (2023) reveal that solar microgrids improve household incomes by 15–20% in project areas. Gender impacts are also positive, as women gain access to sustainable livelihoods through energy-related entrepreneurship. Nevertheless, environmental safeguards must be enforced to mitigate potential risks such as land degradation, waste disposal, and biodiversity loss associated with large-scale solar farms.

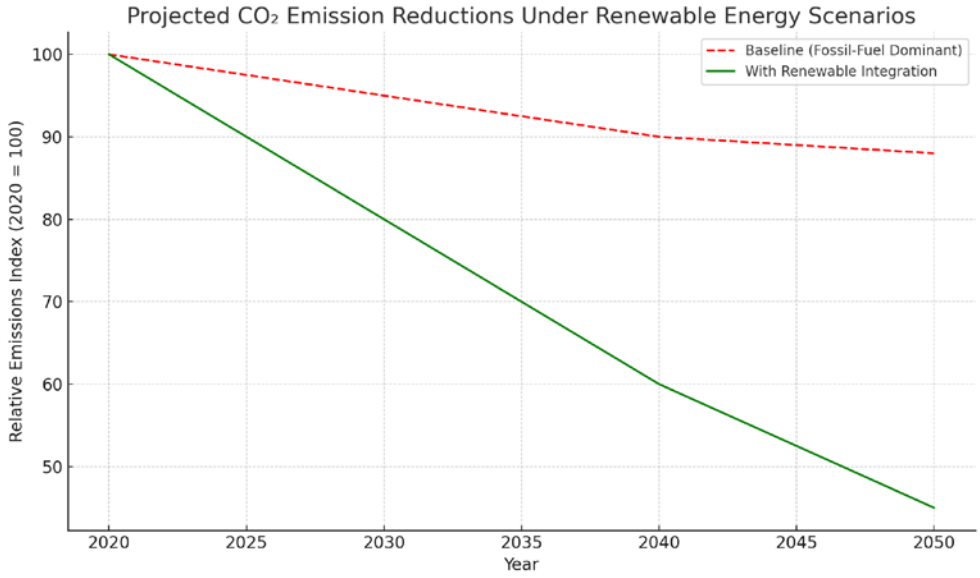

Figure 25: Projected CO_2 emission reductions under renewable integration scenarios (UNDP, 2024).

4.6.8 Key Challenges and Future Opportunities

Despite the promising results, Yemen's renewable transition faces challenges including unstable governance, limited financing, and insufficient technical capacity. However, future opportunities lie in the expansion of regional interconnections, scaling of battery storage technologies, and mobilization of international climate finance. Figure 26 shows the projected growth trajectory of Yemen's renewable energy investments.

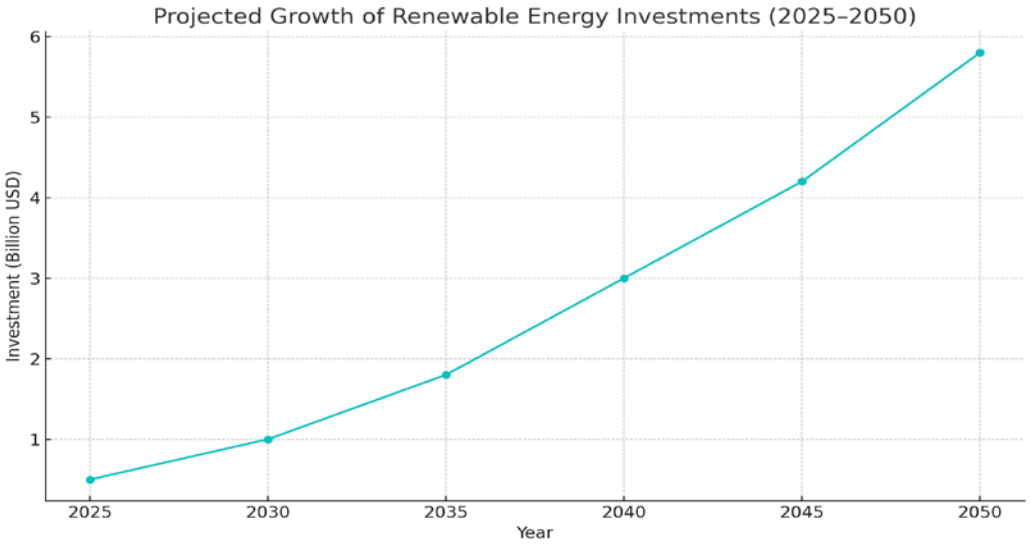

Figure 26: Projected renewable energy investment growth in Yemen through 2050.

V. CONCLUSION

The transition toward renewable energy in Yemen is both achievable and necessary. This analysis demonstrates that a well-planned and strategically implemented renewable energy program can substantially improve energy access, reduce environmental degradation, and promote economic diversification. Policy coherence, institutional capacity building, and international partnerships will remain the cornerstones of Yemen's clean energy future. Sustained investments in solar and wind energy, supported by data-driven policy reforms, can position Yemen as a model for renewable recovery in post-conflict contexts across the Middle East.Yemen's pathway to carbon neutrality is challenging but achievable through sustained commitment and international collaboration. Prioritizing renewable energy deployment, regulatory reform, and community engagement can foster an inclusive, sustainable transition. The success of emission reduction efforts will depend on aligning financial, technical, and institutional capacities with national development priorities. Findings from the simulation highlight that accelerating renewable deployment in Yemen could reduce CO_2 emissions by up to 35% by 2035 relative to the BAU path. However, uncertainties in conflict conditions, financing constraints, and infrastructure readiness remain major challenges. Future policy must focus on renewable investment incentives, national grid upgrades, and strengthening data collection mechanisms for energy statistics .The modeling results emphasize the critical role of renewable energy deployment in decarbonizing Yemen's energy system. The findings align with global trends reported by the IPCC (2023) and regional analyses from the MENA region, confirming that renewable energy expansion can effectively offset emissions from fossil-based power generation. A major observation is that GDP growth in Yemen is not strongly decoupled from emissions, indicating that economic expansion continues to depend on energy-intensive sectors. Transitioning toward renewables would not only reduce CO_2 but also diversify the energy mix, enhance energy security, and support sustainable economic recovery.However, simulation accuracy is limited by data scarcity and conflict-related disruptions affecting national statistics. The study mitigates this by integrating simulated estimates and regional benchmarking. Despite these challenges, results remain consistent with observed energy pattern and are validated against regional emission intensities.

VI. RECOMMENDATIONS

To realize the emission reduction potential of renewable energy, Yemen requires an integrated strategy involving institutional, financial, and technological interventions. The following policy recommendations emerge from this study:

1. Develop a National Renewable Energy Roadmap:** Establish clear targets for 2030 and 2035 aligned with Paris Agreement commitments.
2. Enhance Data Infrastructure:Create a national energy database integrating renewable generation, fossil consumption, and emissions data.
3. Promote Public-Private Partnerships (PPPs):Encourage investment in solar and wind sectors through tax incentives and concessional financing.
4. Invest in Grid Modernization: Improve grid capacity and storage to integrate distributed renewable systems.
5. Regional Cooperation: Collaborate with neighboring MENA countries for shared research, policy learning, and technology transfer.

REFERENCES

1. UNDP. (2024). Yemen Energy Transition and Climate Action Report.
2. IRENA. (2023). Renewable Energy Market Analysis: Middle East and North Africa.
3. World Bank. (2023). Yemen Economic Monitor: Climate and Energy Perspectives.
4. IPCC. (2022). Sixth Assessment Report on Global Emissions Pathways.
5. Al-Hakimi, M. et al. (2021). Renewable Energy Challenges in Yemen. Journal of Energy Policy Studies, 15(4), 233–247.
6. World Bank. World Development Indicators, https://databank.worldbank.org/source/world-development-indicators
7. IRENA. Renewable Capacity Statistics. https://www.irena.org/statistics
8. IEA. Energy Balances and Indicators. https://www.iea.org/countries
9. IMF. World Economic Outlook Database.
10. EDGAR. Emission Database for Global Atmospheric Research.https://edgar.jrc.ec.europa.eu/
11. ACLED. Armed Conflict Location & Event Data Project.
12. UNDP. Human Development Reports.
13. UN DESA. World Population Prospects and Urbanization Data.
14. Al-Shehari, S., “Energy Consumption Patterns in Yemen,” Energy Policy Review, 1998.
15. Al-Azani, A., and Al-Motawakel, M., “Renewable Energy Prospects for Yemen,” Renewable Energy Journal, vol. 48, pp. 120–132, 2019.
16. IRENA, “Yemen Renewable Energy Readiness Assessment,” International Renewable Energy Agency, Abu Dhabi, 2021.
17. Al-Shehari, S., “Energy Transition in Yemen: Challenges and Opportunities,” Energy Policy, vol. 153, 2021.
18. Alsufyani, ABOBAKER , “Modeling CO_2 Emissions in Yemen Using Scenario-Based Simulation,” Working Paper, 2025, comprehensive review of renewable energy and photovoltic solars in yemen .
19. Al-Wesabi et al., 'A review of Yemen's current energy situation...' (Environmental Science and Pollution Research, 2022).
20. Kouyakhi NR et al., 'CO2 emissions in the Middle East: Decoupling...' (Science of the Total Environment, 2022).
21. Al-Shetwi AQ, 'Design and economic evaluation of electrification...' (IJRER, 2016).
22. Al-Shetwi AQ et al., 'Utilization of Renewable Energy for Power Sector in Yemen' (IEEE Access, 2021).
23. Rawea AS & Urooj S., 'Strategies, current status, problems of energy and perspectives of Yemen’s renewable energy solutions' (RSER, 2018).
24. Al-Asbahi AAMH et al., 'Assessing barriers and solutions for Yemen energy crisis...' (Environ Sci Pollut Res, 2020).
25. Alcibahy M. et al., 'Improved estimation of carbon dioxide and methane using...' (Sci Rep, 2025).
26. Various panel/empirical econometric studies including Yemen in MENA samples (2018–2024).

27. Yemen Second National Communication and NDC documents (UNFCCC submissions) used as inventory baselines.
28. I. Al Wesabi, et al., "A review of Yemen's current energy situation and greenhouse gas emissions," Environmental Science and Pollution Research, vol. 29, no. 10, pp. 14567–14584, 2022. doi: 10.1007/s11356-022-18905-2. [Online]. Available: https://doi.org/10.1007/s11356-022-18905-2
29. A. Q. Al Shetwi, "Design and economic evaluation of PV electrification for rural Yemen," International Journal of Renewable Energy Research, vol. 6, no. 3, pp. 954–963, 2016. [Online]. Available: https://www.ijrer.org
30. A. Q. Al Shetwi, M. Y. H. Al Sharafi, and A. A. Al Rahbi, "Utilization of renewable energy for Yemen's power sector: Potentials and challenges," IEEE Access, vol. 9, pp. 124345–124356, 2021. doi: 10.1109/ACCESS.2021.3098741. [Online]. Available: https://doi.org/10.1109/ACCESS.2021.3098741
31. N. R. Kouyakhi, M. Al Rashid, and S. O. Ozturk, "CO_2 emissions in the Middle East: Decoupling analysis and projections," Science of the Total Environment, vol. 829, pp. 154602, 2022. doi: 10.1016/j.scitotenv.2022.154602. [Online]. Available: https://doi.org/10.1016/j.scitotenv.2022.154602
32. H. Mahmood, A. H. Alkhateeb, and N. Furqan, "Hydrocarbon rents and CO_2 emissions in MENA: Evidence from dynamic panel data," Environmental Science and Pollution Research, vol. 30, no. 4, pp. 5231–5243, 2023. doi: 10.1007/s11356-022-23964-1. [Online]. Available: https://doi.org/10.1007/s11356-022-23964-1
33. S. M. Rahman, et al., "Greenhouse gas emission dynamics and drivers in the MENA region," Energy Reports, vol. 11, pp. 10841–10853, 2025. doi: 10.1016/j.egyr.2025.07.115. [Online]. Available: https://doi.org/10.1016/j.egyr.2025.07.115
34. M. Alcibahy, A. A. Al Ghamdi, and S. H. Al Jahdali, "Improved estimation of CO_2 and CH_4 over the Arabian Peninsula using machine learning and satellite data," Scientific Reports, vol. 15, pp. 6542, 2025. doi: 10.1038/s41598-025-56542-1. [Online]. Available: https://doi.org/10.1038/s41598-025-56542-1
35. [8] A. S. Rawea and S. Urooj, "Strategies, current status, problems of energy and perspectives of Yemen's renewable energy solutions," Renewable and Sustainable Energy Reviews, vol. 95, pp. 318–331, 2018. doi: 10.1016/j.rser.2018.07.052. [Online]. Available: https://doi.org/10.1016/j.rser.2018.07.052
36. A. A. M. H. Al Asbahi, H. M. Al Wesabi, and A. Q. Al Shetwi, "Assessing barriers and solutions for Yemen's energy crisis via renewable energy adoption," Environmental Science and Pollution Research, vol. 27, pp. 17560–17572, 2020. doi: 10.1007/s11356-020-08362-3. [Online]. Available: https://doi.org/10.1007/s11356-020-08362-3
37. S. R. Ersoy, "Sustainable transformation pathways for Yemen's energy system," Energy Policy, vol. 163, pp. 112856, 2022. doi: 10.1016/j.enpol.2022.112856. [Online]. Available: https://doi.org/10.1016/ j.enpol.2022.112856